

Erlend Magnus Løvstakken

Grey-box modelling of a domestic hot water tank to be used for flexibility services

Master's thesis in Energy and Environmental Engineering

Supervisor: Karen Byskov Lindberg

June 2022

Erlend Magnus Løvstakken

Grey-box modelling of a domestic hot water tank to be used for flexibility services

Master's thesis in Energy and Environmental Engineering
Supervisor: Karen Byskov Lindberg
June 2022

Norwegian University of Science and Technology
Faculty of Information Technology and Electrical Engineering
Department of Electric Power Engineering

Abstract

Renewable generation can cause challenges in the power grid, such as deviation in the generation/demand balance. Energy storage and grid reinforcement can solve this problem, but are expensive measures. Renewable generation increases the relevance of flexibility in the power system. Flexible loads can even out the demand profile by load shifting, leading to cost savings for system operators. Flexibility is also beneficial for consumers as it can lead to a reduction in their electricity bills. With the new grid tariff structure, flexibility will be even more valuable, making it easier for consumers to shift their loads. Electric water heaters (EWH) have great flexibility potential, and several projects using smart water heaters have been launched in the last couple of years. In Norway, almost every household has a water heater, which stands for approximately 20 % of the household's total energy consumption. By flexibly controlling the water heater, both system operators and consumers could save costs [1].

This master thesis builds on the specialization project "Predicting flexibility potential of domestic hot water" [2]. Both papers aim to make a model of an EWH by using gray box modelling. The model uses thermoelectric analogy to describe the behavior of the water heater. The models tested in this thesis are called 1R1C, 2R2C, and 3R3C-models. R and C describes the system's amount of thermal resistances and thermal capacitances. These unknown parameters are obtained using parameter fitting. Both the laboratory setup and the theoretical models are improved in the master thesis. This led to better results.

High-frequency power and temperature measurements at the NTNU Smart House Lab are performed, and the parameter fitting of R and C are decided using continuous-time-stochastic-modeling (CTSM-R). The thermal resistance is estimated to have a combined value of $0.446 \frac{^{\circ}C}{kW}$. The thermal capacitance is estimated to a value of $170 \frac{kWh}{^{\circ}C}$. This is a significant improvement from the results obtained in the specialization project [2]. Graphical analysis, Log-Likelihood value, and root-means-square-error are used to verify and decide the best EWH-model. The 3R3C-model is chosen as the best model. The new parameter fittings agree more with other scientific papers.

This thesis makes a model of an EWH and decides its unknown parameters. Further work is to make an optimization problem that minimizes the operational cost of EWHs and map their flexibility potential.

Sammendrag

Fornybar produksjon kan gi utfordringer i kraftnettet, som for eksempel ubalanse mellom produksjon og etterspørsel. Energilagring og nettførsterkning kan løse dette problemet, men er kostbare tiltak. Fornybar produksjon øker relevansen av fleksibilitet i kraftsystemet. Fleksible laster kan jevne ut lastprofiler ved å flytte last til andre tider av døgnet. Dette fører til kostnadsbesparelser for systemoperatører. Fleksibilitet er også gunstig for forbrukerne, da det kan føre til en lavere strømregning. Med den nye nettleiestrukturen vil fleksibilitet være enda mer verdifullt, da det kan være en stor økonomisk fordel å spre laster utover døgnet. Elektriske varmtvannsberedere (EVVB) har stort fleksibilitetspotensial, og flere prosjekter med smarte varmtvannsberedere er gjennomført de siste årene. I Norge har nesten hver husholdning en varmtvannsbereder. Denne står for omtrent 20% av husholdningens totale energiforbruk. Ved fleksibel styring av varmtvannsberederen kan både systemoperatører og forbrukere spare kostnader [1].

Denne masteroppgaven bygger på fordypningsprosjektet "Predicting flexibility potential of domestic hot water" [2]. Begge oppgaver kartlegger egenskapene til varmtvannsberederen gjennom eksperimenter, og lager en modell av tanken for å bestemme ukjente parametre. Modellen bruker termoelektrisk sammenheng for å beskrive oppførselen til varmtvannsberederen. Ved å beskrive den termiske modellen med RC-kretser, kan ukjente parametre bli funnet. Modellene som er testet i denne oppgaven kalles 1R1C, 2R2C og 3R3C-modeller, og beskriver modellens mengde av termiske motstander og kondensatorer. Parametertilpasning brukes for å finne disse ukjente parametrene. Både laboratorieoppsettet og modellene er forbedret i masteroppgaven. Dette fører til bedre resultater.

Høyfrekvente effekt- og temperaturmålinger ved NTNU Smart House Lab utføres, og parametertilpasning av R (termisk motstand) og C (termisk kapasitans) bestemmes ved bruk av kontinuerlig-tids-stokastisk-modellering (CTSM-R). Den termiske motstanden er beregnet til å ha en verdi av $170 \frac{^{\circ}\text{C}}{\text{kW}}$. Den totale termiske kapasitansen er beregnet til å ha en verdi på $0.446 \frac{\text{kWh}}{^{\circ}\text{C}}$. Dette er en betydelig forbedring fra resultatene oppnådd i prosjektoppgaven. Grafisk analyse, sannsynlighetsverdi og kvadratisk gjennomsnittsverdi ble brukt for å verifisere og bestemme den beste modellen. 3R3C-modellen ble valgt som den beste modellen. De nye parametertilpasningene stemmer godt overens med andre artikler.

Denne oppgaven beskriver en varmtvannstank-modell og bestemmer dens ukjente parametre. Dette kan brukes til å bestemme fleksibilitetspotensialet til en og flere varmtvannstanker. Videre arbeid vil være å lage et optimaliseringsproblem som minimerer driftskostnadene til varmtvannstanken.

Preface

Several people helped me during the master thesis. My supervisor, Karen Lindberg, has contributed invaluable help and feedback throughout the semester. She is committed and has been positive about my work. This has helped me stay motivated. I would also like to thank Eilif Hugo Hansen and Aksel Andreas Reitan Hansen for their excellent help at the Smart House Lab. They have helped acquire and install new equipment for the lab. I would also like to thank my classmates who have made these five years at NTNU unforgettable.

Table of Contents

List of Figures	v
List of Tables	vii
1 Introduction	1
1.1 Motivation	1
1.2 Hypothesis	1
1.3 Scope	1
1.4 Research Questions	2
1.5 Limitations	2
1.6 Context of thesis	2
2 Theory	4
2.1 Norwegian Power Usage	4
2.2 Grid tariff structure	6
2.3 Flexibility	7
2.3.1 Demand side flexibility	7
2.3.2 Flexibility of EWHs	9
2.4 Water heaters	9
2.4.1 Design and operation of water heater	10
2.4.2 Restrictions due to legionella	12
2.5 Data Communication	12
2.5.1 Logic Machine	12
2.5.2 KNX	13
3 Literature Review	14
3.1 Grey box modelling	14
3.1.1 Thermal equivalent model	15
3.1.2 Continuous Time Stochastic Modelling in R	17
3.2 Parameter fittings of academic papers	18
3.3 Flexibility potential of EWH	19
4 Experimental Setup	20

4.1	Smart House	20
4.2	Control system	20
4.3	Equipment	21
4.3.1	OSO Saga S 300 water heater	21
4.3.2	Temperature sensors	23
4.3.3	Water flow meter	24
4.3.4	Power meter	25
4.3.5	Other Equipment	26
4.4	Physical Setup	26
5	Experimental Method	28
5.1	Case 1: Steady state of the EWH at different set-point temperatures	28
5.2	Case 2: 3-4 showers a day while the EWH is in on-mode	28
5.3	Case 3: 3-4 showers a day while the EWH is in off-mode	28
5.4	Overview of the Cases	29
6	Method and Model	30
6.1	1R1C	30
6.2	2R2C	31
6.3	3R3C	33
6.4	Using The CTSM-R tool	36
6.5	Model Validation	37
7	Experimental Results	38
7.1	Case 1.1: Steady state of the EWH at different set-point temperatures using the upper temperature sensor	38
7.2	Case 1.2: Steady state of the EWH at different set-point temperatures using the upper temperature sensor	40
7.3	Case 2: 3-4 showers a day while the EWH is in on-mode	43
7.4	Case 3.1: 3-4 showers a day while the EWH is in off-mode	45
7.5	Case 3.2: 3-4 showers while the EWH is in off-mode	47
8	Verification of Mathematical Model	51
8.1	Case 1	51
8.2	Case 2	53

8.3	Case 3	55
9	Discussion	57
9.1	Case 1	58
9.1.1	Case 1.1	58
9.1.2	Case 1.2	59
9.1.3	Take home from experiments without draining water	59
9.2	Case 2	60
9.3	Case 3	60
9.3.1	Case 3.1	61
9.3.2	Case 3.2	61
9.4	Take home from experiments where water is drained from the EWH	61
9.5	Parameter fitting computed with CTSM-R	61
10	Further Work	63
11	Conclusion	64
	References	65
12	Appendix	69
12.1	Case 1.1	69
12.1.1	2R2C	69
12.1.2	3R3C	70
12.2	Case 1.2	71
12.2.1	1R1C	71
12.2.2	2R2C	72
12.2.3	3R3C	73
12.3	Case 2	73
12.3.1	1R1C	73
12.3.2	2R2C	74
12.3.3	3R3C	75
12.4	Case 3.1	75
12.4.1	1R1C	75
12.4.2	2R2C	76

12.4.3	3R3C	77
12.5	Case 3.2	77
12.5.1	1R1C	77
12.5.2	2R2C	78
12.5.3	3R3C	79
12.6	Tables	80
12.7	Code	81

List of Figures

1	Monthly total power use and spot-price for Oslo, year 2021.	4
2	Power consumption the first day of each month, June 2021 to May 2022.	5
3	Spot-Price for Oslo the first day of each month, June 2021 to May 2022.	5
4	Grid Tariff Structure of detached house with a consumption of 20 000 kWh/year.	6
5	End user flexibility types [21].	8
6	Illustration of electric water heater [38].	11
7	Illustration of the concept of grey-box modelling [50].	14
8	Analogy between the electrical circuit and the thermal model.	15
9	Heating of insulated enclosure (left) and its electric equivalent circuit between electrical circuit and thermal model (right).	16
10	Logic Machine 4 (to the left) and LogicMachine application interface (to the right).	21
11	OSO S300 Water Heater schematics [37].	22
12	Illustration of thermostat [37].	22
13	T_{lower} and T_{middle} to the left and T_{in} and T_{out} to the right.	23
14	T_{upper} to the left and T_a to the right.	23
15	Thermowell to the left and installation point to the right.	24
16	Illustration of the temperature sensors in the tank.	24
17	GWF Multi Jet Water Meter.	25
18	ELITEpro XC (to the left) and ELOG 15 application interface(to the right).	25
19	Asus router RT-AC3200 and Relay MTN647895 from Schneider Electric.	26
20	The communication system structure of the Smart House.	26
21	OSO Saga S300 with temperature sensor location.	27
22	Final RC-equivalent circuit.	30
23	The thermoelectric equivalent of the system.	31
24	The V_{water} node.	32
25	The V_{wall} node	32
26	The thermoelectric equivalent of the system.	33
27	The thermoelectric equivalent of the system.	34
28	The thermoelectric equivalent of the system.	35
29	The thermoelectric equivalent of the system.	35
30	Iterations performed by CTSM-R.	36

31	Temperatures and power rating measurements of Case 1.1.	38
32	Estimated values for resistances and capacitances for Case 1.1.	39
33	Comparing residuals of Case 1.1 using upper temperature sensor.	40
34	Temperatures and power rating measurements of Case 1.2.	41
35	Estimated values for resistances and capacitances in Case 1.2.	42
36	Comparing residuals of Case 1.2 using middle temperature sensor.	42
37	Temperatures and power ratings of the EWH during Case 2.	43
38	Estimated values for resistances and capacitances in Case 2.	44
39	Comparing residuals of Case 2 using middle temperature sensor.	45
40	Temperatures and power ratings of Case 3.1.	46
41	Comparing residuals of Case 3.1, using middle temperature sensor.	47
42	Temperatures and power ratings of Case 3.2 with the upper temperature sensor.	48
43	The relationship between the different resistances and capacitances of Case 3.1 and Case 3.2.	49
44	Comparing residuals of Case 3.2, using upper temperature sensor.	50
45	Comparing one-step-ahead functions for Case 1.1 using upper temperature sensor.	51
46	Comparing simulated value-plots for Case 1.1 using the upper temperature sensor.	52
47	Comparing one-step-ahead functions for Case 1.2 using middle temperature sensor.	52
48	Comparing simulated-value-plots for Case 1.2 using middle temperature sensor.	53
49	Comparing one-step-ahead plots of Case 2 using middle temperature sensor.	54
50	Comparing simulated-value-plots for Case 2 using the middle temperature sensor.	54
51	Comparing one-step-ahead plots of 1R1C, 2R2C and 3R3C for Case 3.1.	55
52	Comparing simulated-value-plots for Case 3.2, middle temperature sensor.	55
53	Comparing one-step-ahead plots of 1R1C, 2R2C and 3R3C for case 3.2.	56
54	Comparing simulated-value-plots for Case 3.2 using the upper temperature sensor.	56
55	Code for initializing and system equations.	81
56	Code for reading files and setting initial values.	81
57	Code for plotting temperature and power graphs.	82
58	Code for parameter fitting, RMSE and LogLikelihood value and Residual plots.	82

List of Tables

1	Fixed cost price 2022 (Elvia).	6
2	Isolation materials and their specific heat capacity [39].	12
3	Analogies between thermal and electrical systems.	16
4	List of equipment used in the smart house.	21
5	Technical data of OSO Saga S300 water heater.	22
6	Overview of the different experiments.	29
7	CSV-file.	29
8	Coefficient Matrix of the 1R1C-model for case 1.1 with upper temperature sensor.	39
9	Correlation Matrix of the 1R1C-model for Case 1.1 using the upper temperature sensor.	39
10	Estimated values for resistance and capacitance of Case 1.1.	39
11	Estimated values for R and C of Case 1.2.	41
12	Showers performed during Case 2.	43
13	Parameter fitting for Case 2.	44
14	Showers and state of EWH during Case 3.1.	46
15	Parameter fitting for Case 3.1.	46
16	Showers and state of water heater during Case 3.2.	48
17	Parameter fitting of case 3.2.	49
18	Likelihood, RMSE, R and C-values of Case 1.	51
19	R ($\frac{^{\circ}C}{kW}$) and C ($\frac{kWh}{^{\circ}C}$), LogLikelihood and RSME-value for Case 2.	53
20	Resistance ($\frac{^{\circ}C}{kW}$), capacitance ($\frac{kWh}{^{\circ}C}$), LogLikelihood and RMSE-value for Case 3.	55
21	R ($\frac{^{\circ}C}{kW}$) and C ($\frac{kWh}{^{\circ}C}$) compared with other papers.	57
22	R ($\frac{^{\circ}C}{kWkg}$) and C ($\frac{kWh}{^{\circ}Ckg}$) compared with other papers.	57
23	Specific heat capacity of water.	58
24	Specific heat capacity of water at different volumes (L).	58
25	Coefficient Matrix of the 2R2C-model in Case 1.1, using the upper temperature sensor.	69
26	Correlation Matrix for the 2R2C model in Case 1.1 using the upper temperature sensor.	69
27	Coefficient Matrix of the 2R2C-model in Case 1.1, using the lower temperature sensor.	69
28	Correlation Matrix for the 2R2C model in Case 1.1 using the lower temperature sensor.	70

29	Coefficient Matrix for the 3R3C-model in Case 1.1 using the upper temperature sensor.	70
30	Correlation Matrix for the 3R3C-model in Case 1.1 using the upper temperature sensor.	70
31	Coefficient Matrix for the 3R3C-model in Case 1.1 using the lower temperature sensor.	71
32	Correlation Matrix for the 3R3C-model in Case 1.1 using the lower temperature sensor.	71
33	Coefficient Matrix for the 1R1C-model in Case 1.2.	71
34	Correlation Matrix for the 1R1C-model in Case 1.2.	72
35	Coefficient Matrix of the 2R2C-model of Case 1.2 with middle temperature sensor.	72
36	Correlation Matrix of the 2R2C-model for case 1.2 using the middle temperature sensor.	72
37	Coefficient Matrix for the 3R3C-model in Case 1.2 using the middle temperature sensor.	73
38	Correlation Matrix for the 3R3C-model in Case 1.2 using the middle temperature sensor.	73
39	Coefficient Matrix for the 1R1C-model in Case 2.	73
40	Correlation Matrix for the 1R1C-model in Case 2.	74
41	Coefficient Matrix of the 2R2C-model in Case 2, using the middle temperature sensor.	74
42	Correlation Matrix for the 2R2C model in Case 2 using the middle temperature sensor.	74
43	Coefficient Matrix of the 3R3C-model of Case 2 with middle temperature sensor.	75
44	Correlation Matrix of the 3R3C-model for Case 2 using the middle temperature sensor.	75
45	Coefficient Matrix for the 1R1C-model in Case 3.1.	75
46	Correlation Matrix for the 1R1C-model in Case 3.1.	76
47	Coefficient Matrix of the 2R2C-model in Case 3.1 using the middle temperature sensor.	76
48	Correlation Matrix for the 2R2C model in Case 3.1 using the middle temperature sensor.	76
49	The coefficient Matrix of the 3R3C-model for Case 3.1 using the middle temperature sensor.	77
50	Correlation Matrix of the 3R3C-model for Case 3.1 using the middle temperature sensor.	77
51	Coefficient Matrix for the 1R1C-model in Case 3.2.	77
52	Correlation Matrix for the 1R1C-model in Case 3.2.	78

53	Coefficient Matrix of the 2R2C-model in Case 3.2 using the middle temperature sensor.	78
54	Correlation Matrix for the 2R2C model in Case 3.2 using the middle temperature sensor.	78
55	Coefficient Matrix of the 3R3C-model for Case 3.2 using the middle temperature sensor.	79
56	Correlation Matrix of the 3R3C-model for Case 3.2 using the middle temperature sensor.	79
57	Flexibility service for TSO.	80
58	Flexibility services for DSO.	80
59	Flexibility services for BRP.	80
60	Flexibility services for Prosumers.	81

Abbreviations

DHW = Domestic Hot Water

EWH = Electric Water Heater

EVVB = Elektrisk Varmtvannsbereder

KCL = Kirchhoff Current Law

DSO = District System Operator

TSO = Transmission System Operator

BRP = Balancing Responsible Party

EV = Electric Vehicle

PV = Photovoltaics

HVAC = Heating, Ventilation, and Air Conditioning

AMS = Automatic Metering System

CTSM-R = Continuous Time Stochastic Modelling for R

ICT = The Information and Communication Technology Area of Advance

FCR = Frequency Containment Reserves

FRR = Frequency Restoration Reserves

mFRR manually Frequency Restoration Reserves

1 Introduction

Less fossil and more renewable energy sources are needed to reduce the global climatic changes. This was also the conclusion at the 2021 United Nations Climate Change Conference [3]. With more renewable resources, the share of variable generation increases. This generation leads to the establishment of new challenges in the power grid. These challenges include reverse power flows, islanding issues, overvoltage, and voltage fluctuations [4]. An active demand side is critical when dealing with these types of challenges because it enables the opportunity for cheap control and quick reaction time.

The Smart House Lab at NTNU is a part of the National Smart Grid Laboratory and can be used to simulate an active demand side. The Smart House Lab is equipped with standard household equipment, like a water heater. The lab has advanced measurement and control equipment, making it possible to control and monitor the equipment installed. The lab is accessible by both business and research communities.

1.1 Motivation

Flexibility is the power system's ability to change demand, or generation [5]. Demand-side flexibility addresses the possibility of demand-side loads changing their consumption patterns. Smart meters are installed in every household in Norway. Smart meters simplify the opportunity for flexibility. Combined with demand-side loads such as EVs, battery storage and thermostatically controlled loads increase the possibility of flexibility [6]. Flexibility can lead to cost optimization for both system operators and consumers.

Electric water heaters have excellent energy storage potential due to sound insulation, and water's high specific heat capacity [7]. In Norway, almost every household has an EWH, and 20 % of a building's total energy consumption is used by an EWH [1]. This makes the EWH a highly relevant flexible energy source. The water heater's flexibility could decrease costs for end-users and system operators. The water heater installed in the NTNU Smart House Lab is not a "smart water heater," but it is possible to access its data and use it in research projects. This data can be used to quantify available flexibility for a water heater.

During the last couple of years, several test projects on smart water heaters have been performed in Norway. The manufacturer Høiax has already launched their first smart electric water heater. It enables remote control over temperature settings and the opportunity to change this in accordance with the price of electricity. The Norwegian manufacturer OSO will launch their smart water heater devices in 2022.

1.2 Hypothesis

By expanding the thermoelectric model made in the project thesis, [2], and installing new laboratory equipment at the NTNU Smart House Lab, the model will improve, and the parameter fitted values for resistance and capacitance will be better.

1.3 Scope

- Present relevant theoretical background electric water heaters, Power consumption habits in a Norwegian scenario, grid tariff structure, flexibility and data communication systems.
- Perform a literature review of gray box modelling, previous work on parameter fitting and previous work on flexibility of EWHs.

-
- Perform experiments on the water heater at the NTNU Smart House Lab to obtain temperature and power profiles.
 - Make a model of an EWH, and use grey-box modelling to precisely estimate its unknown parameters.
 - Comparing estimated parameters with equivalent parameters of previous and others work.

1.4 Research Questions

- How will draining water from the tank change the value of thermal resistance and capacitance?
- What is the reason for the differences in parameter fitted resistances and capacitances in different scientific papers?
- Will a thermoelectric equivalent with more resistances and capacitances improve the model?
- Will the new equipment improve the results obtained from the lab?
- How does a model based on steady state perform compared to a model based on dynamic behavior.
- Is it appropriate to perform experiments with different set-point temperatures?

1.5 Limitations

There are several limitations with the equipment used at the NTNU Smart House Lab. There are no temperature sensors inside the tank. There is not possible to remotely control the power or the set-point temperature of the EWH. This has to be done manually. Some draining of hot water may occur as the Lab is used by several people.

1.6 Context of thesis

- Section 1: Introduction, presents the motivation, hypothesis, Scope, Research Questions and Limitations of the master thesis
- Section 2: Theory, presents general theory on electric water heaters, Norwegian power usage, grid tariff structure, flexibility and data communication
- Section 3: Literature review, presents background on grey-box modelling and reviews several papers on gray box-modelling. This section also reviews flexibility potential of an EWH.
- Section 4: Experimental setup, presents a thorough description of the experimental setup.
- Section 5: Experimental Method, presents the method of how experiments are performed. mathematical model
- Section 6: Mathematical Model, presents the mathematical models.
- Section 7: Experimental Results, presents the results of parameter fitting in tables and by graphs. The residuals are also shown in this section.

-
- Section 8: Verification of Mathematical Model establishes the one-step-ahead plots, simulated-value plots, RMSE and LogLikelihood.
 - Section 9: Discussion, analyses the results.
 - Section 10: Further work, provides recommendations for further work.
 - Section 11: Conclusion, provides a summary of the main findings in the report.

2 Theory

This section is based on the theory section written in the project thesis [2]. The section is reviewed and modified, and more theory has been added.

This section gives insight into the Norwegian power usage, grid tariff structure, flexibility, operation of an EWH and data communication systems.

2.1 Norwegian Power Usage

Due to significant climatic variations, Norwegian electrical power use varies throughout the year. Figure 1 shows Norway's monthly power consumption and the spot price for 2021. Figure 2 shows the average power use throughout a day for the first day of each month in Norway. Figure 3 shows the spot price for this scenario [8]. There are typically power peaks around 09:00 and another peak in the afternoon. There is usually a strong correlation between power peaks and power price, as can be seen when comparing Figure 2 and Figure 3. In the last two years, the electricity price has been very high, especially in the southern parts of Norway. With dry years, new overseas cables, and bottlenecks in the grid, this may not change at first. Utilizing flexible loads could make society save money.

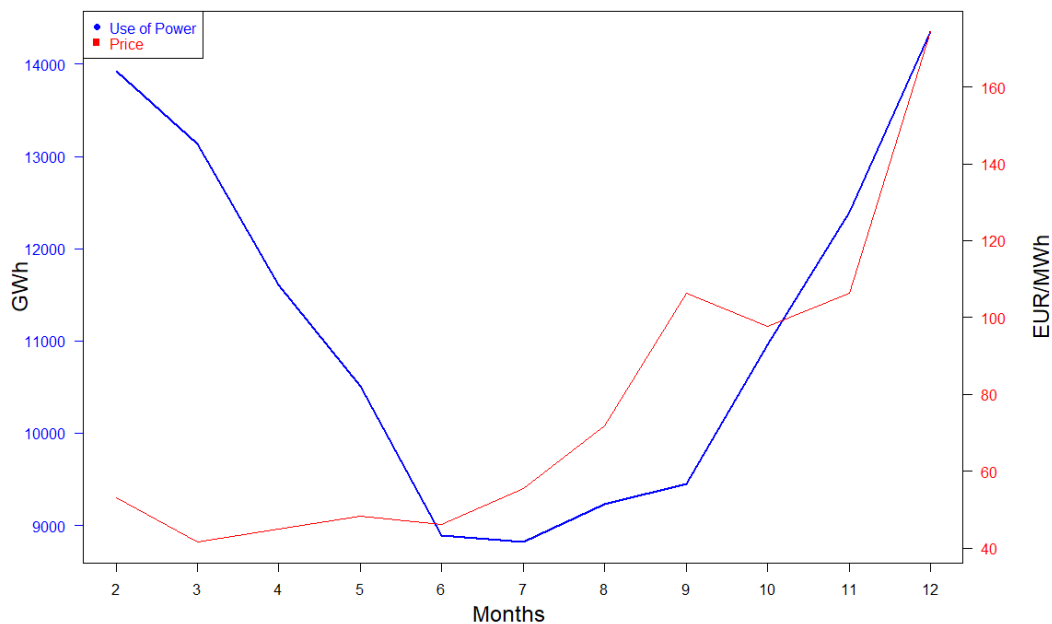


Figure 1: Monthly total power use and spot-price for Oslo, year 2021.
[8]

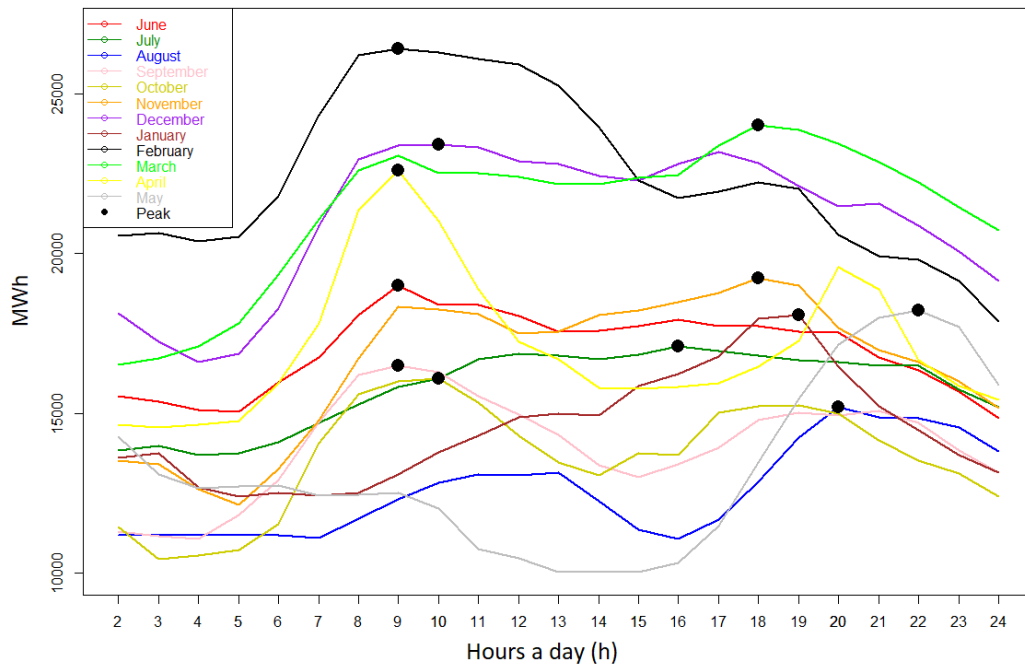


Figure 2: Power consumption the first day of each month, June 2021 to May 2022. [8]

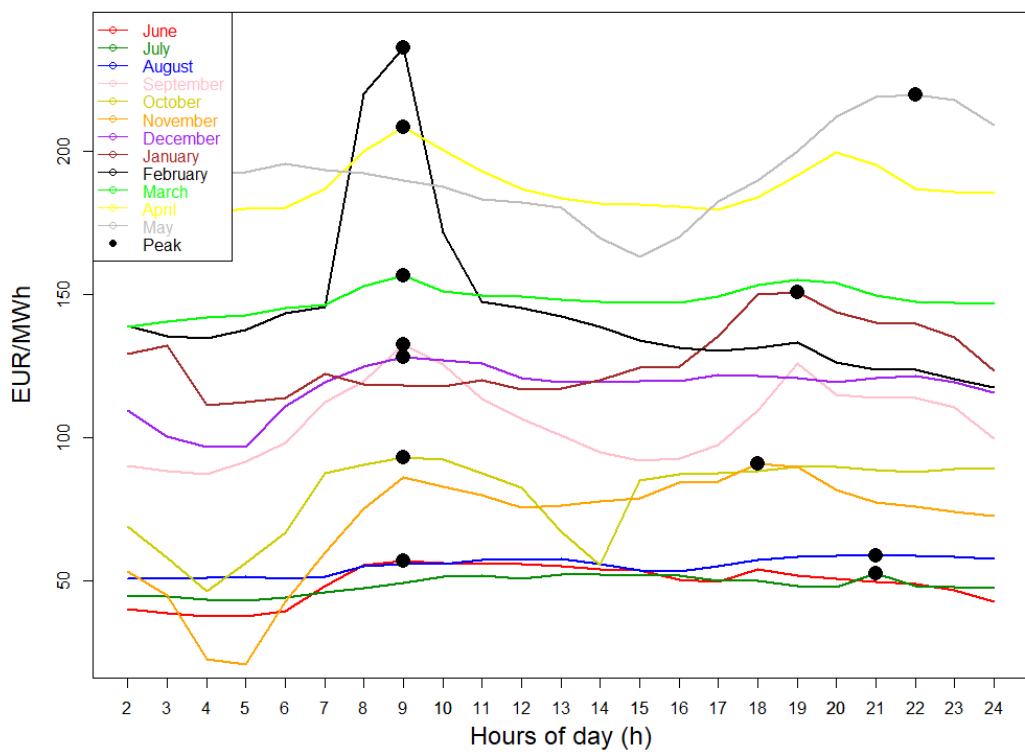


Figure 3: Spot-Price for Oslo the first day of each month, June 2021 to May 2022. [8]

2.2 Grid tariff structure

Until 2022, the grid tariff was divided into fixed costs, taxes, and electricity costs, given in NOK/kWh. Figure 4 shows the average amount of each part. The fixed part was used to cover the grid owner’s fixed cost of operation. This part was fixed throughout the year but varied for different system operators. The most significant part of the grid tariff was the public taxes [9]. The public taxes consists of value-added tax (25%), electrical power fee (16.69 øre/kWh in 2021 [10]), and the ENOVA fee (1 øre/kWh).

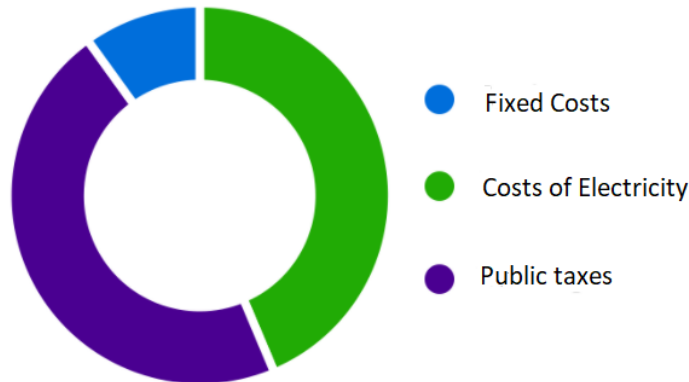


Figure 4: Grid Tariff Structure of detached house with a consumption of 20 000 kWh/year. [9]

In 2022 the grid tariff still consists of a fixed cost, the cost of electricity, and public taxes. The cost of electricity is the same as in earlier years, and taxes represent a substantial part of the electricity bill. The former fixed part is changed, as it now considers the amount of power used by the consumer simultaneously. Table 1 shows Elvia’s price ranges for power [11]. This means that if a person uses 8 kW maximum at the same time a month, the person must pay 280 NOK in fixed costs that month.

Table 1: Fixed cost price 2022 (Elvia).

Step	Fixed Cost (NOK/month)
0 - 2 kW	130
2 - 5 kW	190
5 - 10 kW	280
10 - 15 kW	375
15 - 20 kW	470
20 - 25 kW	565
25 - 50 kW	1250
50 - 75 kW	1720
75 - 100 kW	2190
Over 100 kW	4180

The additional cost of power is an incentive for power peak reduction. It, therefore, is an incentive for flexibility. According to NVE [12], the change in structure provides efficient utilization and development of the power grid.

2.3 Flexibility

There are many definitions of flexibility. Flexibility can be seen as the power system's ability to change demand, or generation [5]. Flexibility states the changes and modifications that can be performed to optimize desired parts of the system. There are several drivers for flexibility, such as uncertain and uncontrollable generation, increasing distributed energy resources, synergies with multi-vector energy systems, ICT (Information and Communication Technology Area of Advance), and changes in consumer attitude and outlook [5].

District System Operator(DSO), Transmission System Operator(TSO), and Balancing Responsible Party (BRP) are willing to buy flexibility services. BRP's role is to maintain supply and demand in the grid and use flexibility services to reduce sourcing costs and obtain system balance. The TSO uses flexibility services to manage transmission capacity, system balance, and facilitate flexible trading across Europe. The DSO uses flexibility services due to increased grid capacity demand from electric vehicles (EV), solar (PV), and heating, ventilation and air-conditioning (HVAC). Grid reinforcements are expensive and time-consuming. It is also costly to balance power, but flexible services could reduce costs. People tend to use electrical power at the same time during the day. This pressurizes the capacity of the power grid. Therefore, end users are vital in flexibility services as they change from passive consumers to prosumers [5], [13]. Tables of flexibility services for TSO, DSO, BRP and Prosumers are given in Table 57 - 60 in Section 12.

2.3.1 Demand side flexibility

There are flexible resources at the supply, grid, and demand sides. An EWH is a part of demand-side flexibility. Demand-side flexibility is the capacity of demand-side loads to change their consumption patterns. Demand-side flexibility can help customers use less power when prices are high and reduce stress on the grid [14] The demand-side flexibility can therefore be an alternative to network reinforcement [15] [6]

Different types of demand-side flexibility resources are following [16]:

- PV
- Battery Storage
- EV
- Thermostatically controlled loads (TCL) such as EWH and HVAC

Following flexibility services can be provided [17]:

- Frequency control
- Voltage control
- Congestion Management
- Reduce maintenance and development costs of the power grid
- Grid capacity management
- Better planning and increased efficiency in grid operation

In Norway, automatic metering systems (AMS) were installed in all households in 2018. AMS increases the data availability and gives insights on consumption and consumption patterns to facilitate smart electricity solutions. It also detects power failures in the grid more efficiently and reduces the risk of congestion and power failure [18]. AMS installation is one step towards a more flexible and smart power grid.

80% of the energy demand in the Norwegian building sector is met by electricity [12]. This facilitates a considerable potential for flexibility because of the storage opportunities of electricity. Electricity can be stored in batteries, but the energy can also be stored as heat. The main goal of energy flexibility in Norway is to avoid substantial power peaks to reduce the strain on the distribution grid [19]. Typical load-shifting types are described below and shown in Figure 5. [20]

- **Peak clipping** = Reducing load (mainly in-peak hours but also in general)
- **Load Shifting** = Reducing load in-peak hours and distribute this load to off-peak hours
- **Valley Filling** = Increase load during off-peak hours

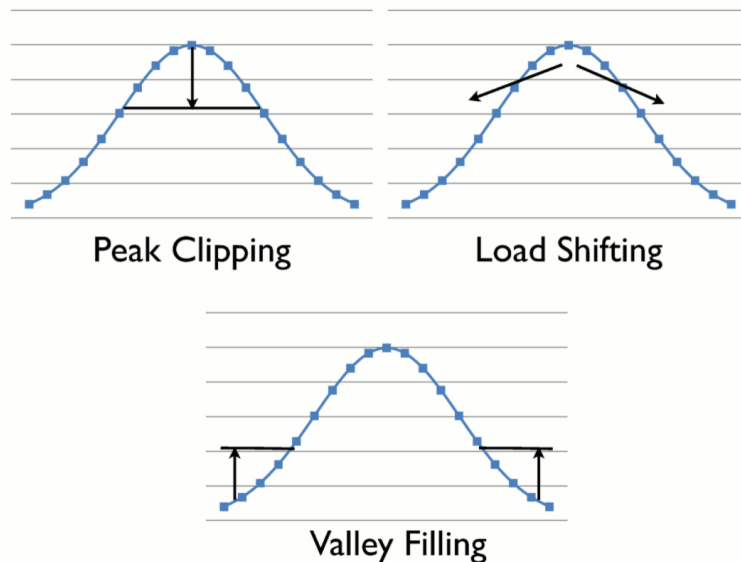


Figure 5: End user flexibility types [21].

Frequency response is also a vital flexibility service, and it is separated into different types of control with different working periods. There is Primary, Secondary, and Tertiary control.

Primary control: frequency response control or frequency containment reserves (FCR). FCR has the fastest reaction time. It is an automatic function used when there is an imbalance between generation and demand in the power grid. Imbalance leads to a change in frequency which is unwanted. The primary control wants to bring the system back to stable conditions. For example, if the load in the grid increases, the frequency will drop. The generated power does not instantly increase, and compensation from kinetic energy from the rotating generators is needed. This leads to a decrease in the velocity of the generator. The governor(speed controller) increases generated power to recover speed and balance to the system [22]. The primary control response time is 0 to 30 seconds, and it is operational for 15 minutes [23].

Secondary control: Frequency restoration reserves (FRR) brings the frequency back to its nominal value and restores the power reserve of the generators used for the primary frequency control [22]. It has a response time of 30 seconds and can last 120 minutes.

Tertiary control: Manually frequency restoration reserves (mFRR) or replacement reserves. mFRR is executed on request from the grid operator [24]. It shall restore the power reserve of the generators used for the secondary frequency control [22]. The response time is 15 minutes.

A negative consequence of flexibility is load rebound. Load rebound is an unwanted power peak that occurs when the consumer compensates for the previous outage or resets the load state. For example, if many users take advantage of the flexibility of the EWH and turn them off to avoid the power peaks at a given the time of day, their EWH eventually needs to turn on, which leads to new power peaks. This phenomenon may mislead grid operators to make non-optimal regulations. One solution to this is to flatten the load profile of end-users [25].

2.3.2 Flexibility of EWHs

EWHs are perfect for storing energy because of the high heat capacity of water. High heat capacity means storing more energy per mass at a given temperature than other substances such as air [7]. An EWH is also insulated, which further increases the heat capacity and reduces energy loss. Minor loss in energy enables the possibility of turning off the EWH in given periods while the water temperature is still at a desirable level. The EWH can be switched on and off in seconds, and heating patterns can change without loss in comfort [12]. This makes an EWH flexible. The operation of an EWH is highly dependent on the lifestyle of consumers. The number of showers, length of showers, and time of day of showers depend on the user. Therefore, the consumers are set to significantly impact the flexibility aspect of an EWH [26].

There are several projects today where smart, flexible EWHs are used to support the strain on the grid, like reducing power peaks and optimizing costs for system operators and consumers. There is, among others, a project in Gjøvik where Elvia and OSO Energy collaborate on a pilot project where 20 households with smart EWHs are analyzed [27]. The results are good, and OSO smart water heaters will be available in 2022. The Norwegian company Høiax has also developed a smart hot water tank in collaboration with Futurhome, and NxTech [28]. The smart water heater is named Høiax CONNECTED. Both Høiax CONNECTED and OSO Charge enable the opportunity of control via an application. This application enables cost savings as the user can use the water heater as energy storage when power prices are high and recharge the storage when prices are low. The water heaters could avoid heating when prices are high [29] [30]. A smart water heater costs around 5000 - 7000 NOK more than a standard water heater. Enova gives up to 5000 NOK in support of buying a smart water heater. There are also possible to install smart metering on already installed water heaters. This will also give financial support by Enova [31]. Tibber sells products that make it possible to control high-power units, such as water heaters. This makes it possible to remotely turn on and off the power of the water heater [32].

Several projects abroad, such as Tucson Electric Power in Arizona, use solar power plants to heat water heaters when the energy demand is low, and plenty of solar energy is available [33]. This provides cheap power to customers and works as a grid service for the system operators. There is also a project by Bonneville Power Administration where 600 homes can participate in a similar project with the same goal of reducing power peaks by utilizing a smart EWH. The EWH will respond to demand response signals [34]. Smart water heaters and smart controllers are available from several suppliers in response to these projects' good results. Rheem [35] and Aquanta [36] are some manufacturers introducing new smart technology for water heaters.

2.4 Water heaters

Water heaters are standard units in households. There are several types of water heaters, such as

conventional storage-tank water heaters or tankless water heaters. These heaters use electricity or gas as an energy source.

2.4.1 Design and operation of water heater

Figure 6 shows the main components of an electric water heater. EWHs are insulated to prevent loss of energy. Cold water flows into the bottom of the tank, and hot water flows out of the top of the tank. The exchange of water happens in the mixing valve. The water is heated by heating elements placed in the tank. The number of heating elements usually varies from 1 to 3. A thermostat can adjust the set-point temperature of the heating element, which decides the temperature of the water in the tank. There is also a pressure relief valve and a safety valve/drain valve. The pressure valve is needed to ensure that pressure does not exceed the given limitations of the tank. A safety/drain valve is used to empty the tank when maintenance is needed [37].

The EWH wants to maintain the water temperature at the set-point temperature. In the manufacturer settings, the set-point temperature usually is 75°C . It is possible to change the set-point temperature between 60°C and 90°C . The tank has a built-in ΔT which defines the tank's upper and lower temperature limit. This ΔT depends on the set-point temperature. If the set-point temperature is 75°C and the ΔT is 5°C , the tank could have an upper limit on temperature of 77.5°C and a lower limit on temperature of 72.5°C . It is also possible to have an upper limit of 75°C and a lower limit of 70°C . The ΔT may also vary for different set-point temperatures. It can be 1°C for a set-point temperature of 60°C and 5°C for a set point temperature of 85°C . The heating element in the EWH is either on or off. If the water heater has a 3kW heating element, the EWH will heat the water at maximum power until the temperature reaches the desired temperature. Temperature sensors register the temperature of the water in the tank. The heating element turns on when the temperature has decreased to the lower limit. The heating element will turn off when the desired temperature level is reached.

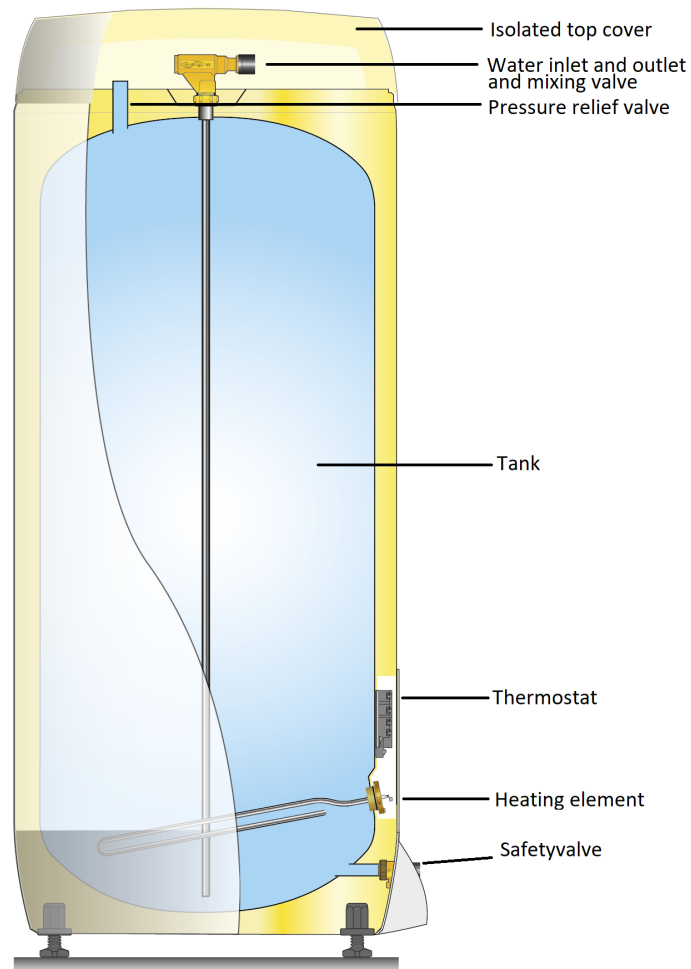


Figure 6: Illustration of electric water heater [38].

The general formula for heating an EWH:

$$E = \frac{V \cdot C_w \cdot \Delta T}{t} \quad (1)$$

where:

- $E = (\text{kWh})$
- $V = \text{Volume of tank } (m^3)$
- $C_w = \text{Specific heat capacity of water } (\frac{\text{kJ}}{\text{°Ckg}})$
- $\Delta T = \text{change in temperature } (^\circ\text{C}) \text{ from start temperature to set point temperature}$
- $t = \text{Time (h)}$

The most standard water heater in Norway is the OSO Saga water heater. There are several sizes of the OSO Saga. The water heater used in this thesis is also an OSO Saga water heater. The most common isolation material is glass wool, Glava. Table: 2 shows the specific heat capacity of some isolation materials.

Table 2: Isolation materials and their specific heat capacity [39].

Type Insulation	$C(\frac{kWh}{^{\circ}Ckg})$
Rock wool, glass wool	0.000286
Plastic insulation (EPS, XPS, PUR)	0.000403
Foam glass	0.000278

2.4.2 Restrictions due to legionella

To avoid the development of the legionella bacterias, it is essential to have the hot water tank at a set-point temperature above $60^{\circ}C$. Temperatures of $20 - 55^{\circ}C$ are critical when considering the growth of legionella bacterias. Following measures should be maintained according to FHI [40]:

- Hot water temperature of minimum $60^{\circ}C$
- Cold water temperature of maximum $20^{\circ}C$
- Good water circulation
- Opportunity for cleaning and disinfection

The EWH can operate in the critical temperature zone for short periods, but the growth of Legionella can occur after only a few days in the temperature zone of $20 - 55^{\circ}C$.

2.5 Data Communication

Data communication systems are necessary for smart houses and homes where smart/flexible solutions are implemented. An application that makes it possible to control and communicate with the system is needed. In the application, the user can control and monitor the system. Further, there is a need for switches and sensors, making smart/flexible solutions possible. A solution can be smart light that dims or turns on/off by itself or a flexible EWH. There are often several interfaces interconnected in the smart house. This is because many companies specialize in smart solutions. For example, DALI (Digital Addressable Lighting Interface) focuses on lights. KNX is a standard that focuses on a broader amount of electrical instruments. A control system is needed to control and interconnect the components in the smart house. These control systems need to understand several types of interfaces due to the different suppliers.

2.5.1 Logic Machine

Logic Machine is developed by Embedded Systems, a control system and a central unit of the data communication system. The primary purpose of the logic machine is its network interface. It has an online application that gives a complete overview of the equipment connected to the machine. The Logic Machine can also be programmed in the way the user desires. The logic machine supports the KNX system and other interfaces and works as the system's "brain." It sends and receives information to and from the different units connected to the machine. The Logic machine gives a logical name to every unit connected, which simplifies the system [41].

2.5.2 KNX

KNX is an open standard for building automation both commercial and domestic buildings. KNX is an intelligent way of managing heating, lighting, and access control systems. This is a way of efficiently using energy [42]. With KNX, every device in the building can be interconnected, making it possible to get a complete overview of the installations [43].

3 Literature Review

This section is based on the literature review written in the project thesis [2]. The section is reviewed and modified, and additional content has been added.

This section will review previous work on grey-box modeling based on thermal-electric equivalent circuits, and electric water heaters as a flexible load will be investigated.

3.1 Grey box modelling

To understand the grey-box modeling, a description of both black-box and white-box modeling is necessary. A physical model with parameters of physical significance describes a white-box model. The white-box model is also referred to as a clear-box or open-box model because it has full physiological knowledge of the system [44]. The negative part of white-box modeling is that it is often hard to derive the physical parameters. The model is also complicated due to its differential equations [45] [46]. A black-box model has its name from the lack of insight into its internal workings. Black-box models are based purely on the analysis of measured data. This model's inputs are known, and the following outputs are observed. It is then possible to map the outputs when trying several different inputs [47], [45]. Black-box modeling is technically tricky and highly dependent on the availability of appropriate inputs [48]. Grey-box models refer to a combination of black-box and white-box modeling. The Grey-box model is partially theoretical and data-driven [49] [45]. It uses stochastic differential equations and combines the advantages of white-box, and black-box modeling [48].

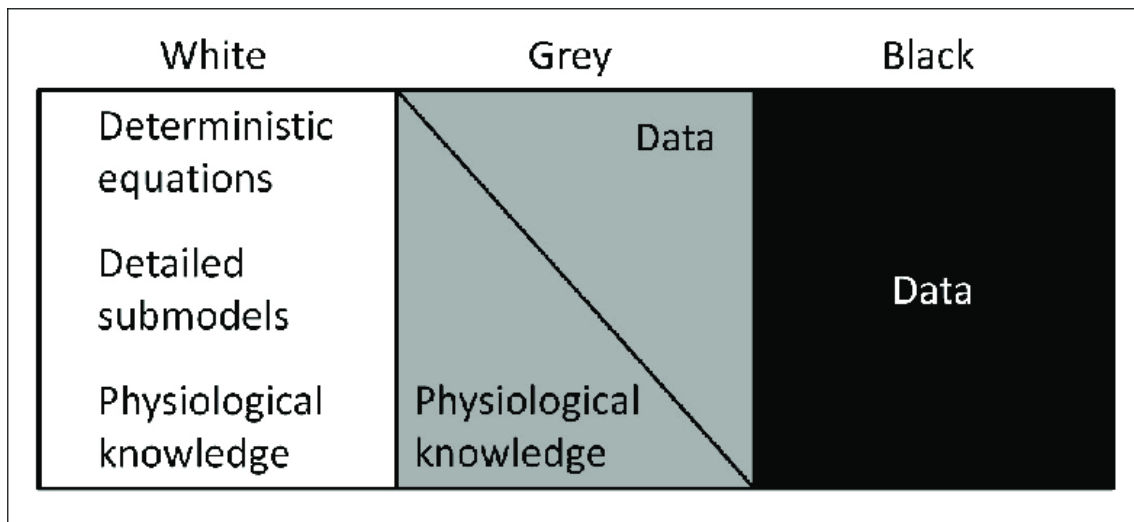


Figure 7: Illustration of the concept of grey-box modelling [50].

The grey-box model can be used with a thermal-electric equivalent. The thermal-electric equivalent uses an electrical analogy to quantify and analyze the thermal behavior. These equivalent circuits use resistance-capacitance networks (RC-circuits). A thermal system that is constructed using electrical component values enables the derivation of the necessary differential equations based on simple electric circuit analysis. The electrical resistance and capacitance are parameters needed to solve these differential equations. These values can be obtained by performing parameter fitting [51], [52], [50].

3.1.1 Thermal equivalent model

The analogy between the thermal behavior and electric circuits makes the transformation between the two systems possible. Figure 8 shows this analogy, which is presented in Table 3.

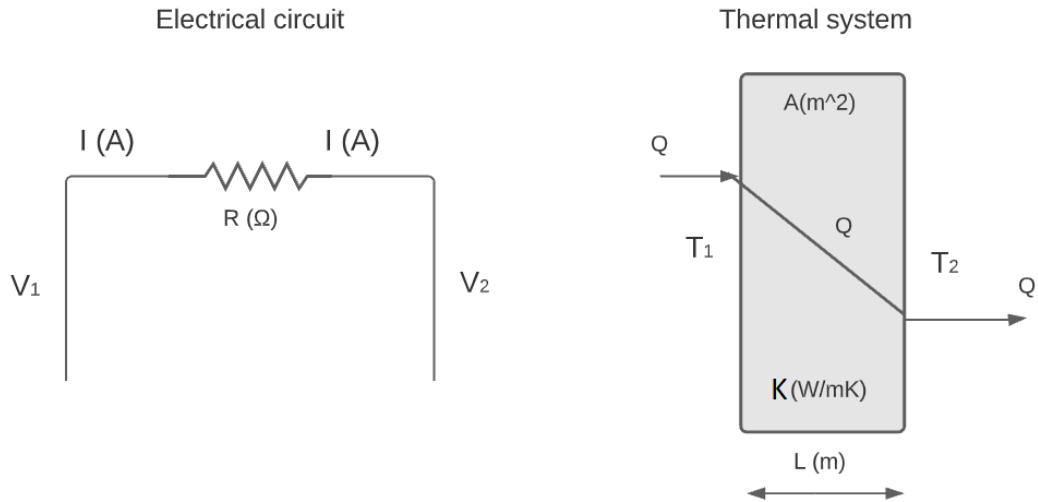


Figure 8: Analogy between the electrical circuit and the thermal model.

In the electrical circuit, to the left, V_1 is assumed to be greater than V_2 . The current will flow from left to right due to potential differences. This gives the following correlation known from ohms law:

$$I = \frac{(V_1 - V_2)}{R} \quad (2)$$

In the thermal system (to the right), a wall with thickness L (m) is considered. The Thermal conductivity of the wall is given as K ($\frac{W}{mK}$). The area of the wall is given as A (m^2). There are two different temperatures on each side of the wall. T_1 is here greater than T_2 . The heat-flow Q always goes from the highest to the lowest temperature. This gives the following equation:

$$Q = \frac{(T_1 - T_2)}{\frac{L}{KA}} \quad (3)$$

When comparing the 2 and 3, the analogy between the electric circuit and the thermal behavior can be observed. Table 3 presents analogies between thermal and electrical systems [52].

Table 3: Analogies between thermal and electrical systems.

Thermal	Electrical
Thermal resistance, $\frac{L}{KA}, R_{Th}[W/K]$	Electrical resistance, $R_{el}[\Omega]$
Temperature, $T[K]$	Voltage, $U[V]$
Heat Transfer, $Q[W]$	Current, $I[A]$
Thermal Capacitance, $C[J/K]$	Electrical capacitance, $C_{el}[F]$
Steady Heat Conduction. Relationship Between Temperature And Heat Flow, $\Delta T = Q \cdot R$	Ohm's Law, $\Delta U = I \cdot R_{el}$
Thermal Capacitance. Relationship Between Heat Flow and Change In Temperature, $Q = C \frac{dT}{dt}$	Current Through Capacitor, $I = C \frac{dV}{dt}$
Heat Balance	Kirchoff's Current Law

The thermal-electrical model can be categorized as circuits with a given amount of resistors and capacitors, such as $1R1C, 2R2C, \dots nRkC$. The resistors represent thermal resistance, and the capacitor represents thermal capacitance. Thermal capacitance measures how much heat the object can store. Other parameters in the RC-circuit can be inputs, such as a power source or a temperature source [53]. There can also be disturbances in the model, such as solar gains or draft. With an increase in resistances and capacitors, the complexity of solving the system enhances, but the model's accuracy often improves [45].

An example of a thermal-electric circuit is the model of an insulated water tank that is heated. R_{wall} is defined as the thermal resistance in the water between the ambient and the enclosure. The water in the tank has a thermal capacitance C_{water} because the enclosure can store heat. The water temperature is T_{water} , and the ambient temperature is $T_{ambient}$. It also flows heat into the enclosure, stated as Q . The system will have a physical setup as left in Figure 9 and have the thermal-electric model as shown to the right.

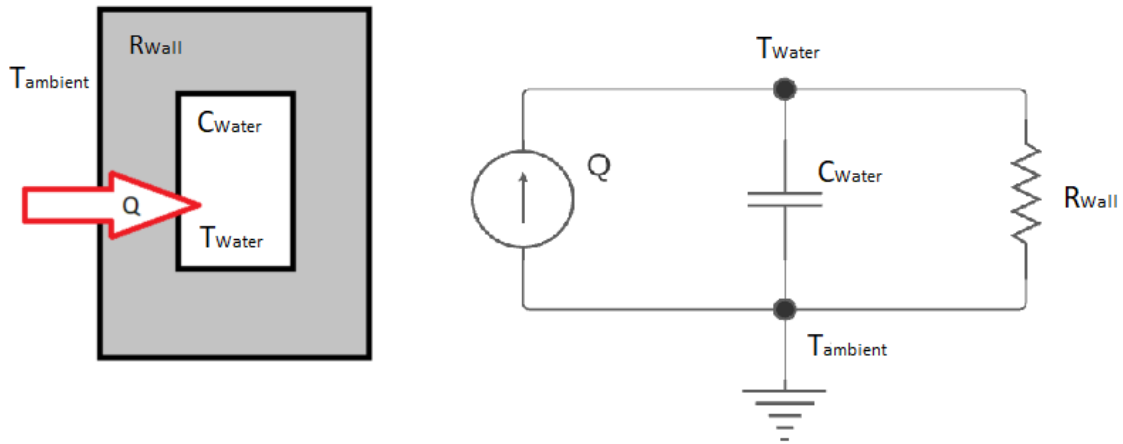


Figure 9: Heating of insulated enclosure (left) and its electric equivalent circuit between electrical circuit and thermal model (right).

Q = Heating element. T_{water}^* = Temperature of the water. $T_{ambient}$ = Temperature of the ambient C_{water} = heating capacity of water R_{wall} = Thermal resistance in wall

The capacitance needs to be connected to the earth. This connection point equals the reference temperature. The heat into the system is shown as a temperature source (Q). The temperature

in the ambient and the temperature in the water tank are measured and therefore need a node. The system is a parallel connection between heat, resistance, and capacitance. Figure 9 shows the thermal-electric equivalent of the system.

When the thermal-electric equivalent is obtained, the differential equations can be established. The general form of the differential equation used in a stochastic-differential-equation-based model is on the form [50]:

$$dx_t = f(x_t, u_t, t, \theta)dt + \sigma(u_t, t, \theta)d\omega \quad (4)$$

$$y_k = h(x_k, u_k, t_k, \theta) + e_k \quad (5)$$

Equation 4 describes the dynamics of the states of the system. It is separated into two parts, $f(x_t, u_t, t, \theta)$ = drift term and $\sigma(u_t, t, \theta)$ = diffusion term (approximations and noise from disturbances). Including u_t that represents inputs while θ represents the parameters. Equation 5 describe the observation equation and e_k represents an error [50].

To be able to find the equations, it is necessary to decide on a base node. Looking at the node called T_{water} , one can find the equations by looking at the currents entering and leaving this node. Kirchhoff's current law (KCL) states that the algebraic sum of all currents entering and exiting a node must equal zero. The differential equation of the system, described in Figure 9, will look like the following:

$$dT_{Water} = \left(\frac{\dot{m} \cdot c_w}{C_{water}} (T_{in}(t) - T_{water}(t)) + \frac{T_{ambient} - T_{Water}}{R_{Wall} C_{Water}} + \frac{\dot{Q}}{C_{Water}} \right) dt + ed\omega \quad (6)$$

The first part of the equation describes the water leaving the tank. The second part of the equation describes the heat loss of the tank. The third part describes the heat added to the system. The last part describes the error.

Expanding the model by bringing more resistors and capacitors to the system is possible. When expanding the model, it becomes more complex and precise. The derivation of a 2R2C-model and a 3R3C-model is located in Section 6.

3.1.2 Continuous Time Stochastic Modelling in R

When the equations are decided, CTSM-R is used for parameter fitting. It uses the equations obtained in the thermal-equivalent model and estimates the unknown parameters, like resistance and capacitance. CTSM-R is open source and developed by DTU Compute. CTSM-R, or Continuous-Time Stochastic Modelling for R, is a tool for identifying and estimating partial observable models using real-time series data. CTSM uses the known data, such as temperature and power input, to estimate the unknown parameters. These parameters are obtained using the maximum likelihood theory. CTSM is an additional package in R, and the modeling is referred to as grey-box modeling. CTSM-R can handle both non-linear and linear models. Its basic structure consists of a continuous-time stochastic differential equation and a discrete-time observation of underlying physical systems. The differential equation is a physical description of the system [54].

3.2 Parameter fittings of academic papers

The section presents seven different papers that all look at parameter fitting. These build a basis for parameter comparison.

Reference [51](Svendsen Master) establishes the flexibility potential of EWHs. To collect necessary data for parameter fitting, experiments are performed at the NTNU Smart House Lab. The set-point temperature was $75^{\circ}C$ and there was no water removed from the tank. The thermal-electric model used in this work is a 1R1C and a 2R2C model. With parameter fitting, the following R and C values were calculated for the 1R1C model: $R = 286.6 \frac{\text{C}}{\text{kW}}$ and $C = 0.17 \frac{\text{kWh}}{\text{C}}$. Following R and C values were calculated for the 2R2C model: $R_{wa} = 232.5 \frac{\text{C}}{\text{kW}}$, $R_{ww} = 50.74 \frac{\text{C}}{\text{kW}}$ and $C_{water} = 0.172 \frac{\text{kWh}}{\text{C}}$ and $C_{wall} = 0.00213 \frac{\text{kWh}}{\text{C}}$.

Reference [2] (Project thesis Løvstakken) has the same lab setup as Reference [51], Svendsen. The project thesis uses CTSM-R to obtain the unknown parameters. A 1R1C-model is used, and no water is removed from the tank. Using grey box modeling, the following R and C values are estimated: $R = 296 \frac{\text{C}}{\text{kW}}$ and $C = 0.157 \frac{\text{kWh}}{\text{C}}$.

Reference [6](Lakshmanan) finds flexibility potential of EWHs. The authors use a first-order differential equation-based EWH-model to calculate flexibility activation time. The water heaters used in this work have a capacity of 200 Liters and a power rating of 2kW. The temperature settings are $70 - 75^{\circ}C$. This reference also used a 1R1C thermal-electric equivalent circuit. The unknown parameters are calculated to be $C = 0.335 \frac{\text{kWh}}{\text{C}}$ and $R = 600 \frac{\text{C}}{\text{kW}}$. The heat demand curve used in this paper varies a lot during the day. The EWH has high heat demand between 7 and 9 in the morning and quite high heat demand in the afternoon and evening. It is noticeable that the EHW is used actively throughout the day.

Reference [55](Yu) establishes an optimized schedule of EWH operation to minimize the electrical bill. A thermal-electric equivalent circuit of an EWH is established, and CTSM-R is used to find necessary parameters. The EWH analyzed in this paper is approximately 2.8 kW and has a volume of 92 Liters. The predefined temperature zone is $25^{\circ}C - 80^{\circ}C$. The paper compared four models, T_i , T_iT_h , T_iT_e and $T_iT_hT_e$. This refers to single-, two- or three-stage models, or 1R1C, 2R2C or 3R3C models. Subscript i refers to inside tank, subscript h refers to the heating element, and subscript e refers to EWH envelope. The authors concluded that the $T_iT_hT_e$ model was the best due to better properties and less root-mean-square error than the other models. Parameters were obtained for C (heat capacity of water inside the tank) and R (wall resistance). All four models have $C = 0.1069 \frac{\text{kWh}}{\text{K}}$ but some difference in R values. For T_i $R = 1055 \frac{\text{K}}{\text{kW}}$. For T_iT_h $R = 929 \frac{\text{K}}{\text{kW}}$. For T_iT_e model $R = 1017 \frac{\text{K}}{\text{kW}}$ and for $T_iT_hT_e$ model $R = 1004 \frac{\text{K}}{\text{kW}}$.

In Reference [56] (DTU), a solar thermal collector using a domestic hot water tank to store energy. The tank has three heating elements of 3 kW each and a volume of 788 Liters. The method presented in the paper also uses CTSM to estimate parameters. Their parameters were $C = 1.0781 \frac{\text{kWh}}{\text{K}}$ and $UA = 8.29(\pm 0.0278) \frac{\text{W}}{\text{K}}$. UA equals U-value times area and needs to be inverse to find the desired parameter, namely R. $R = 120.627 \frac{\text{K}}{\text{kW}}$.

Reference [48] uses economic model predictive control to optimize the electricity cost of a three storage house. CTSM-R is used with a total of 6 differential equations to find unknown parameters. This article considers the heat capacity of air and thermal resistance of walls, which gives different values for C and R, but the method used is similar to the other articles. Reference [57] research optimal control of an HVAC system and use the same method as the above paper. It states 4 differential equations. These papers show that the method is usable for several thermal systems.

3.3 Flexibility potential of EWH

The total electricity consumption of an EWH equals 20 % of the building's total electricity consumption [58]. Moving this load away from power peaks is vital for the future development of the power grid and will be financially favorable for both consumers and distributors. With the new grid tariff structure, end-users will experience a noticeable change in expenses if they can shift their EWH away from power peaks. The new grid tariff structure motivates smart technology and energy storage to reduce power peaks in the grid. Incentives to invest in smart technology and energy storage leads to the development of flexibility management. A flexible EWH that controls consumption away from power peaks can be essential with the new grid tariff structure [59].

Several articles have researched the flexibility of an EWH. Reference [12], NVE, evaluates a European case. The EU's daily controllable storage capacity equals the storage capacity of 3 million Nissan Leaf batteries. In numbers, this is equal to 20 GW daily flexible capacity and 120 GWh daily storage capacity. The reference also states that one tank of 200-liter capacity and 2 kW heating element has a capacity of 14 kWh. A 300 liter, 3 kW EWH has a capacity of 21 kWh. Reference [51], Svendsen, estimates a population of 12 EWHs to shift a load of 7kWh during one hour. Reference [6], Lakshmanan, introduces a model that uses a population of 1000 EWHs, and the authors calculate the flexibility potential and rebound rates. They conclude with a maximum flexibility potential of 53.9% but will lead to a rebound of 60%. With the flexibility of 13.5%, the total rebound will be 15%. Reference [55], Yu, optimizes the energy cost of an EWH and concludes with a savings of 11.965 %. Reference [56], Halvgaard, states an economic model predictive control which gave savings in electricity cost of 25 – 30%.

Demand response is the change of power consumption to match the demand and the supply. An EWH can store energy, and by load shifting, it is possible to adjust the demand to fit the supply. Reference [60], Saele, shows that the potential for demand response of an EWHs is 0.6 kWh/h, and if half of the Norwegian households use remote load control on their EWH. A total of 600 MWh/h demand response is possible.

The EWH can be used in frequency regulation by storing energy, using more energy when the frequency is high, and avoiding using energy when the frequency is low. Reference [61], Haider, states that when the frequency is high, the water heater can heat the water in the tank to a higher temperature. The frequency will be reduced, and energy will be stored in the tank. Reference [6], Lakshmanan, states that EWHs flexibility activation can serve as FCR at peak demand hours with high ramp-up and ramp-down rates of 48.5% and 23.8% per minute and as FRR during non-peak hours.

According to NVE, EWHs can also contribute to voltage control in the power grid as they can react fast, provide up and down-regulation, automated response and are a highly distributed resource. Voltage control is necessary as equipment connected to the grid has specific operating ranges. EWH can be used in grid capacity management by shifting the loads in the power grid, as shown in Figure 5. EWH can also be used in congestion management, using the power available without violating system constraints [12].

4 Experimental Setup

The section is based on the equivalent section written in the project thesis [2]. The section is reviewed and modified, and theory has been added.

During the expansion of the lab setup, a weakness was discovered in the already existing lab setup. The surrounding air temperature influenced the temperature sensor used in the project thesis. This temperature sensor is called T_{low} . Insulation was used to improve this. The lab equipment and setup are described in this section.

4.1 Smart House

The Smart House Lab at NTNU is a part of the National Smart Grid Laboratory. It is accessible by both business and research communities. The Smart House has equipment like a regular Norwegian household, i.e., shower and washing machine. It also has advanced measurement and control equipment, enabling it to control and monitor all the equipment installed. The function of the laboratory is to research the electrical loads in the smart house. It is also used to research the future digitized power markets where interaction between production, power grid, and end-user is essential. The laboratory is used for research, demonstration, verification, testing, and instruction of future electrical solutions [62].

There is no remotely controlled equipment in the existing lab. Set-point temperature, on/off-state, and power measurements must be initialized/changed manually. The lab is a working bathroom, meaning other people can influence the measurements. The shower and washing machine in the bathroom is sometimes used by NTNU employees and could disturb the measurements. The EWH is connected to either TN or IT network. It is only the TN network that is measurable. Weeks of experiments were lost when plumbers changed connections during maintenance and installation of new equipment. It was unfortunate, but the new equipment improved the measurements drastically.

4.2 Control system

To be able to take advantage of the equipment, a control system is needed. This will tie every piece of equipment together. The control system used at the NTNU Smart House Lab is a Logic Machine 4. The PC in the lab is connected to the router, which is connected to the Logic Machine4. LogicMachine is used to read the temperature data from the logic machine. It is developed by Embedded Systems and accessed by typing the IP address in the web browser's tab. In LogicMachine, every KNX-device is visible and has its logical address. There are several addresses used in this specific lab.

- 5/1/0(Bathroom/Temperature/lower EWH)
- 5/1/1(Bathroom/Temperature/Inlet Water)
- 5/1/2(Bathroom/Temperature/Outlet Water)
- 5/1/3(Bathroom/temperature/inside EWH)
- 5/1/4(Bathroom/temperature/inside EWH)
- 5/1/5(Bathroom/Watermeter/Watermeter)
- 5/2/2(Bathroom/Temperature/Bathroom)

Logic machine enables to view trend logs of the different KNX equipment. LogicMachine has a measurement interval of 5 minutes.

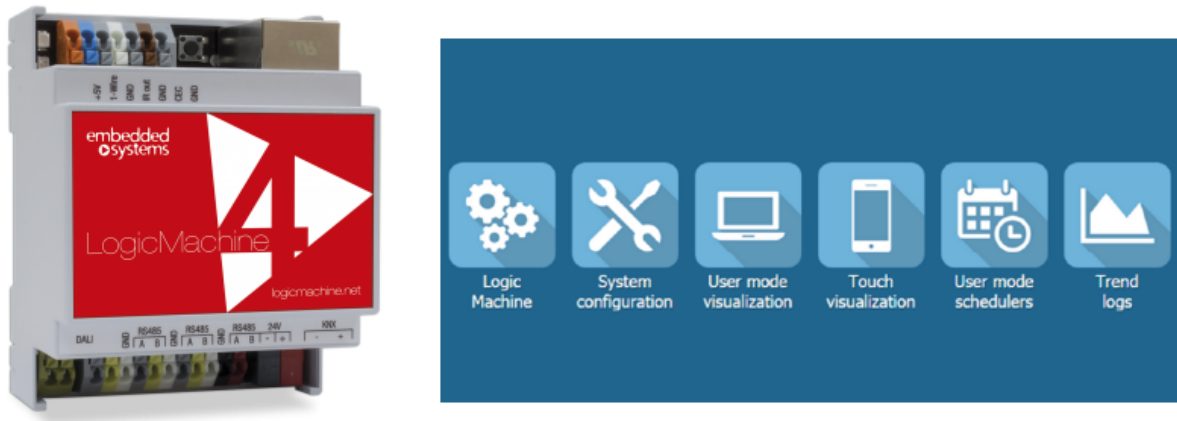


Figure 10: Logic Machine 4 (to the left) and LogicMachine application interface (to the right).

4.3 Equipment

The experiments performed at the NTNU Smart House Lab will use the EWH with attached temperature sensors, power meter and volume flow meter. Table 4 shows the equipment is used in the lab.

Table 4: List of equipment used in the smart house.

Producer	Model	Interface	Function	Application
Embedded Systems	Logic machine 4	KNX, Modbus Bac-net, ENOcean, DALI, 1-Wire	Controls	LogicMachine
Schneider Electric	MTN647895	KNX	Relay	-
ASUS	RT-AC3200	USB, ethernet	Wireless Router	-
OSO Hotwater	S300 - 3kW/1x230v SAGA heater	-	Water heater	-
DENT Instruments	ELITEpro XC	USB, ethernet	Power meter	ELOG 15
Lingg and Janke	GWF Multi-JET WATER METER	KNX	Water meter	-
Arcus	SK10-TC-HTF	KNX	Temperature sensor	-
Arcus	SK10-TC-ALTF1 contacting/tube sensor	KNX	Temperature sensor	-
Arcus	SK10-TC-ETF3 WITH SCREW-IN	KNX	Temperature sensor	-

4.3.1 OSO Saga S 300 water heater

The OSO Saga S300 water heater is an electrical water heater. It is only used for the bathroom at the smart house. It has one heating element at the bottom of the tank with a power rating of 3 kW. OSO Saga S300 was the best-insulated water heater when introduced in 2017 [19]. The ΔT of the tank is variable with the set-point temperature. A smaller set-point temperature gives a smaller ΔT . Table 5 presents technical data of the water tank [37].

Table 5: Technical data of OSO Saga S300 water heater.

Product code	S 300 - 3kW / 1x230 V
Capacity (persons)	5.5
Capacity (L)	281
Factory thermostat setting ($^{\circ}C$)	75
Time to heat the water to 65 $^{\circ}C$ (h)	7.2
Heating elements	1

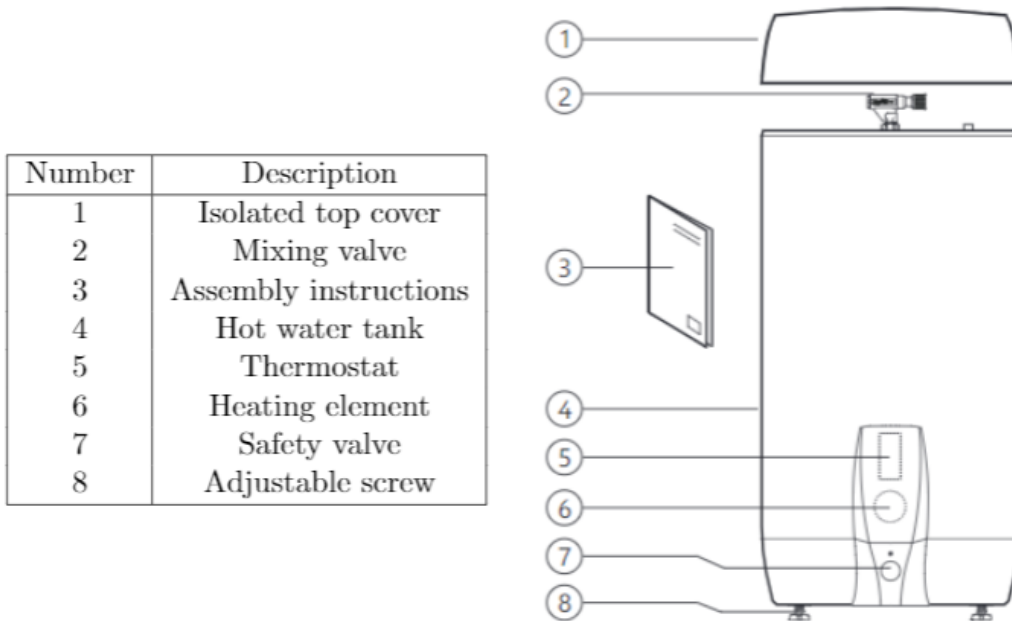


Figure 11: OSO S300 Water Heater schematics [37].

The thermostat located at point 5 in Figure 11 will be adjusted to obtain different temperatures. The temperature is manually adjusted using a screwdriver. The temperature can be set between $60^{\circ}C$ and $90^{\circ}C$. Figure 12 shows design of thermostat.

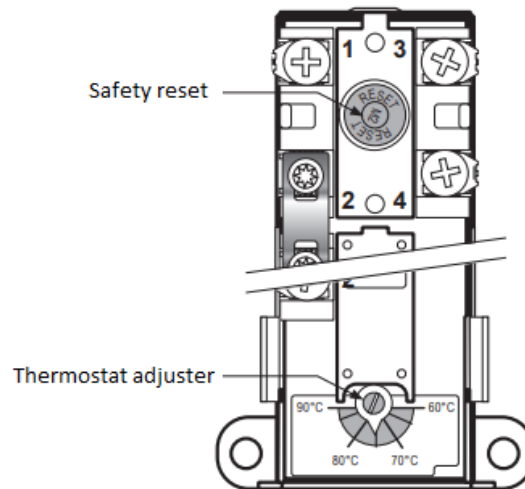


Figure 12: Illustration of thermostat [37].

4.3.2 Temperature sensors

Six temperature sensors are fitted at different places surrounding the tank. There are two temperature sensors on the water tubes connected to the EWH. One measures the temperature of the outlet water, T_{out} , and one measures the temperature of the inlet water, T_{in} . Three sensors measure the temperature inside the tank. T_{lower} is located at the heating element. This is placed on the metal next to the thermostat. This sensor was not insulated, but several layers of Glava is placed on the outside of this sensor. The temperature sensor is located 15 cm from the bottom of the tank. There are two sensors inside the tank. They cannot be fitted simultaneously because they use the same thermowell. T_{upper} describes the temperature sensor in the tank's upper parts. This is placed 10 cm down in the thermowell. T_{middle} is located in the middle of the tank. This is placed 55 cm down the thermowell. One temperature sensor measures the temperature of the room, T_a . This is placed on the wall next to the water heater. The temperature sensors are shown in Figure 13 and Figure 14.



Figure 13: T_{lower} and T_{middle} to the left and T_{in} and T_{out} to the right.



Figure 14: T_{upper} to the left and T_a to the right.

Figure 15 shows the thermowell and its installation point. Figure 16 shows the location of the temperature sensors.

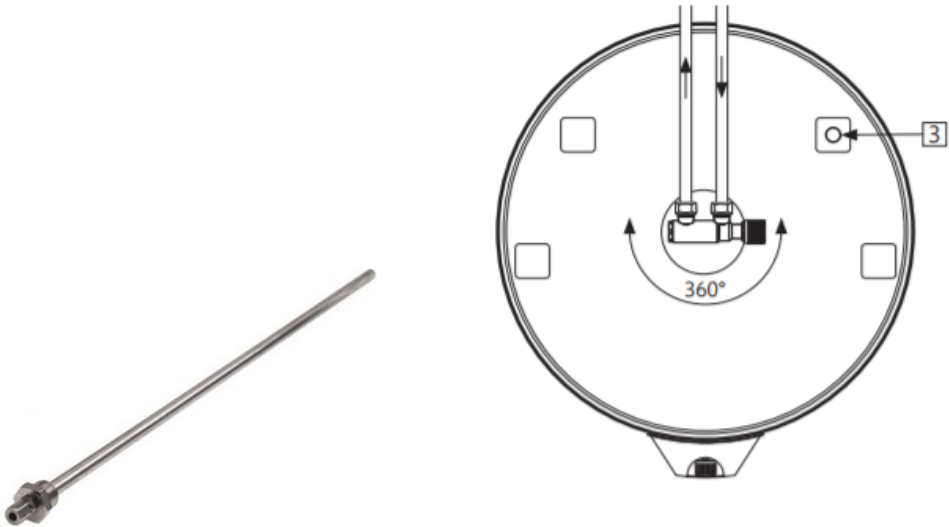


Figure 15: Thermowell to the left and installation point to the right.

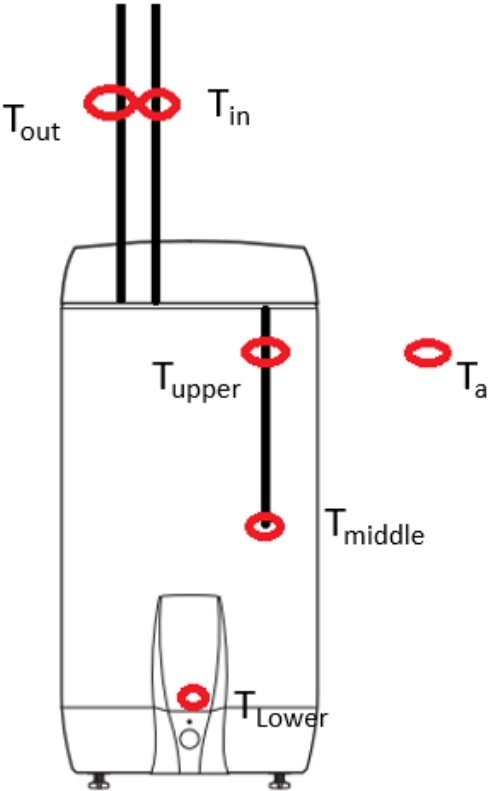


Figure 16: Illustration of the temperature sensors in the tank.

4.3.3 Water flow meter

The water flow meter is installed at the outgoing hot water tube. Figure 17 shows the water flow meter used in the lab. The water flow meter is connected to hot water only. This makes it

possible to observe the amount of water leaving and entering the tank.



Figure 17: GWF Multi Jet Water Meter.

4.3.4 Power meter

A separate system is used to read the power ratings. The power is measured with a power meter called ELITEpro XC. ELITEpro XC uses a clamp and probes to get current and load profiles. The power meter is connected to The PC in the lab by a USB port. To easily read the values gathered by the power meter, an application called ELOG 15 is used. DENT Instruments develop ELOG15. ELOG 15 collects measurements but can also control and specify how the measurements will be performed. It can specify how many measurements we will perform in a given time frame. In these experiments, a 5-minute interval is used. This is to get measurements of the same time profile as LogicMachine. The clamp uses a relationship of 1mV to 1mA and reads on one phase, phase 2, which is the physical power channel that must be specified in ELOG 15. Figure 18 shows the power meter.

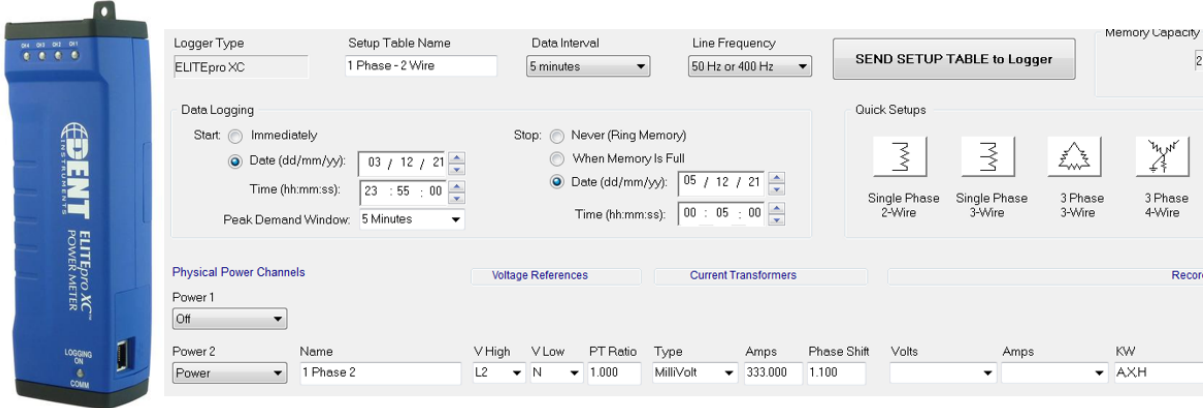


Figure 18: ELITEpro XC (to the left) and ELOG 15 application interface(to the right).

4.3.5 Other Equipment



Figure 19: Asus router RT-AC3200 and Relay MTN647895 from Schneider Electric.

4.4 Physical Setup

Figure 20 shows the physical setup of the lab. Temperature sensors, power meter, and water flow meter enable to obtain temperature and power profiles. A control system controls the system, and the router and the relay are essential to communicate and send signals between different physical components.

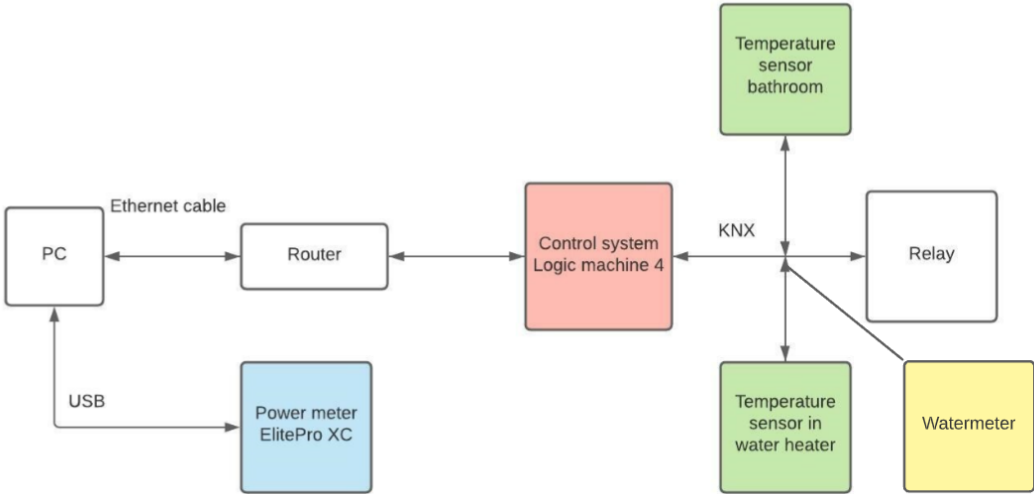


Figure 20: The communication system structure of the Smart House.

Figure 21 shows the installation points of the temperature sensors and the water flow meter.

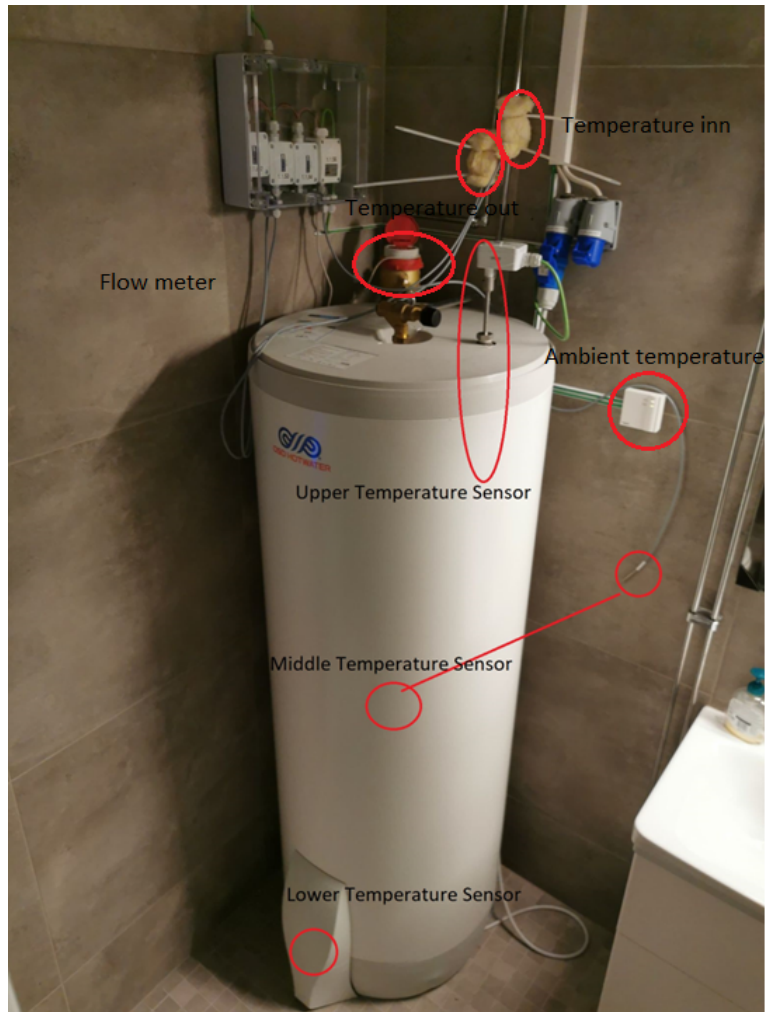


Figure 21: OSO Saga S300 with temperature sensor location.

5 Experimental Method

The experiments address three different cases. The set-point temperature is changed between three different temperatures in all cases. These set point temperatures are 60 °C (minimum temperature), 75 °C (normal factory setting) and 85 °C (maximum temperature). The reason for choosing 85 °C as a maximum is that a set-point temperature of 90 °C makes the fuse blow. To drain water from the tank, the shower is used. The shower is adjusted to 38 °C and drains water at the maximum flow rate. This is chosen as it gives equal water flow during all the experiments. The flow meter measures that the tank uses around 40 liters of hot water every five minutes. Enova estimates 160 liters of water is used per ten-minute shower.

The experiments use different temperature sensors located on/in the tank. This is to see if they give different parameter fittings and if there are some temperature-change delays in the tank's different areas. The lower temperature sensor is always available. The upper and the middle-temperature sensor cannot be used simultaneously because they have to be put into the thermowell, which only fits one sensor at a time. This is manually changed.

5.1 Case 1: Steady state of the EWH at different set-point temperatures

Case 1 considers a scenario where no water is drained from the tank. Case 1 is executed two times. This is because it is desirable to do measurements for three different temperature sensor locations, and only two sensors can be used at the same time. Case 1 is therefore divided into Case 1.1 and Case 1.2. Case 1.1 considers the upper and the lower temperature sensor. It will start with a set-point temperature of 70°C, decrease to 60°C, and then immediately increase to 85°C before returning to the set-point temperature of 75°C. Case 1.2 considers the middle and the lower temperature sensor, and the set-point temperature starts at 85°C, then is adjusted to 60°C and then increased to 75°C. The goal with the different temperature settings is to get a rich dataset.

5.2 Case 2: 3-4 showers a day while the EWH is in on-mode

Case 2 considers a scenario where the water heater is connected to a power source and water is drained from the tank. The middle temperature sensor is used in Case 2. Showers will be taken throughout the day to simulate hot water usage by an average family. Three showers will be taken at the start of the day, then 1-to 2 showers will occur later the same day. The length of the showers varies between 5, 10, and 15 minutes and does not occur at the same hours each day. This is to make a realistic dataset. Experiments will last for three days to see how the tank behaves. Set-point temperatures start at 60°C, then adjusted to 75°C and then adjusted to 85°C the last day.

5.3 Case 3: 3-4 showers a day while the EWH is in off-mode

Case 3 considers a scenario where the water heater is not connected to a power source in the period where water is drained. Case 3 is divided into Case 3.1 and Case 3.2 to test both upper and middle temperature sensor. 1-3 showers occur every day. The length of the showers varies between 5, 10, and 15 minutes and does not occur at the same hours each day. This is to make a realistic dataset. This case is equal to experiment 2, but the EWH is turned off between the first and the last shower every day. This case is performed two times. One for the upper temperature sensor and one for the middle temperature sensor. The set-point temperature of Case 3.1 starts at 85°C, then adjusted down to 75°C, then further down 60°C, and then back

to 75°C again. The set-point temperature of Case 3.2 starts at 75°C , adjusted down to 60°C , increased to 85°C , and then back to 75°C . Case 3.2 does only show the upper temperature sensor. This is because the data file obtained from the lower temperature sensor was damaged due to maintenance in the KNX-system.

5.4 Overview of the Cases

Table 6 shows an overview of the experiments performed at the lab.

Table 6: Overview of the different experiments.

Case	T_{upper}	T_{middle}	T_{lower}	Showers	Set-point temperature	EWH
1.1	X		X	No	75-60-85	On
1.2		X	X	No	85-60-75	On
2		X	X	Yes	60-75-85	On
3.1		X	X	Yes	85-75-60-75	Off in periods
3.2	X			Yes	75-60-85-75	Off in periods

The power ratings are gathered in ELOG 15. The data is stored in CSV-files/xlsx-files. The temperature ratings are gathered from Logic Machine and stored in a separate CSV-file/xlsx-files. The water flow is manually read from the water flow meter. The files are merged on the computer in the lab. The files include 8 columns (time, \dot{Q} , T_{lower} , $T_{upper/middle}$, T_a , T_{in} , T_{out} , Mass of water) with a measurement every fifth minute. Figure 7 shows an example of a data file. The file is sent to the author's personal computer.

Table 7: CSV-file.

t	\dot{Q}	T_{lower}	T_{middle}	T_a	T_{in}	T_{out}	M
0	1.229	73.56	76.256	22.84	54.024	39.76	0
0.083333333	0	73.328	76.328	22.86	52.568	37.144	0
0.166666666	0	73.296	76.296	22.87	47.808	34.9	0
0.249999999	0	73.192	76.192	22.89	43.32	33.248	0
0.333333332	0	72.96	76.16	22.9	39.964	31.784	0
0.416666665	0	72.86	76.136	22.89	37.368	30.708	0
0.499999998	0	72.72	76.072	22.9	35.84	29.812	0
0.583333331	0	72.7	76.112	22.9	34.856	29.176	0
0.666666664	0	72.634	76.024	22.89	34.056	28.544	0
0.749999997	0	72.57	75.96	22.87	34.424	28.032	0
0.833333333	0	72.47	76.024	22.88	33.38	27.612	0
0.916666663	0	72.45	75.976	22.9	32.792	27.28	0
0.999999996	0	72.44	75.944	22.89	32.656	26.992	0

6 Method and Model

The system is represented as an 1R1C, 2R2C and 3R3C-circuit.

6.1 1R1C

The thermal equivalent circuit of the EWH can be represented as an 1R1C-circuit as shown in Figure 22.

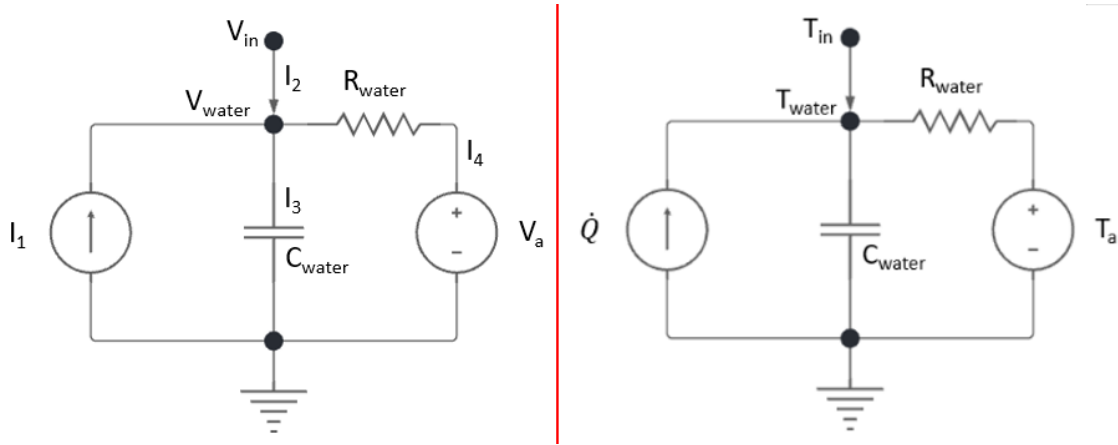


Figure 22: Final RC-equivalent circuit.

R_{water} = Resistance between wall and ambient. V_{water} = Voltage water. T_{water} = Temperature water. C_{water} = Heat capacity of water. A = Current source \dot{Q} = heat source V_{in} = Voltage in T_{in} = Temperature of inlet water I = currents

Heat is added when the temperature drops below a given set-point temperature, as stated in 2.4. This heat is added in \dot{Q} . The water in the EWH can store heat, giving a temperature T_{water} and a thermal capacity C_{water} . Between the ambient and the water in the tank, there is a resistance named R_{wall} .

To obtain the differential equation for the system in Figure 22 KCL is used. Using node V_{water} as a reference, currents into this point must equal the outgoing currents. Current I_1 is the current/heat added to the system, and the current I_2 is the water that flows into the system. I_2 equals $V_{in} - V_{water}$. I_1 and I_2 come into V_{water} and must be equal to the outgoing currents I_3 and I_4 . I_3 equals the current over the capacitor, $C \frac{dV}{dt}$, and I_4 equals the current over the resistor, $\frac{V_{water} - V_a}{R}$. This gives us the following equations:

$$I_1 + I_2 = I_3 + I_4 \quad (7)$$

$$I_1 + (V_{in} - V_{water}) = C \frac{dV_{water}}{dt} + \frac{V_{water} - V_a}{R_{water}} \quad (8)$$

Given this is a thermal-electrical equivalent, it is known that $\dot{Q} = I$ and $T = V$.

$$\dot{Q} + (T_{in} - T_{water}) = C_{water} \frac{dT_{water}}{dt} + \frac{T_{water} - T_a}{R_{water}} \quad (9)$$

It is desirable to look at the equation regarding dT_{water} . It is also important to add the diffusion term, being an error and stated as $\sigma d\omega$. This leads to the following equation:

$$dT_{water} = \left(\frac{\dot{m} \cdot c_w}{C_{water}} (T_{in} - T_{water}) + \frac{T_a - T_{water}}{R_{water} C_{water}} + \frac{\dot{Q}}{C_{water}} \right) dt + \sigma d\omega \quad (10)$$

The observation equation is essential when using CTSM-R. The observation equation gives the model information about the actual parameter values. This makes it possible for the model to perform accurate parameter fitting. The observation equation used in calculations is as follows:

$$YT_{water} = T_{water} + \sigma \quad (11)$$

A comparison between measured and simulated data will be performed to verify the model. This comparison will happen through one-step-ahead plots and simulated-value plots. To obtain simulated data, Equation 10 will be solved using Euler's method. Equation 12 is solved for $T_{EWH}(t + 1)$. This equation finds all T_{water} values by using the initial measured values and parameter fitted values. The equation will iterate through the entire spreadsheet of measured data, making $T_{water}(t + 1)$ into $T_{water}(t)$ in the next iteration.

$$T_{water}(t + 1) = T_{water}(t) + dt \cdot \left(\frac{\dot{m} \cdot c_w}{C_{water}} (T_{in}(t) - T_{water}(t)) + \frac{T_a(t) - T_{water}(t)}{R_{water} C_{water}} + \frac{\dot{Q}(t)}{C_{water}} \right) \quad (12)$$

6.2 2R2C

The literature review indicated that models using more resistances and capacitors gained more accurate results. The following thermoelectric model is used in the 2R2C model:

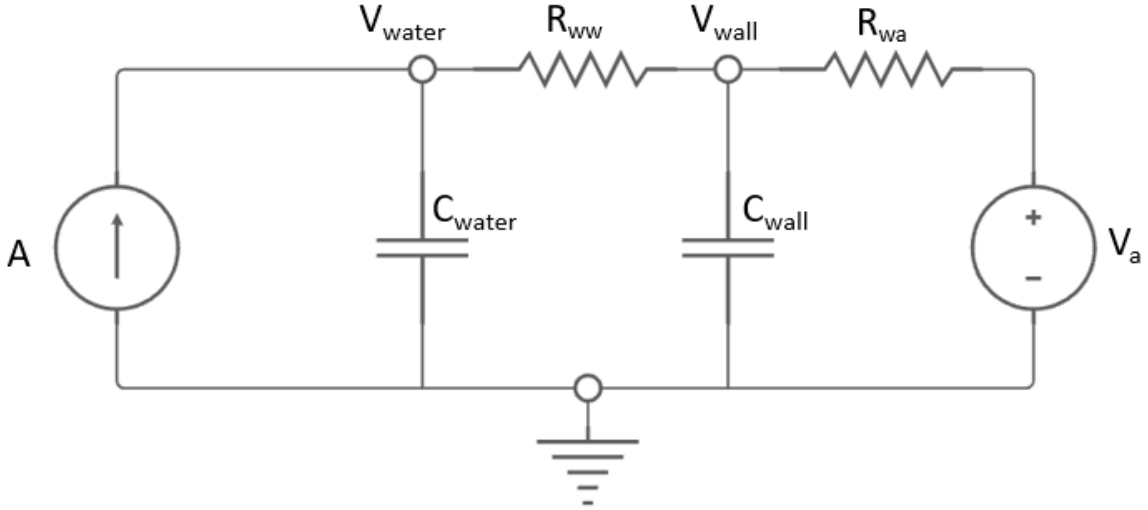


Figure 23: The thermoelectric equivalent of the system.

R_{ww} = Resistance between water and wall. R_{wa} = Resistance between wall and ambient. V_{water} = Voltage water. V_{wall} = Voltage wall. C_{water} = Heat capacity of water. C_{wall} = Heat capacity of wall. A = Current source V_a = Voltage source

This model is expanded with one more R and one more C. It is the same system, but the water and the ambient are further divided with a wall. It is not just one resistance between the water and the ambient, but there is a water-wall resistance and a wall-ambient resistance in this system. It is also a specific heat capacity for water and a specific heat capacity for the wall. This is the same approach as previous work, stated in reference [51].

In the 1R1C model, KCL is used to obtain the differential equations for the system. The currents flowing in and out of node V_{water} and node V_{wall} must be the same.

When looking at node V_{water} , currents I_1 and I_4 equals the currents I_2 and I_3 . This is almost the same circuit as the 1R1C model. I_1 equals the heat added to the system and I_4 equals the water flowing into the system, given as $V_{in} - V_{water}$. Current I_3 is the current through R_{ww} , given as $\frac{V_{water} - V_{wall}}{R_{ww}}$. The current I_2 is the current through the capacitor, given as $C \frac{dV}{dt}$. Figure 24 shows the circuit as seen from V_{water} .

$$I_1 + I_4 = I_2 + I_3 \quad (13)$$

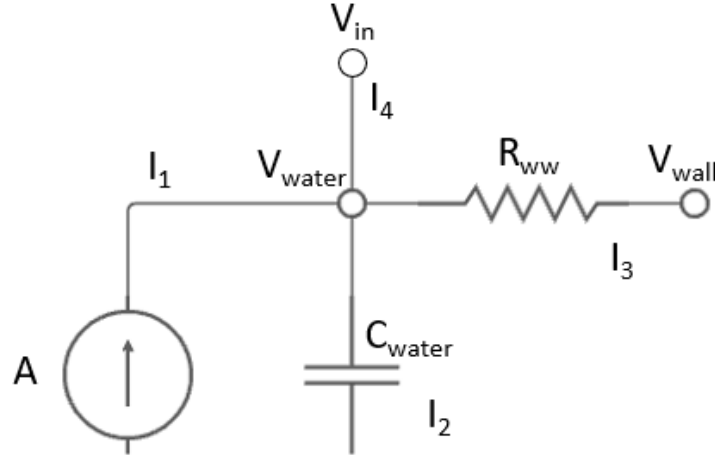


Figure 24: The V_{water} node.

$$I_1 + (V_{in} - V_{water}) = C_{water} \frac{dT_{water}}{dt} + \frac{V_{water} - V_a}{R_{water}} \quad (14)$$

Looking at node V_{wall} , one have to consider three currents. I_3 represents the current through R_{ww} , I_5 represents the current through C_{wall} and I_6 represents the current through R_{wa} .

$$I_3 = I_5 + I_6 \quad (15)$$

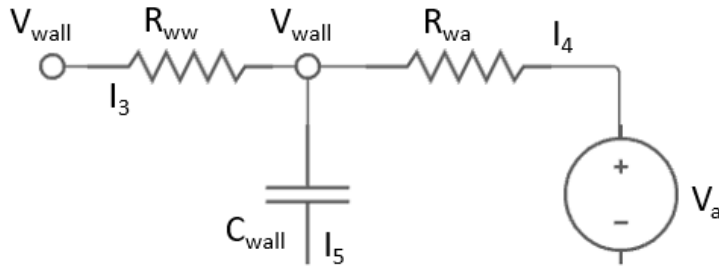


Figure 25: The V_{wall} node

This gives us the following equation:

$$\frac{V_{water} - V_{wall}}{R_{ww}} = C_{water} \frac{dV_{wall}}{dt} + \frac{V_{wall} - V_a}{R_{wa}} \quad (16)$$

The above Equations 14 and 16 are changed to thermo-electric analogy and shown with regard to dT. The diffusion term, $\sigma d\omega$, is added. This leads to the following equations:

$$\frac{dT_{water}}{dt} = \frac{\dot{m} \cdot c_w (T_{in} - T_{water})}{C_{water}} + \frac{T_{wall} - T_{water}}{R_{ww} C_{water}} + \frac{\dot{Q}}{C_{water}} + \frac{\sigma_{water} d\omega}{dt} \quad (17)$$

$$\frac{dT_{wall}}{dt} = \frac{T_{water} - T_{wall}}{R_{ww} C_{wall}} + \frac{T_a - T_{wall}}{R_{wa} C_{wall}} + \frac{\sigma_{wall} d\omega}{dt} \quad (18)$$

The observation equation is the same as for the 1R1C model.

$$Y_{T_{water}} = T_{water} + \sigma \quad (19)$$

Equation 17 and 18 is solved using Euler's to be able to find $T_{water}(t+1)$ and $T_{wall}(t+1)$.

$$T_{water}(t+1) = T_{water}(t) + dt \cdot \left(\frac{\dot{m} \cdot c_w (T_{in}(t) - T_{water}(t))}{C_{water}} + \frac{T_{wall}(t) - T_{water}(t)}{R_{ww} C_{water}} + \frac{\dot{Q}}{C_{water}} \right) \quad (20)$$

$$T_{wall}(t+1) = T_{wall}(t) + dt \left(\frac{T_{water}(t) - T_{wall}(t)}{R_{ww} C_{wall}} + \frac{T_a(t) - T_{wall}(t)}{R_{wa} C_{wall}} \right) \quad (21)$$

6.3 3R3C

The system is also solved as a 3R3C-model. The following thermoelectric model is used:

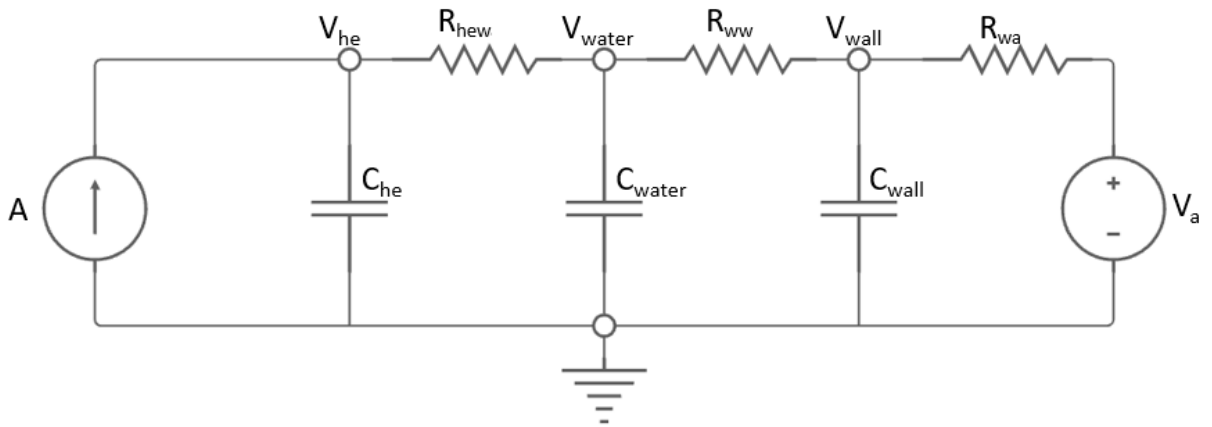


Figure 26: The thermoelectric equivalent of the system.

R_{hew} = Resistance between heating element and water. R_{ww} = Resistance between water and wall. R_{wa} = Resistance between wall and ambient. V_{he} = Voltage heating element. V_{water} = Voltage water. V_{wall} = Voltage wall. C_{he} = Heat capacity of heating element. C_{water} = Heat capacity of water. C_{wall} = Heat capacity of wall. A = Current source V_a = Voltage source

This is the same system as the 1R1C-model and the 2R2C-model. The difference is that it also considers the heating element. This gives another node described as V_{he} . The heating element has a heating capacity of C_{he} . There is a resistance between the heating element and the water, and also a resistance between the water and the wall and between the wall and the ambient. The water and the wall both have their thermal capacities.

To obtain the differential equation for the system in Figure 26 KCL is used. There are three nodes in the model, V_{he} , V_{water} and V_{wall} . The currents flowing into these nodes must equal the currents flowing out of the nodes. The circuit is divided into these three nodes and then analyzed.

The first node, V_{he} , as seen in Figure 27 represents the heating element. I_1 needs to be the same as the two other currents. Current over a capacitor equals, $C_{he} \frac{dV}{dt}$ and current over the resistor equals $\frac{V_{he}-V_{water}}{R_{he}}$. Equation 23 shows the complete equation.

$$I_1 = I_2 + I_3 \quad (22)$$

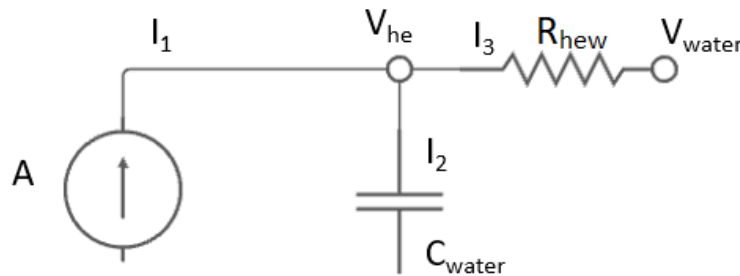


Figure 27: The thermoelectric equivalent of the system.

$$I_1 = \frac{V_{he} - V_{water}}{R_{hew}} + C_{water} \frac{dV_{he}}{dt} \quad (23)$$

The second node, V_{water} , describes the water inside the EWH. The current I_3 and I_4 equals the current I_5 and the current I_6 . The current over the resistor R_{ehw} , I_3 , is equal to $\frac{V_{he}-V_{water}}{R_{ehw}}$. Since water is withdrawn from the tank, some water will enter the tank. This will be seen as the current I_4 and will be stated as $T_{in} - T_{water}$. The current over the capacitor, I_5 equals $C_{water} \frac{dV}{dt}$ and current over the resistor R_{ww} , I_6 is equal to $\frac{V_{water}-V_{wall}}{R_{ww}}$. This gives the complete equation as shown in Equation 25.

$$I_3 + I_4 = I_5 + I_6 \quad (24)$$

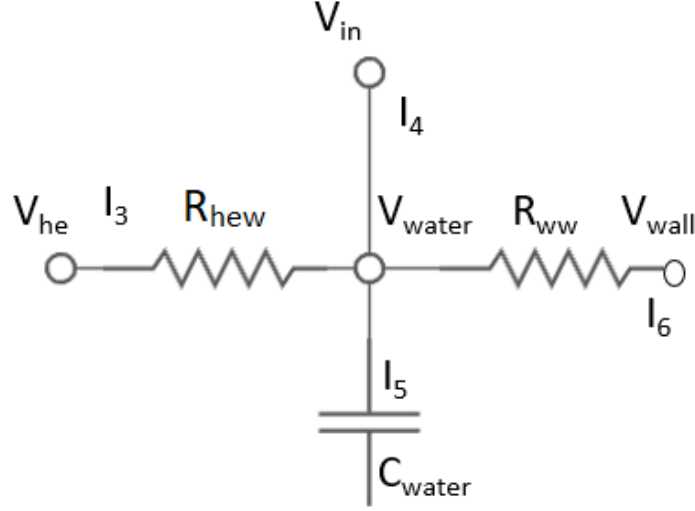


Figure 28: The thermoelectric equivalent of the system.

$$\frac{V_{he} - V_{water}}{R_{hew}} + (V_{in} - V_{water}) = \frac{V_{water} - V_{wall}}{R_{ww}} + C_{water} \frac{dV_{water}}{dt} \quad (25)$$

Looking at node V_{wall} , one have to consider three currents. I_6 represents the current through R_{ww} , I_7 represents the current over C_{wall} and I_8 represents the current over R_{wa} . Equation 27 shows this.

$$I_6 = I_7 + I_8 \quad (26)$$

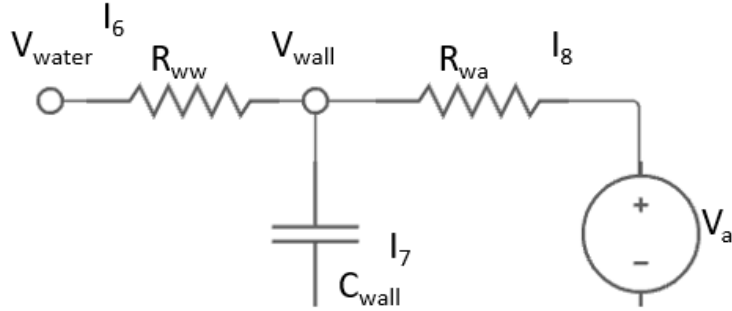


Figure 29: The thermoelectric equivalent of the system.

$$\frac{V_{water} - V_{wall}}{R_{ww}} = C_{wall} \frac{dV_{wall}}{dt} + \frac{V_{wall} - V_a}{R_{wa}} \quad (27)$$

Given this is a thermal-electrical equivalent, it is known that $Q = I$ and $T = V$. It is also important to add the diffusion term, stated as $\sigma d\omega$. This leads to the following equations:

$$\frac{dT_{he}}{dt} = \frac{T_{water} - T_{he}}{R_{hew}C_{he}} + \frac{\dot{Q}}{C_{he}} + \frac{\sigma_{he}d\omega}{dt} \quad (28)$$

$$\frac{dT_{water}}{dt} = \frac{\dot{m} \cdot c_w (T_{in} - T_{water})}{C_{water}} + \frac{T_{wall} - T_{water}}{R_{ww}C_{water}} + \frac{T_{he} - T_{water}}{R_{hew}C_{water}} + \frac{\sigma_{water}d\omega}{dt} \quad (29)$$

$$\frac{dT_{wall}}{dt} = \frac{T_{water} - T_{wall}}{R_{ww}C_{wall}} + \frac{T_a - T_{wall}}{R_{wa}C_{wall}} + \frac{\sigma_{wall}d\omega}{dt} \quad (30)$$

The observation equation is the same as for the 1R1C and the 2R2C model.

$$Y_{T_{water}} = T_{water} + \sigma \quad (31)$$

A comparison between measured and simulated data will be performed to verify the model. To obtain simulated data, Euler's method is used. It is interesting to solve for $T_{water}(t + 1)$, $T_{he}(t + 1)$ and $T_{wall}(t + 1)$. Equation 33, Equation 32 and Equation 34 shows these equations.

$$T_{he}(t + 1) = T_{he}(t) + dt \cdot \left(\frac{T_{water}(t) - T_{he}(t)}{R_{hew}C_{he}} + \frac{\dot{Q}(t)}{C_{he}} \right) \quad (32)$$

$$T_{water}(t+1) = T_{water}(t) + dt \cdot \left(\frac{\dot{m} \cdot c_w (T_{in}(t) - T_{water}(t))}{C_{water}} + \frac{T_{wall}(t) - T_{water}(t)}{R_{ww}C_{water}} + \frac{T_{he}(t) - T_{water}(t)}{R_{hew}C_{water}} \right) \quad (33)$$

$$T_{wall}(t + 1) = T_{wall}(t) + dt \left(\frac{T_{water}(t) - T_{wall}(t)}{R_{ww}C_{wall}} + \frac{T_a(t) - T_{wall}(t)}{R_{wa} - C_{wall}} \right) \quad (34)$$

6.4 Using The CTSM-R tool

With CTSM-R, the unknown resistances and capacitances are obtained for each case. All cases will use three models for parameter fitting. It is an 1R1C-model, a 2R2C-model and a 3R3C-model. Script of the CTSM-R code can be found in Figure 55 - Figure 58 in Section 12. This bases on the CTSM-R examples found on the CTSM.info homepage [63]. The specific system equations, inputs, observation equation, and variance were changed to fit the experiments performed at the NTNU Smart House Lab. Initial values of parameters are stated to fit the cases. Changing initial values and their boundaries is essential to obtain accurate parameter fitting. The boundaries are decided based on examples, references, and trial and error. The boundaries specify the upper and lower limit of where the parameters are allowed to move during iterations. A wide area of movement may lead to poor parameter fitting. By adjusting the initial values and their range, it is possible to get the best possible parameter fitting. Figure 7 shows how the CSV file looks like. Using the known parameters from the file, CTSM-R iterates through to find the optimal solution to the unknown. Figure 30 shows the iteration. CTSM-R uses trial and error on different R and C values to find maximum likelihood values.

```
Iteration 37, F(x) = -1.2991269736794829e+03, max|g(x)| = 2.2515e-02
Parameter:
[1] 77.3199990 0.4253076 -22.1515738 -0.3243255 405.9718080

Iteration 38, F(x) = -1.2991269736823385e+03, max|g(x)| = 3.6274e-03
Parameter:
[1] 77.3199990 0.4253076 -22.1184196 -0.3243255 405.9715327

Iteration 39, F(x) = -1.2991269736823606e+03, max|g(x)| = 6.4985e-04
Parameter:
[1] 77.3199990 0.4253076 -22.1207521 -0.3243255 405.9714505

Iteration 40, F(x) = -1.2991269736823656e+03, max|g(x)| = 5.0252e-04
Parameter:
[1] 77.3199990 0.4253076 -22.1215139 -0.3243255 405.9714358
```

Figure 30: Iterations performed by CTSM-R.

The developers do not specify the units used for R and C in their examples on CTSM-R. CTSM-R is therefore applied with different units. Further, the results are compared with the results of other references. Professors at DTU were contacted for the verification of units. Units are decided as following: R ($\frac{^{\circ}C}{kW}$), C ($\frac{kWh}{^{\circ}C}$) and Q(kW).

6.5 Model Validation

Model validation is essential. When running CTSM-R, one retrieves a coefficient matrix and a correlation matrix. There are four essential observations to these two matrixes. These are as follows:

- The p-value of the t-tests ($\Pr(> |t|$ is below 0.05 for all parameters. Helping parameters can exceed this limit.
- dF/dPar is close to zero.
- dPen/dPar is not significant compared to dF/dPar
- The correlation matrix do not have any off diagonal values close to +/- 1. This does not apply for non-important parameters.

By looking at residuals, ACF, cumulated periodogram, one-step-ahead plot, simulated-value plot, LogLikelihood, and the root-mean-square error(RMSE), it is possible to analyze what model is the best.

Residual means the amount leftover after the operation. The residuals ACF plot is the autocorrelation in the residuals and shows the independence of the residuals. If there is autocorrelation in the residuals, which extends beyond the dotted line in the plot, it would suggest that the forecast is inefficient. The results are not wrong, but they may have a larger prediction interval than necessary [64]. The Cumulated periodogram is also plotted and shows the dominant frequencies of the time series. If the frequencies are inside the blue dotted interval, the residual has satisfactory white noise properties [55]. The script used for plotting residuals, ACF, and cumulated periodogram can be seen in Figure 58 in the Attachments.

The one-step-ahead plot shows the temperature of the water and is solved by an inbuilt function in R. To compute these plots, Euler's method is used. Equation 12 for the 1R1C-model, Equation 20 for the 2R2C-model and Equation 33, for the 3R3C-model. The measured parameter values of temperature and power and fitted parameters of R and C are used as inputs in the equations. The one-step-ahead plot is compared with the measured temperature plot. A simulated-value plot shows the water temperature plots using the last step's simulated values instead of the measured values. For the 1R1C-model, Equation 12 is used. For the 2R2C-model, Equation 21 and Equation 20 are used. For the 3R3C-model Equation 33, Equation 32 and Equation 34 are used. It is only the temperature of the water that is interesting to plot. The values of the other parameters must be obtained to plot this graph. When all values are calculated, the simulated temperature plots are compared with the actual measured-value plot.

Log-likelihood and root-mean-square-error are calculated using built-in functions in R. The script is shown in Figure 58. A higher likelihood is positive, while it is desirable with the lowest possible RMSE. These values indicate how good the models are compared to each other. Equation 35 shows the equation for finding the RMSE manually.

$$RMSE = \sqrt{\sum_{i=n}^N \frac{(Predicted_i - Actual_i)^2}{N}} \quad (35)$$

7 Experimental Results

In this section, graphs of experiments, results from parameter fitting and residual plots are shown.

7.1 Case 1.1: Steady state of the EWH at different set-point temperatures using the upper temperature sensor

Case 1.1 uses an experimental setup where the upper and the lower temperature sensors are fitted. Figure 31 shows measured power ratings and measured temperature ratings of the lower and the upper-temperature sensor. The black line indicates the set-point temperature. Some draining of water occurred around hour 45. The lower temperature sensor reacts more to little water draining than the upper sensor. The upper-temperature sensor measures temperatures closer to the set-point temperature, except for the set-point temperature of 85 °C.

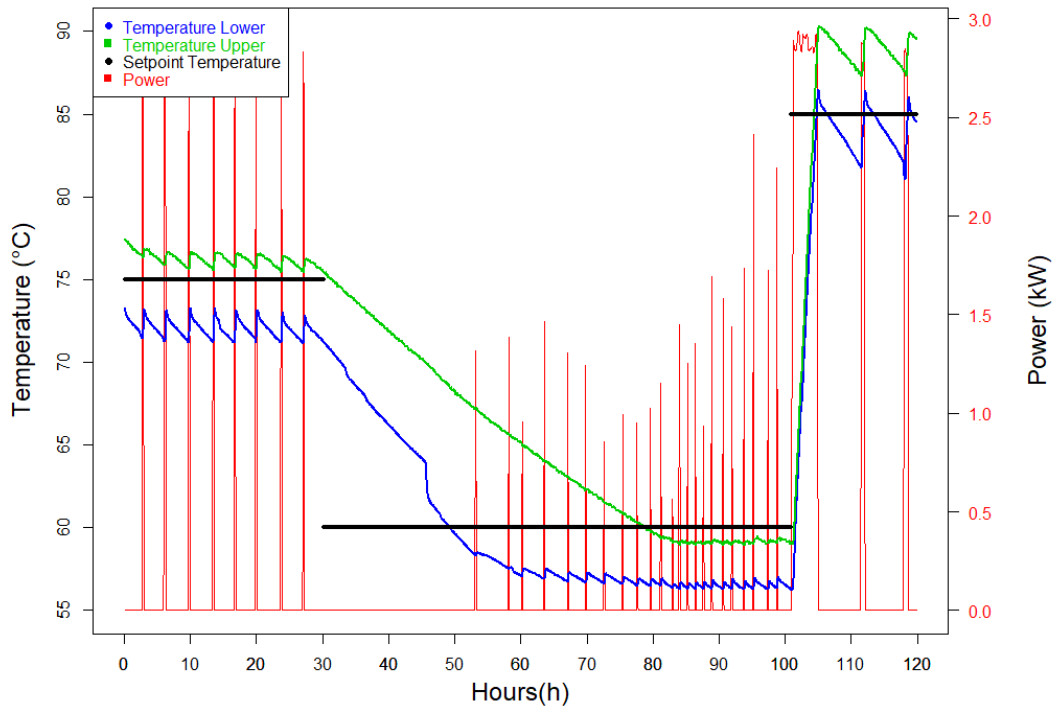


Figure 31: Temperatures and power rating measurements of Case 1.1.

The coefficient matrix and the correlation matrix indicate how good the parameter fittings are. It shows if the results check the four important points stated in Section 6.4. Table 8 and Table 9 shows the coefficient and correlation matrix of experiment 1.1 with upper temperature sensor for the 1R1C model. The coefficient and correlation matrixes of the 2R2C and 3R3C cases can be found in Table 25 - 32 in Section 12, Attachments. The coefficient matrix of experiment 1.1 shows that the model validates considering the four points stated in Section 6. The correlation matrix shows that the diagonal is close to 0, validating the model.

Table 8: Coefficient Matrix of the 1R1C-model for case 1.1 with upper temperature sensor.

	Estimate	Std. Error	t value	Pr(> t)	dF/dPar	dPen/dPar
Tewh0	7.7320e+01	8.9519e-02	8.6372e+02	0.0000e+00	5.9866e-05	0.0023
C	4.2531e-01	8.7496e-03	4.8609e+01	0.0000e+00	2.6738e-08	0.0000
e11	-1.7800e+01	2.4193e+01	-7.3573e-01	4.6202e-01	-2.0570e-07	0.0073
p11	-1.1260e+00	2.0597e-02	-5.4668e+01	0.0000e+00	-2.4300e-06	0.0000
R	4.0597e+02	4.0836e+01	9.9415e+00	0.0000e+00	5.6887e-07	0.0001

Table 10 shows the R and C values obtained. Table 32 shows the R and C values graphically. Figure 33 shows the residual, ACF and cumulated periodograms of case 1.1.

Table 9: Correlation Matrix of the 1R1C-model for Case 1.1 using the upper temperature sensor.

	Tewh0	C	e11	p11
C	0.04			
e11	0.01	0.06		
p11	0.00	0.15	0.00	
R	0.01	0.26	0.02	0.00

Table 10: Estimated values for resistance and capacitance of Case 1.1.

Case	T_{set} ($^{\circ}C$)	$R(\frac{^{\circ}C}{kW})$	$C(\frac{kWh}{^{\circ}C})$	Iterations
1.1 (1R1C) Upper	60-85	405.970	0.425	39
1.1 (2R2C) Upper	60-85	409.19, 1.1899*	0.425, 0.0114*	31
1.1 (3R3C) Upper	60-85	333.14, 3.2258*, 2.3335**	0.22917, 0.1623*, 0.10608**	133
1.1 (1R1C) Low	60-85	271.636	0.343	34
1.1 (2R2C) Low	60-85	270.83, 0.794*	0.343, 0.00774*	49
1.1 (3R3C) Low	60-85	251.07, 20.357*, 1.0955**	0.19289, 0.14419*, 0.088475**	282

R = Resistance between water and wall/(water and ambient for the 1R1C-model). R* = Resistance between wall and ambient. R** = Resistance between heating element and water.

C = Heat capacity of water. C* = Heat capacity of wall. C** = Heat capacity of heating element.

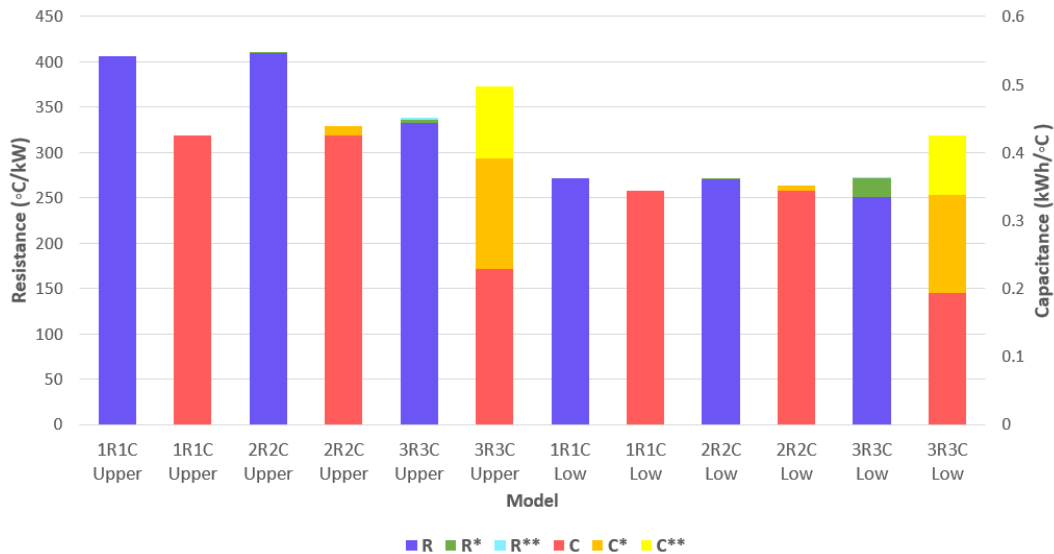


Figure 32: Estimated values for resistances and capacitances for Case 1.1.

The resistance and capacitance values are higher for the upper-temperature sensor experiments. The 3R3C models have the highest combined capacitance values.

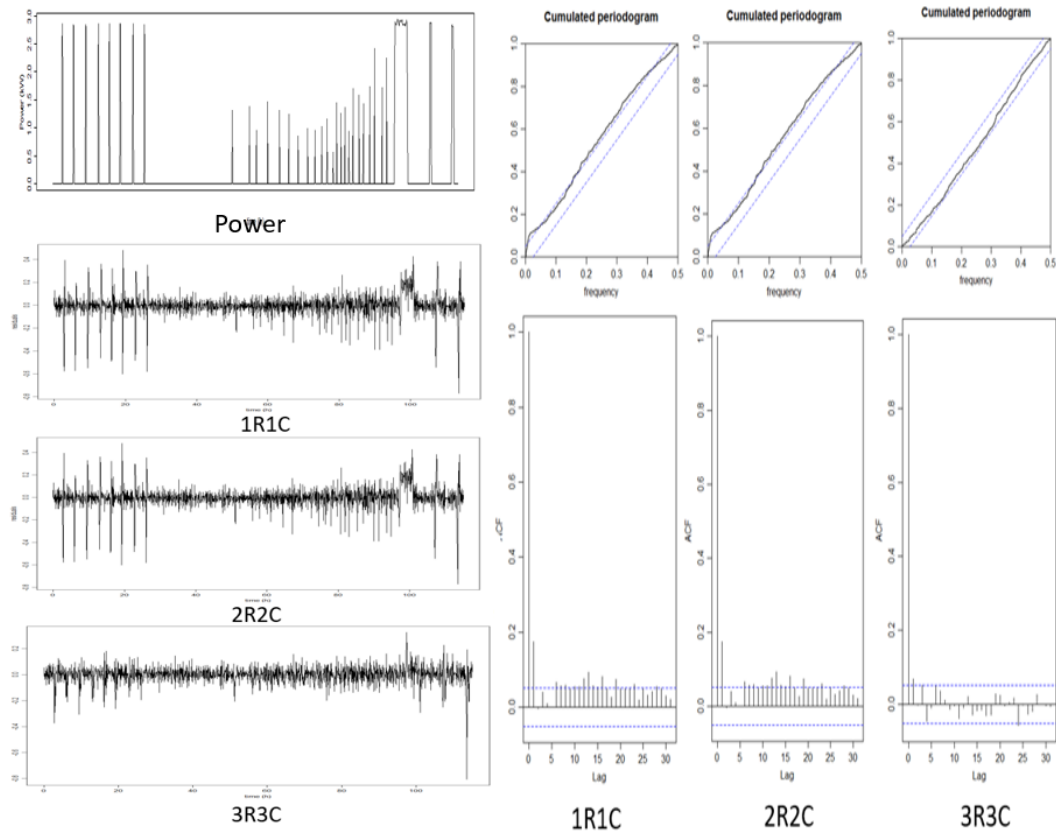


Figure 33: Comparing residuals of Case 1.1 using upper temperature sensor.

The residual plot, cumulated periodogram, and ACF plots show fewer disturbances in the 3R3C-model than in the 1R1C and 2R2C models.

7.2 Case 1.2: Steady state of the EWH at different set-point temperatures using the upper temperature sensor

Case 1.2 uses an experiment setup with the lower and the middle-temperature sensor. The procedure is the same as for Case 1.1. Figure 34 shows power use and temperature measured during Case 1.2. There occurred some water draining around hour 75, but not as much as in Case 1.1. The temperature profile of the middle sensor is above the temperature profile of the lower temperature sensor.

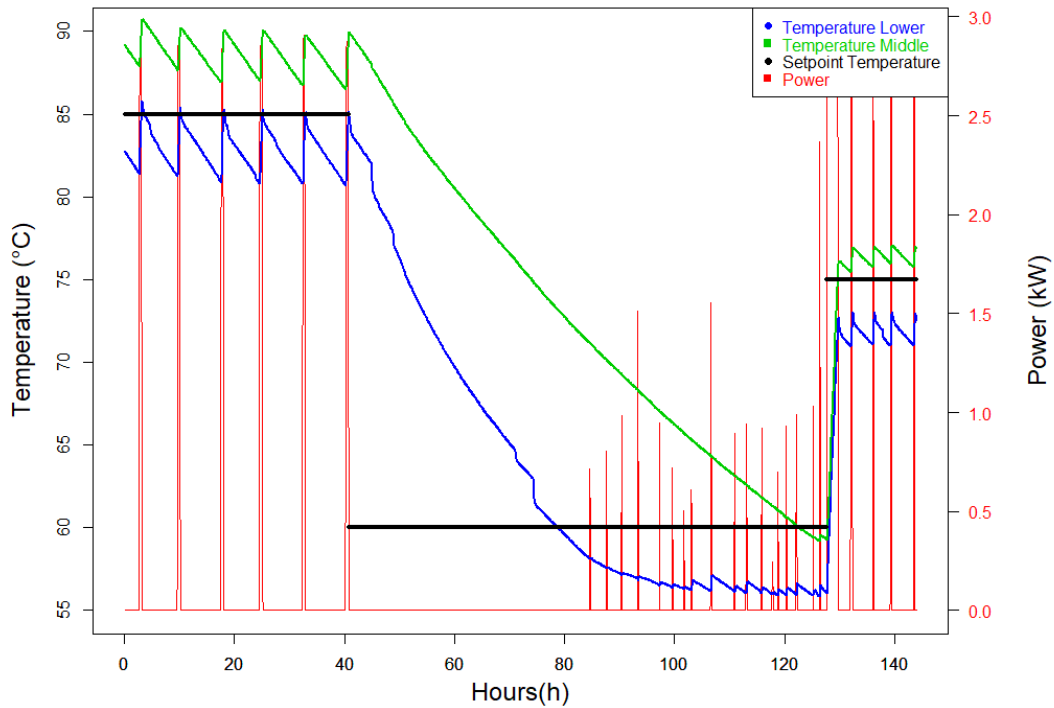


Figure 34: Temperatures and power rating measurements of Case 1.2.

Coefficient matrixes and correlation matrixes of Case 1.2 with middle temperature sensor are shown in Table 33 - 38 in the Section 12 Attachment. They give a good validation of the model. Table 11 shows the predicted R and C values. Figure 35 shows the correlation in R and C-values graphically. Figure 36 shows the residual, ACF and cumulated periodograms of Case 1.2.

Table 11: Estimated values for R and C of Case 1.2.

Reference	T_{set} ($^{\circ}C$)	R ($\frac{^{\circ}C}{kW}$)	C ($\frac{kWh}{^{\circ}C}$)	iterations
1.2 (1R1C) Middle	60-90	357.98	0.367	40
1.2 (2R2C) Middle	60-90	352.1, 1.738*	0.3759, 0.0159*	130
1.2 (3R3C) Middle	60-90	355.17, 4.0647*, 1.1736**	0.31734, 0.01065*, 0.01165**	84
1.2 (1R1C) Low	60-90	302.07	0.3031	40
1.2 (2R2C) Low	60-90	288.46, 1.7295*	0.3211, 0.018206*	100
1.2 (3R3C) Low	60-90	313.57, 9.735*, 5.356**	0.2447, 0.1304*, 0.01206**	97

R = Resistance between water and wall/(water and ambient if it is 1R1C). R* = Resistance between wall and ambient. R** = Resistance between heating element and water.

C = Heat capacity of water. C* = Heat capacity of wall. C** = Heat capacity of heating element.

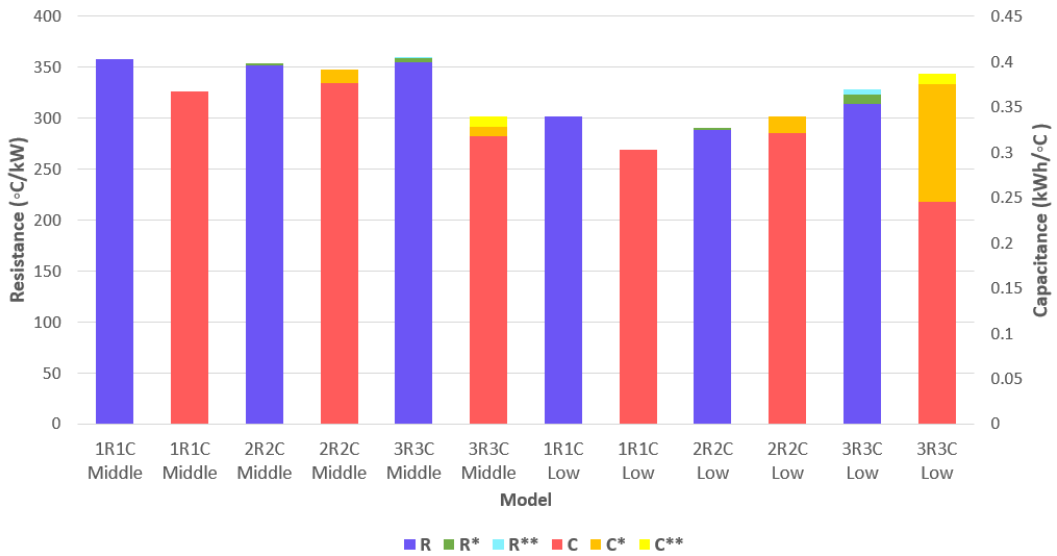


Figure 35: Estimated values for resistances and capacitances in Case 1.2.

The capacitance values are similar for both middle- and lower-temperature sensor predictions. The measurements are better for Case 1.2 than for Case 1.1 because of fewer disturbances from water draining. The resistance obtained for the middle-temperature sensor is higher than for the lower-temperature sensor.

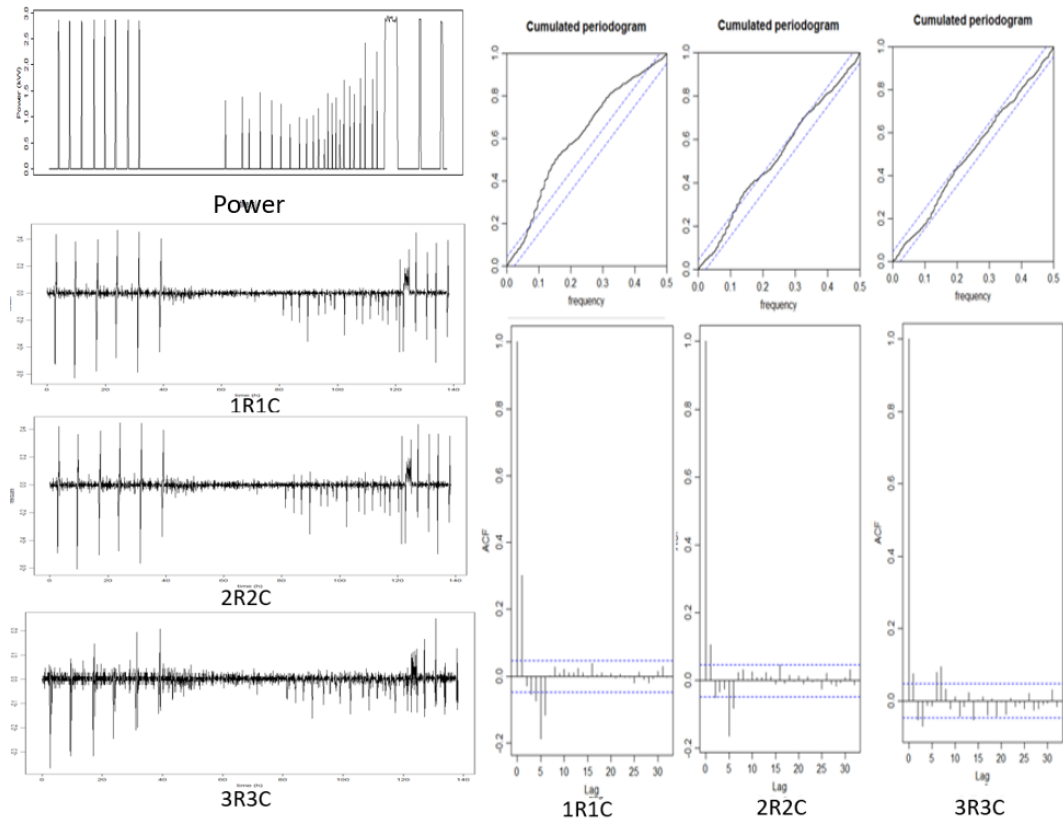


Figure 36: Comparing residuals of Case 1.2 using middle temperature sensor.

The residual plot, cumulated periodogram, and ACF plots show fewer disturbances in the 3R3C-model than in the 1R1C and 2R2C models. The 1R1C model is the worst of the three models.

7.3 Case 2: 3-4 showers a day while the EWH is in on-mode

This case simulates the operation of an EWH in a family home. 3-to 4 showers are performed each day. The showers occur at different times a day, and the duration of the showers varies to simulate the hot water usage in a family home. The water heater is connected to a power source during showering periods. Figure 37 shows the temperature and power ratings of Case 2, and Table 12 shows the number of showers with duration and time. The graph shows that the lower temperature sensor is susceptible to inlet water.

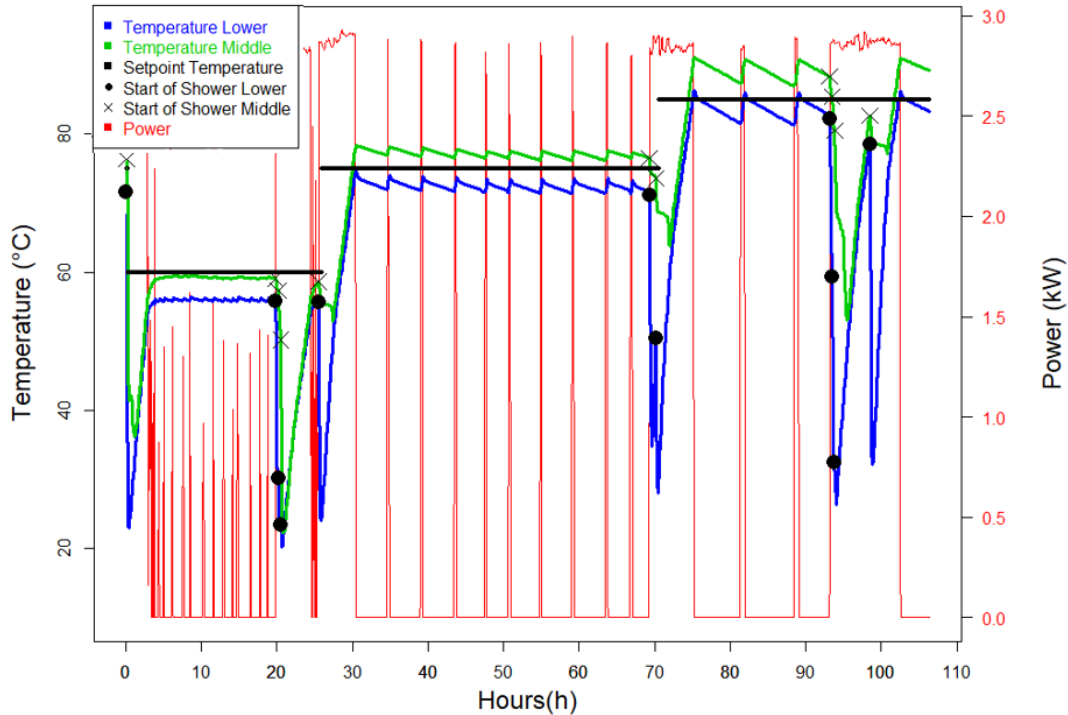


Figure 37: Temperatures and power ratings of the EWH during Case 2.

Table 12: Showers performed during Case 2.

Shower number	Duration	Time
1	10 min	15:20
2	10 min	15:40
3	10 min	16:00
4	15 min	20:00
6	10 min	63:50
7	10 min	64:40
8	10 min	87:40
9	10 min	88:00
10	10 min	88:20
11	15 min	93:00

Coefficient matrixes and correlation matrixes of Case 2 with middle temperature sensor are shown in Table 39 - 44 in Section 12 Attachments. Table 13 shows this experiment's fitted R and C values. Figure 38 compares the models' different R and C values. The values for the lower sensor are not shown, as the measurements are poor due to the sensor being too sensitive to inlet water. Figure 39 shows the residual, ACF and cumulated periodogram of Case 2.

Table 13: Parameter fitting for Case 2.

Case	T_{set} ($^{\circ}C$)	R ($\frac{^{\circ}C}{kW}$)	C ($\frac{kWh}{^{\circ}C}$)	Iterations
2 (1R1C) Mid	60-85	167.69	0.507	44
2 (2R2C) Mid	60-85	123.82, 4.5471*	0.3845, 0.04013*	58
2 (3R3C) Mid	60-85	119.58, 3.985*, 1.9024**	0.14499, 0.16214*, 0.028879**	174

R = Resistance between water and wall/(water and ambient if it is 1R1C). R* = Resistance between wall and ambient. R** = Resistance between heating element and water.

C = Heat capacity of water. C* = Heat capacity of wall. C** = Heat capacity of heating element.

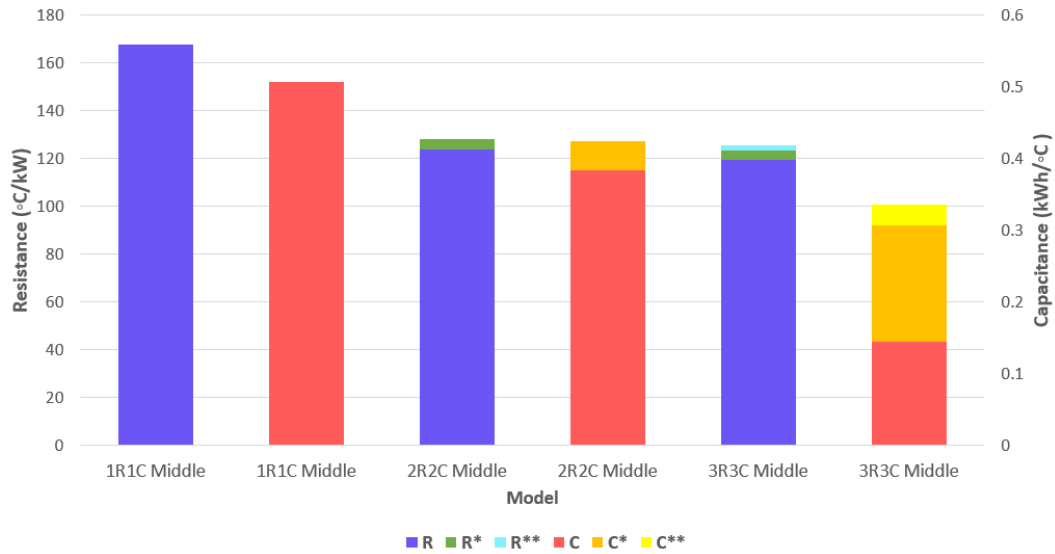


Figure 38: Estimated values for resistances and capacitances in Case 2.

The resistance is much lower in Case 2 than in Case 1. The capacitance is at the same level as in Case 1. Resistance and capacitance values reduce some when the model increases the number of resistances and capacitances.

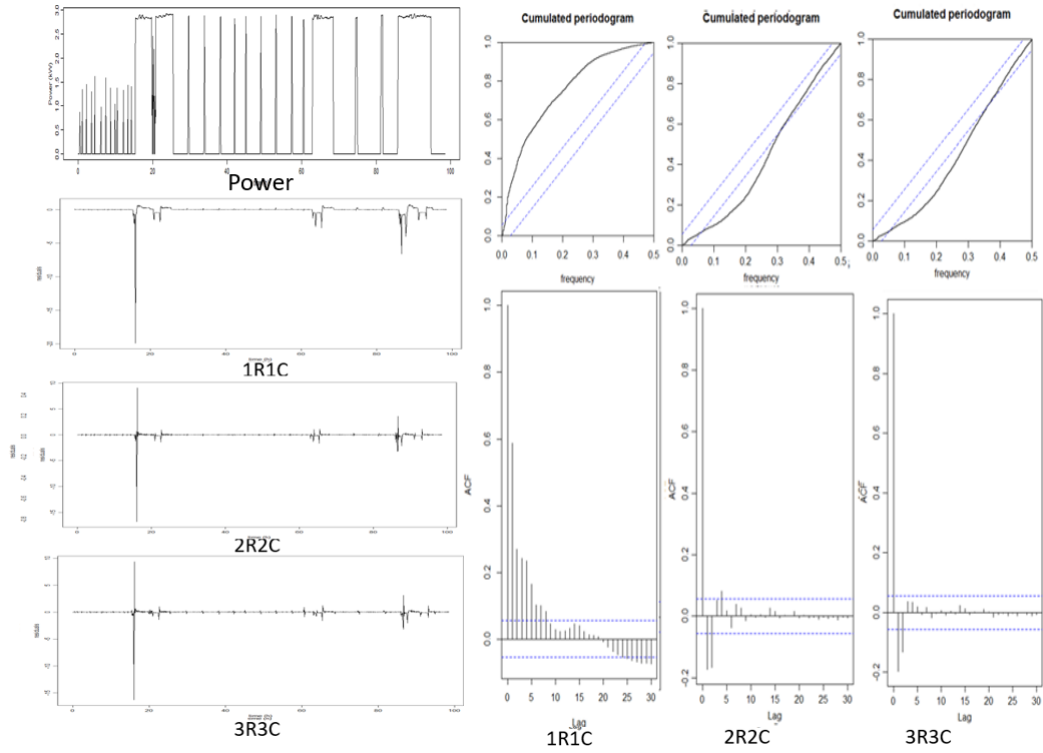


Figure 39: Comparing residuals of Case 2 using middle temperature sensor.

The residual plots, cumulated periodogram, and ACF plots show that the 1R1C-model varies greatly. The 3R3C model is favorable.

7.4 Case 3.1: 3-4 showers a day while the EWH is in off-mode

This case simulates the operation of an EWH in a family home, but the EWH is turned off during the period when showers occur. 3-to 4 showers are performed each day. Showers occur at different times of the day. This is to simulate a flexible water heater in a normal family home. The middle and the lower-temperature sensor is used in this experiment. Figure 40 shows the experiment, and Table 14 shows the number of showers with duration, time, and on-time for EWH. The plot shows that the lower temperature sensor is very dependent on cold water entering the tank.

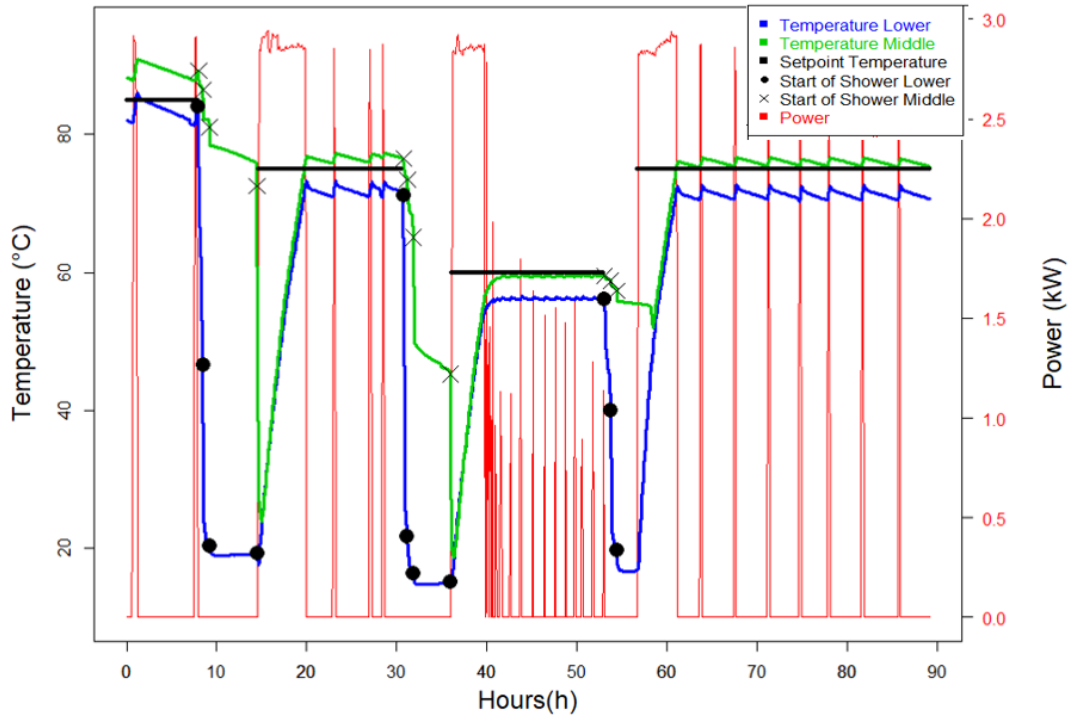


Figure 40: Temperatures and power ratings of Case 3.1.

Table 14: Showers and state of EWH during Case 3.1.

Shower number	Duration	Time
1	10 min	08:00
2	10 min	08:30
3	5 min	09:15
4	10 min	14:30
6	10 min	30:40
7	10 min	31:20
8	5 min	31:50
9	5 min	36:00
10	5 min	53:00
11	5 min	53:45
12	5 min	54:30

Time	State
0-8:00	On
8:00-14:40	Off
14:40-30:40	On
30:40-36:00	Off
36:00-53:00	On
53:00-56:45	Off
57:00-89:00	On

The coefficient matrix and correlation are shown in Table 45 - 50 in Section 12 Attachments. Table 15 shows the calculated R and C values. Figure 41 shows the residual plots for Case 3.1.

Table 15: Parameter fitting for Case 3.1.

Case	T_{set} ($^{\circ}C$)	R ($\frac{^{\circ}C}{kW}$)	C ($\frac{kWh}{^{\circ}C}$)	Iterations
3.1 (1R1C) Middle	60 - 85	195.94	0.316	43
3.1 (2R2C) Middle	60 - 85	180.74, 2.194*	0.311, 0.0452*	84
3.1 (3R3C) Middle	60 - 85	168.13, 1.5448*, 0.86995**	0.12567, 0.16464*, 0.1552**	178

R = Resistance between water and wall/(water and ambient if it is 1R1C). R* = Resistance between wall and ambient. R** = Resistance between heating element and water.

C = Heat capacity of water. C* = Heat capacity of wall. C** = Heat capacity of heating element.

The resistance decreases as the model is expanded. The combined capacitance is higher for increasing model complexity. Both resistance and capacitance for water decrease as the model get more complex.

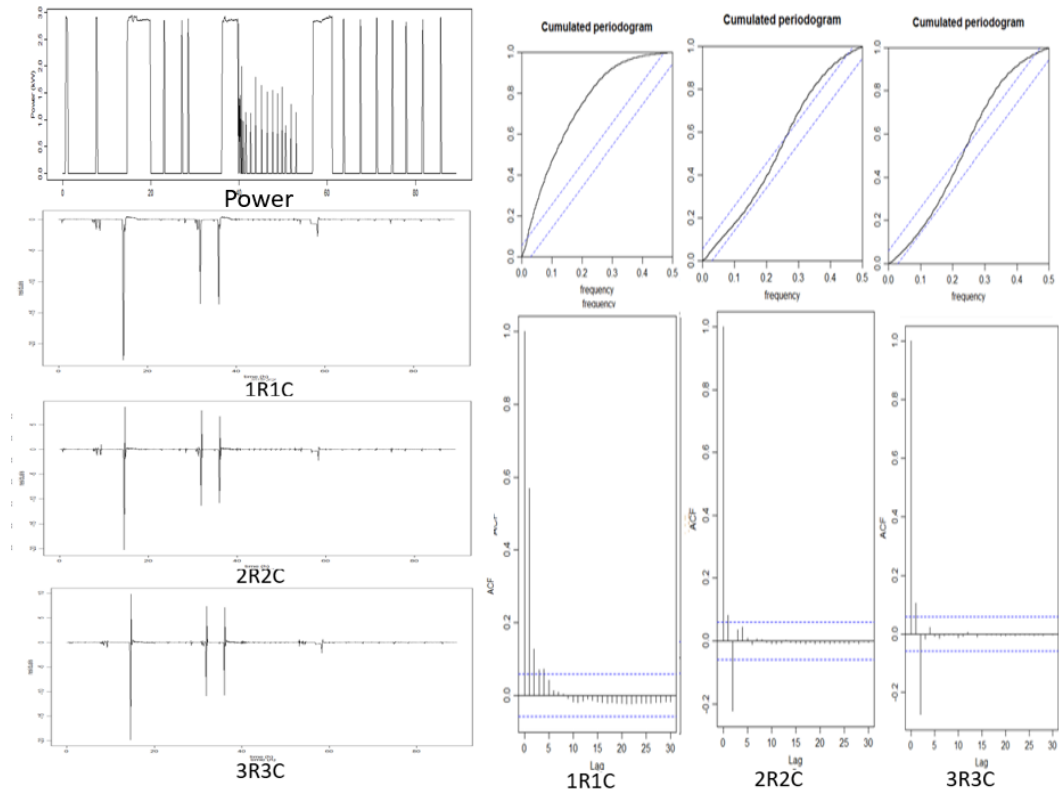


Figure 41: Comparing residuals of Case 3.1, using middle temperature sensor.

The residual plots, cumulated periodogram, and ACF plots show that the 1R1C-model is the weakest. The best model considering these plots is the 3R3C-model.

7.5 Case 3.2: 3-4 showers while the EWH is in off-mode

This experiment has the same procedure as Experiment 3.1, but the upper-temperature sensor is used. Figure 42 shows the plot of the experiment, and Table 16 shows the duration, time of showers, and the state of the EWH. Only the upper sensor temperatures are shown because the lower sensor temperatures were too dependent on the inlet water.

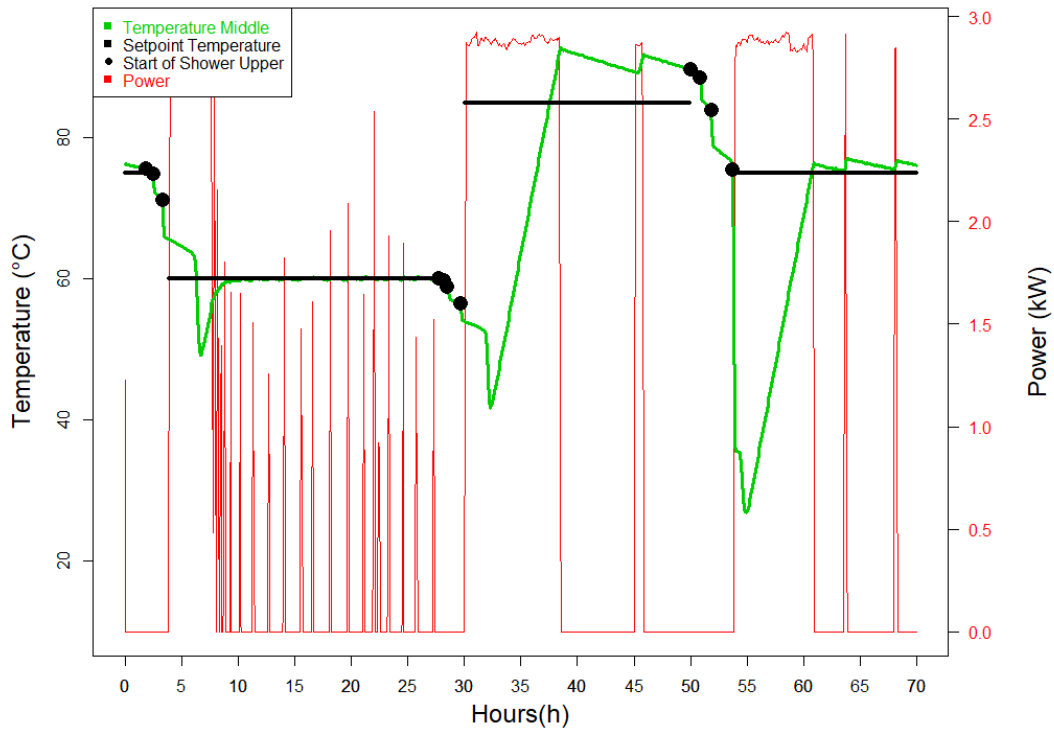


Figure 42: Temperatures and power ratings of Case 3.2 with the upper temperature sensor.

Table 16: Showers and state of water heater during Case 3.2.

Shower Number	Duration	Time
1	10 min	01:45
2	10 min	02:25
3	10 min	03:15
4	10 min	27:40
5	5 min	28:10
6	5 min	28:30
7	5 min	29:40
8	5 min	45:00
9	10 min	49:55
10	10 min	50:45
11	10 min	51:45
12	10 min	53:40

Time	State
0-3:50	Off
3:50-27:20	On
27:20-30:00	Off
30:00-45:00	On
45:00-54:00	Off
54:00-70:00	On

Coefficient matrix and correlation matrix of Case 3.2 with upper temperature sensor are shown in Table 51 - 56 in the Attachments. Table 17 shows the parameter fittings of Experiment 3.2, and Figure 43 shows the graphical presentation of R and C-values of both Experiment 3.1 and Experiment 3.2. Figure 44 shows the residuals, ACF, and cumulated periodogram of case 3.2.

Table 17: Parameter fitting of case 3.2.

Case	T_{set} ($^{\circ}C$)	$R(\frac{^{\circ}C}{kW})$	$C(\frac{kWh}{^{\circ}C})$	Iterations
3.2 (1R1C) Upper	60 - 85	137.83	0.4795	28
3.2 (2R2C) Upper	60 - 85	102.08, 1.373*	0.361, 0.181*	72
3.2 (3R3C) Upper	60 - 85	97.877, 4.8837*, 1.5251**	0.214, 0.1701*, 0.1731**	82

R = Resistance between water and wall/(water and ambient if it is 1R1C). R* = Resistance between wall and ambient. R** = Resistance between heating element and water.

C = Heat capacity of water. C* = Heat capacity of wall. C** = Heat capacity of heating element.

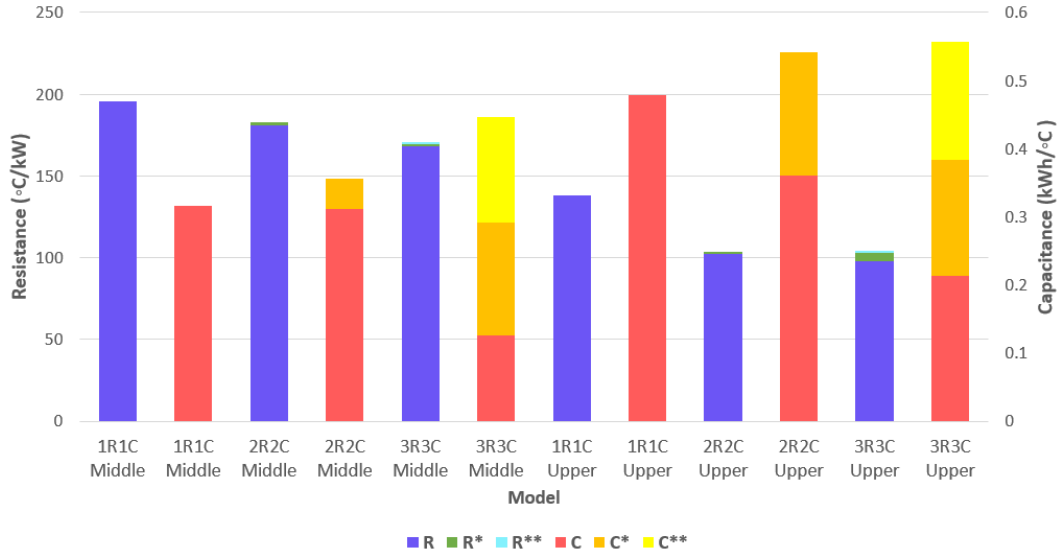


Figure 43: The relationship between the different resistances and capacitances of Case 3.1 and Case 3.2.

When plotting the middle and upper experiments of Case 3, it is interesting to see that the resistance decreases while the capacitance increases for the combined plots. The resistance and capacitance of water decrease with a more complex model with more resistances and capacitances.

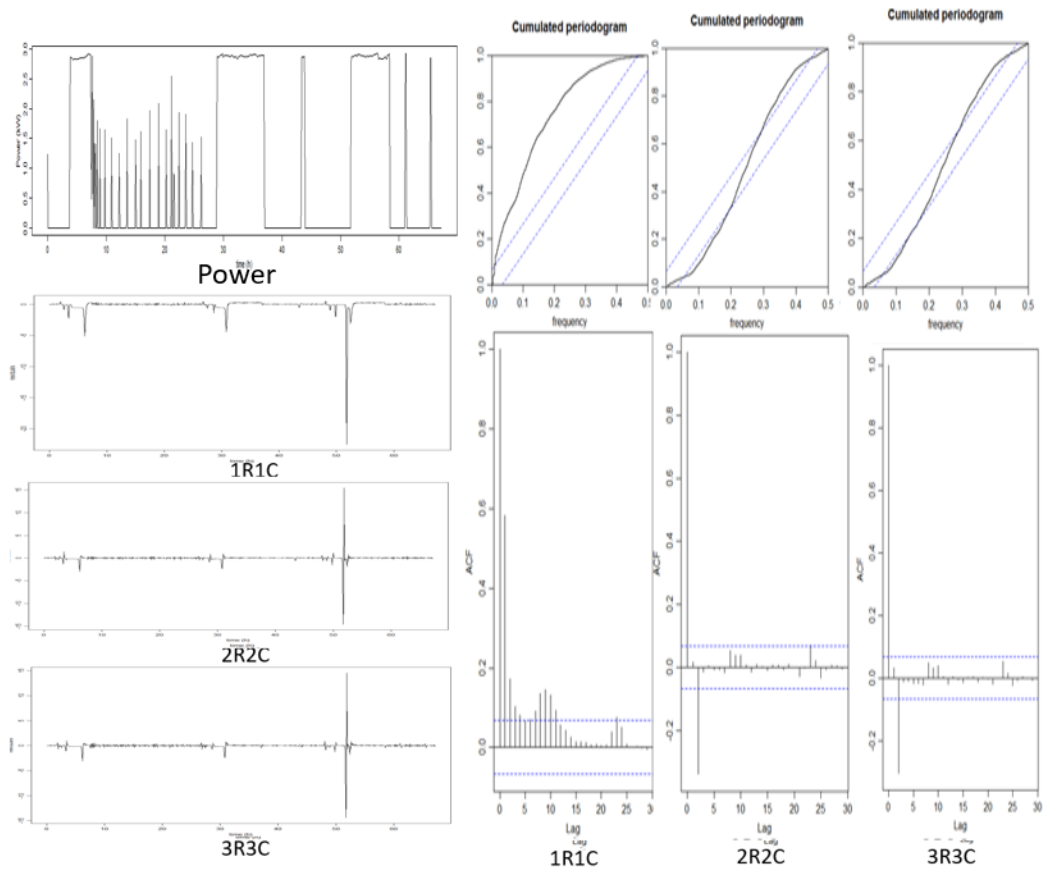


Figure 44: Comparing residuals of Case 3.2, using upper temperature sensor.

The residual plots, cumulated periodogram, and ACF plots show that the 1R1C-model is the poorer model. 2R2C and 3R3C-models are very similar considering these plots.

8 Verification of Mathematical Model

Simulated-value plots, one-step-ahead plots, Log-Likelihood values, and Root-means-square-error are evaluated. Simulated-value plots and one-step-ahead plots are found using the Eulers method. The difference between the two is that the simulated-value plots always use the simulated value of the last iteration to predict the next value. The one-step ahead uses the last measured value to predict the next simulated value. Euler’s method is shown in Section 6. Log-Likelihood is an inbuilt function in R, and RMSE is solved using the formula stated in Section 6.

8.1 Case 1

Table 18: Likelihood, RMSE, R and C-values of Case 1.

Case	$R(\frac{^{\circ}C}{kW})$	Combined($\frac{^{\circ}C}{kW}$)	$C(\frac{kWh}{^{\circ}C})$	Combined($\frac{kWh}{^{\circ}C}$)	LogLikelihood	RMSE
1.1 (1R1C) Upper	405.970	405.970	0.425	0.425	1299.120	0.102
1.1 (2R2C) Upper	409.190, 1.189*	410.379	0.425, 0.011*	0.436	1299.180	0.099
1.1 (3R3C) Upper	333.140, 3.226*, 2.334**	338.699	0.229, 0.162*, 0.106**	0.498	1879.070	0.068
1.1 (1R1C) Low	271.636	271.636	0.343	0.343	1320.427	0.109
1.1 (2R2C) Low	270.830, 0.794*	271.624	0.343, 0.008*	0.351	1337.936	0.106
1.1 (3R3C) Low	251.070, 20.357*, 1.096**	272.523	0.193, 0.144*, 0.089**	0.426	1882.659	0.074
1.2 (1R1C) Middle	357.980	357.980	0.367	0.367	2626.700	0.066
1.2 (2R2C) Middle	352.100, 1.738*	353.838	0.376, 0.016*	0.392	2698.819	0.062
1.2 (3R3C) Middle	355.17, 4.0647*, 1.173**	360.4077	0.317, 0.011*, 0.012**	0.340	3474.716	0.036
1.2 (1R1C) Low	302.070	302.070	0.303	0.303	1925.644	0.091
1.2 (2R2C) Low	288.460, 1.730*	290.190	0.321, 0.018*	0.339	1984.102	0.087
1.2 (3R3C) Low	313.570, 9.735*, 5.356**	328.661	0.245, 0.130*, 0.012**	0.387	2804.914	0.055

The RMSE and Likelihood values show that the 3R3C model is favorable for all models and both experiments. The combined resistance and capacitance are also shown in this table.

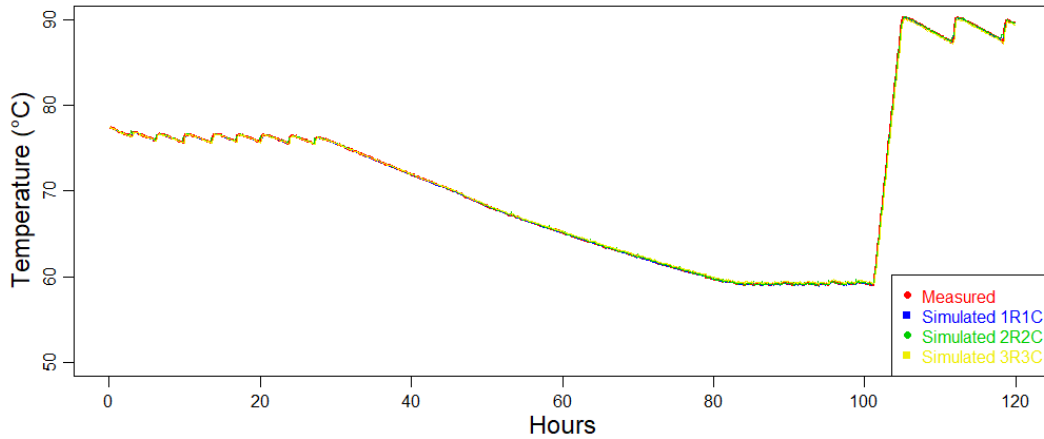


Figure 45: Comparing one-step-ahead functions for Case 1.1 using upper temperature sensor.

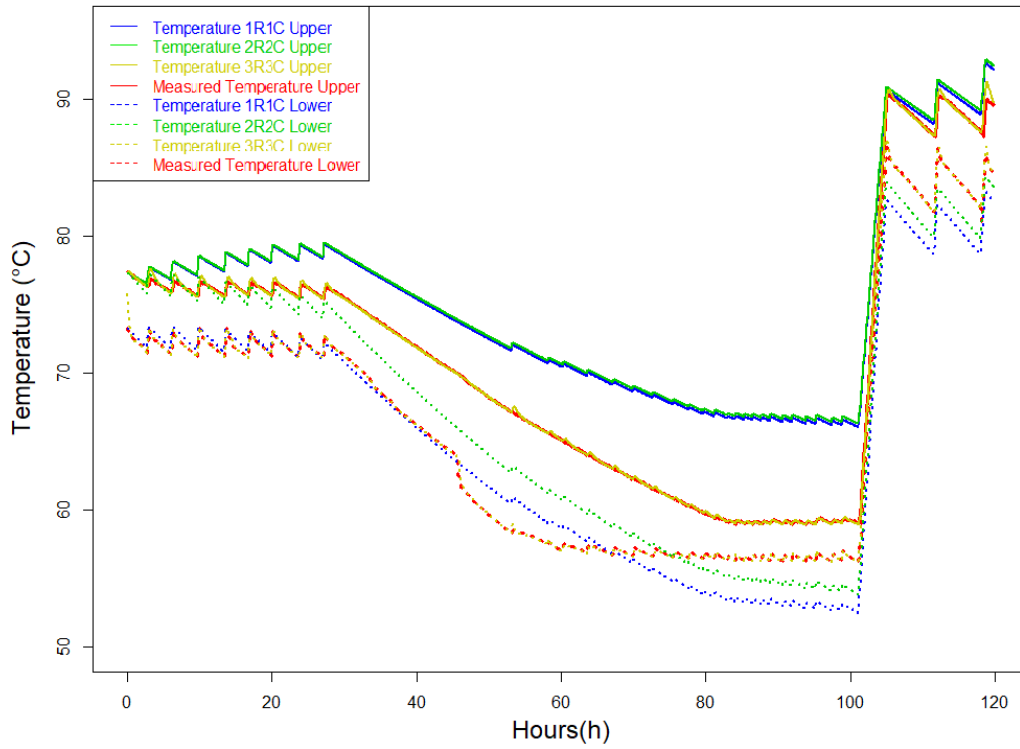


Figure 46: Comparing simulated value-plots for Case 1.1 using the upper temperature sensor.

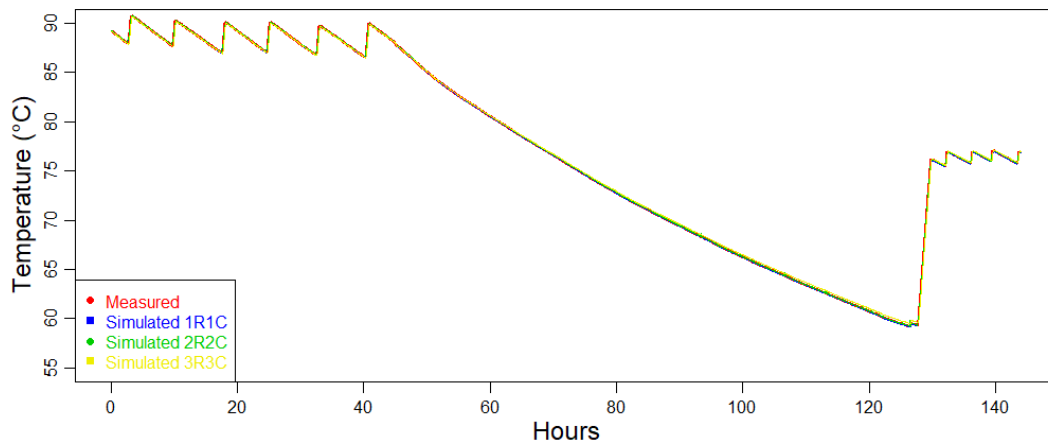


Figure 47: Comparing one-step-ahead functions for Case 1.2 using middle temperature sensor.

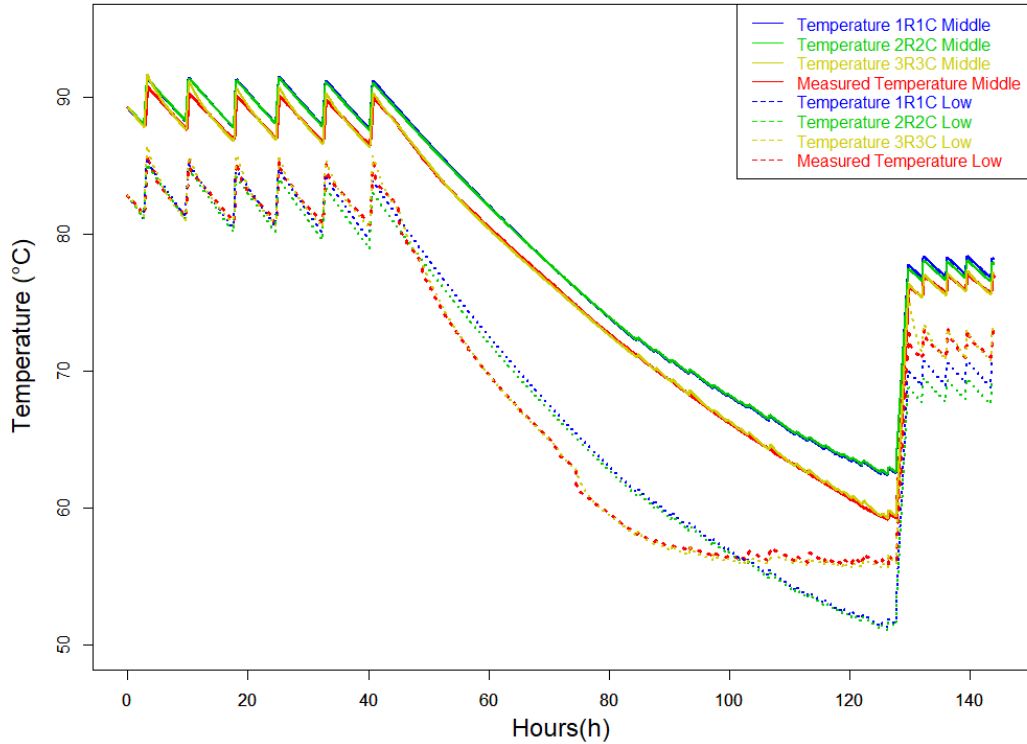


Figure 48: Comparing simulated-value-plots for Case 1.2 using middle temperature sensor.

The one-step-ahead plots for Case 1.1 and Case 1.2 show that all models fit the measured temperature well. The simulated-value plots show that the 3R3C model almost equals the measured temperature. The 2R2C and 1R1C models are not great compared to the measured values. The 2R2C-model is better than the 1R1C-model.

8.2 Case 2

Table 19: R ($\frac{^{\circ}C}{kW}$) and C ($\frac{kWh}{^{\circ}C}$), LogLikelihood and RSME-value for Case 2.

Case	$R(\frac{^{\circ}C}{kW})$	Combined($\frac{^{\circ}C}{kW}$)	$C(\frac{kWh}{^{\circ}C})$	Combined($\frac{kWh}{^{\circ}C}$)	LogLikelihood	RMSE
2 (1R1C) Mid	167.690	167.690	0.507	0.507	-685.195	0.746
2 (2R2C) Mid	123.820, 4.547*	128.3671	0.3845, 0.040*	0.425	-146.092	0.605
2 (3R3C) Mid	119.580, 3.985*, 1.902**	125.467	0.145, 0.162*, 0.0289**	0.336	-127.612	0.613

The LogLikelihood-value is negative, but the most negligible negative value is the 3R3C, which means that this is the best model. The RMSE-value favors the 3R3C-model too.

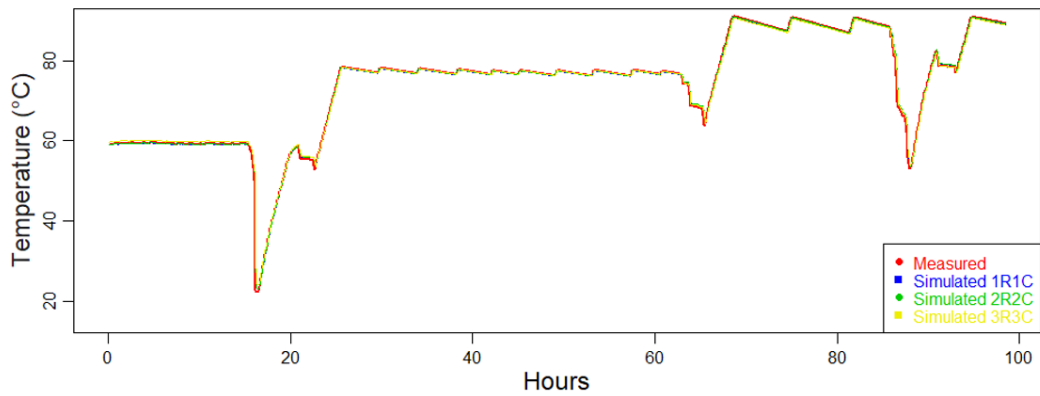


Figure 49: Comparing one-step-ahead plots of Case 2 using middle temperature sensor.

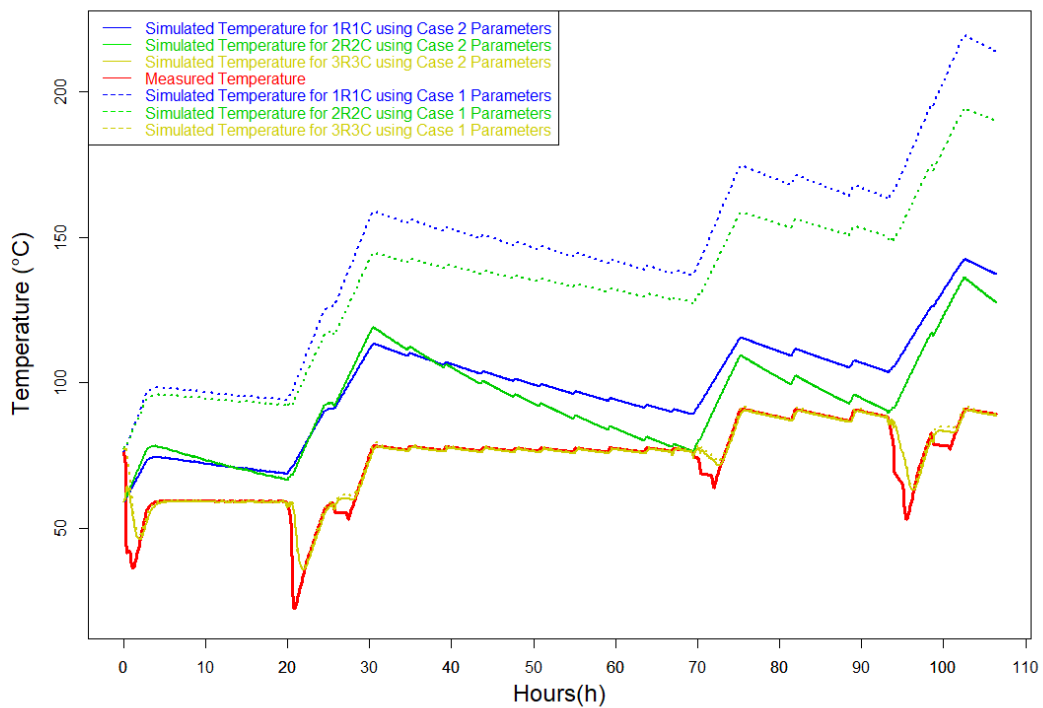


Figure 50: Comparing simulated-value-plots for Case 2 using the middle temperature sensor.

The one-step ahead functions are good for all models. They are all equal to the measured plot. The simulated-value plot shows that the 3R3C-model is very similar to the measured plot. The 1R1C and 2R2C models are off, but the 1R1C model is the least good of the two. The models fit better for the parameters of Case 2.

8.3 Case 3

Table 20: Resistance ($\frac{^{\circ}C}{kW}$), capacitance ($\frac{kWh}{^{\circ}C}$), LogLikelihood and RMSE-value for Case 3.

Case	R($\frac{^{\circ}C}{kW}$)	Combined($\frac{^{\circ}C}{kW}$)	C($\frac{kWh}{^{\circ}C}$)	Combined($\frac{kWh}{^{\circ}C}$)	LogLikelihood	RMSE
3 (1R1C) Middle	195.940	195.940	0.316	0.316	-810.797	1.174
3 (2R2C) Middle	180.740, 2.194*	182.934	0.311, 0.045*	0.356	-647.904	0.928
3 (3R3C) Middle	168.130, 1.545*, 0.869**	170.545	0.126, 0.165*, 0.155**	0.446	-594.504	0.921
3 (1R1C) Upper	137.830	137.830	0.479	0.479	-676.247	1.053
3 (2R2C) Upper	102.080, 1.373*	103.453	0.361, 0.181*	0.542	-404.300	0.851
3 (3R3C) Upper	97.877, 4.884*, 1.525**	104.286	0.214, 0.170*, 0.173**	0.557	-409.125	0.844

The Loglikelihood and RMSE favor the 3R3C model for the middle-temperature sensor. For the experiments with the upper-temperature sensor, RMSE-value favors the 3R3C, and LogLikelihood favors the 2R2C model.

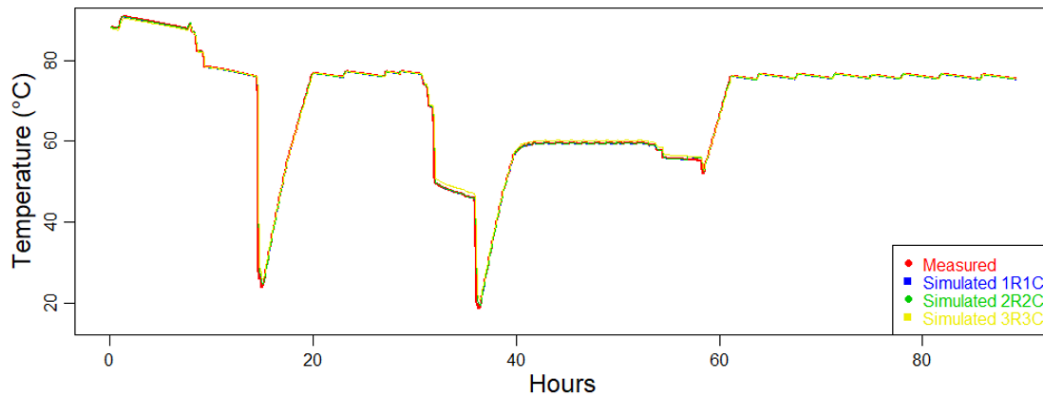


Figure 51: Comparing one-step-ahead plots of 1R1C, 2R2C and 3R3C for Case 3.1.

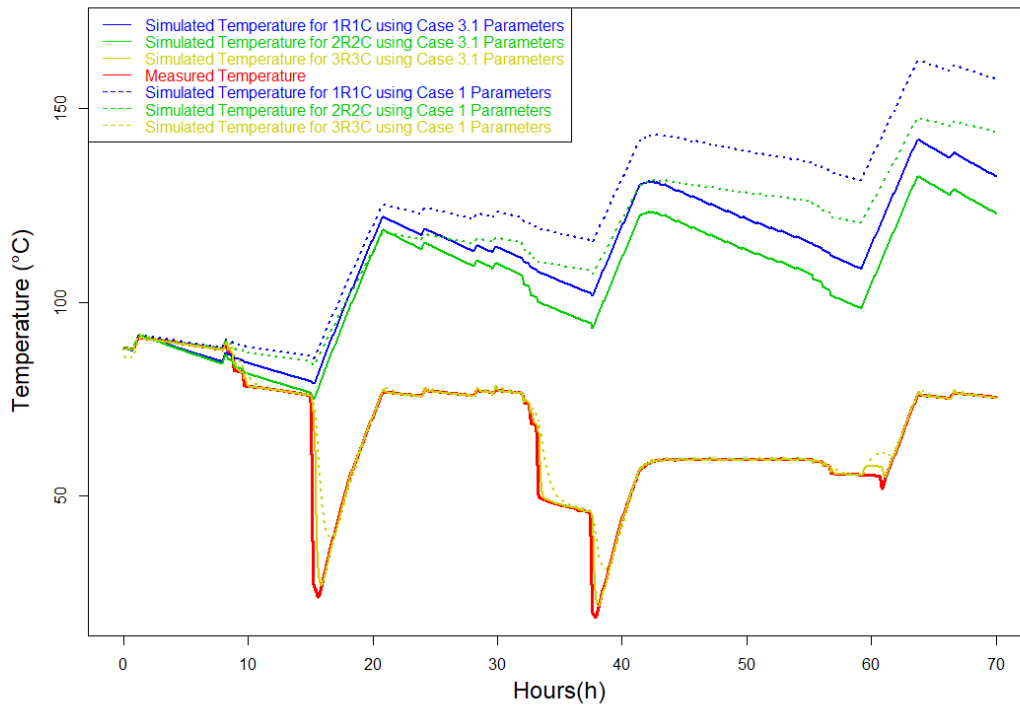


Figure 52: Comparing simulated-value-plots for Case 3.2, middle temperature sensor.

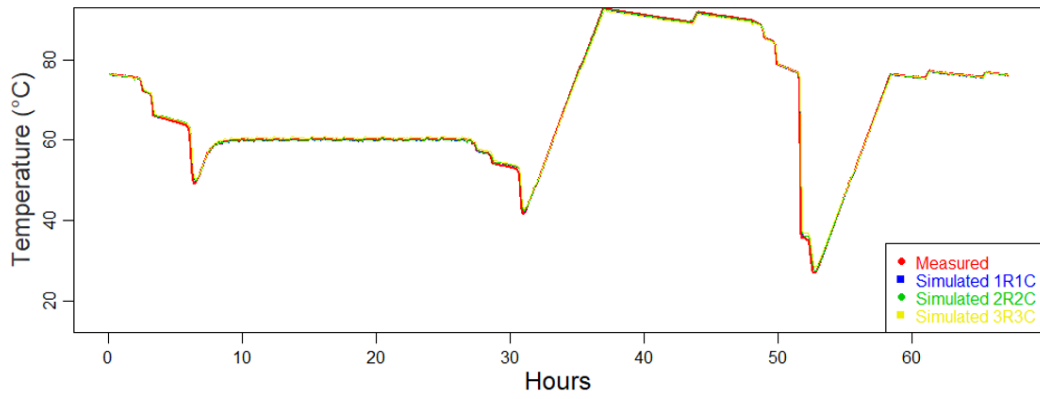


Figure 53: Comparing one-step-ahead plots of 1R1C, 2R2C and 3R3C for case 3.2.

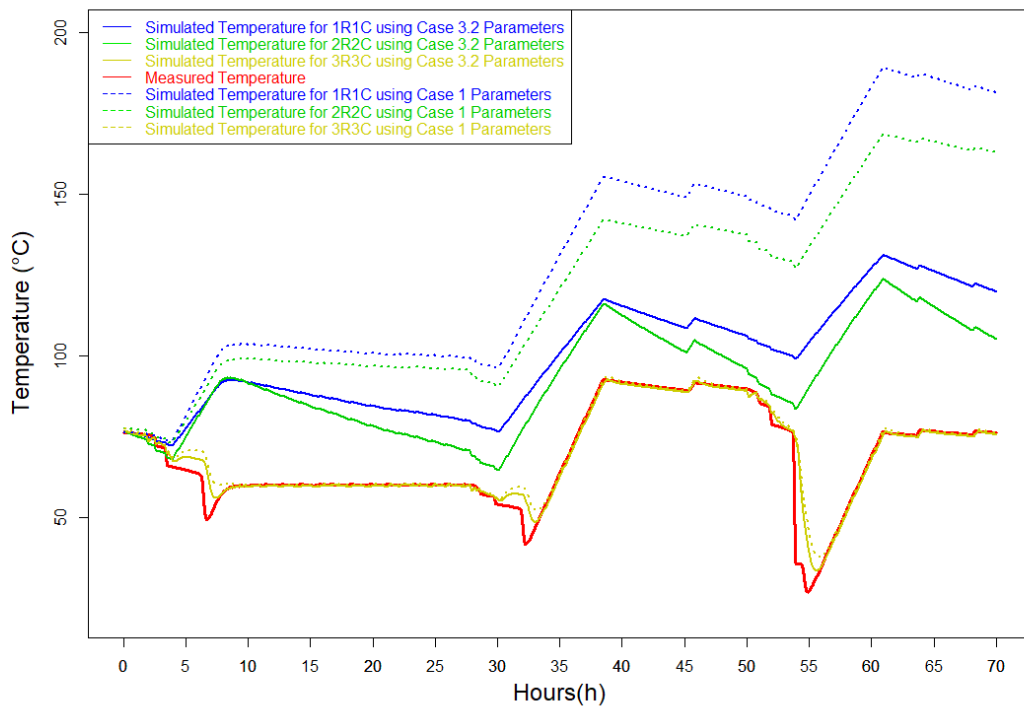


Figure 54: Comparing simulated-value-plots for Case 3.2 using the upper temperature sensor.

The one-step-ahead function shows that the models fit well with the measured temperature. The predicted-value plots show that the 3R3C models fit well, and the 1R1C and 2R2C models do not fit well. The models fit better for the parameters of Case 3.

9 Discussion

In this section, the results of every case are discussed. Table 21 and Table 22 shows a comparison between resistances and capacitances of different research papers. Table 21 shows values of $R \frac{^{\circ}C}{kW}$ and $C \frac{kWh}{^{\circ}C}$. Table 22 shows values of $R \frac{^{\circ}C}{kWkg}$ and $C \frac{kWh}{^{\circ}Ckg}$. Case 1.2, the middle-temperature sensor, is chosen as the best parameter fitted values of Case 1. Case 1.1 had too much disturbance from water being drained from the water heater. The lower temperature sensor is not stated in the tables because it was too dependent on the temperature of the inlet water. For Case 2 and 3, only the 3R3C-model are stated in the tables. This is because RMSE, LogLikelihood, one-step-ahead predictions, predicted-value-plot, residual, ACF, and cumulated periodograms all state that the 3R3C model is the best model for almost every case and experiment.

Table 21: $R \left(\frac{^{\circ}C}{kW} \right)$ and $C \left(\frac{kWh}{^{\circ}C} \right)$ compared with other papers.

Reference	T_{set} ($^{\circ}C$)	V (L)	P (kW)	$R \left(\frac{^{\circ}C}{kW} \right)$	$C \left(\frac{kWh}{^{\circ}C} \right)$
Case 1.2 (1R1C) Middle	60-85	281	3	357.98	0.367
Case 1.2 (2R2C) Middle	60-85	281	3	352.1, 1.738*	0.3759, 0.0159*
Case 1.2 (3R3C) Middle	60-85	281	3	333.29, 26.142*, 7.2524**	0.31734, 0.01065*, 0.01165**
Case 2 (3R3C) Middle	60-85	281	3	119.58, 3.985*, 1.9024**	0.14499, 0.16214*, 0.028879**
Case 3 (3R3C) Middle	60-85	281	3	168.13, 1.5448*, 0.86995**	0.12567, 0.16464*, 0.1552**
Case 3 (3R3C) Upper	60-85	281	3	97.877, 4.8837*, 1.5251**	0.214, 0.1701*, 0.1731***
[2] Løvstakken (1R1C)	70	281	3	286.21	0.185
[2] Løvstakken (1R1C)	75	281	3	296	0.157
[2] Løvstakken (1R1C)	80	281	3	295.2	0.158
[2] Løvstakken (1R1C)	85	281	3	247.11	0.185
[51] Svendsen (1R1C)	75	281	3	286.6	0.17
[51] Svendsen (2R2C)	75	281	3	283.24	0.174
[6] Lakshmanan (1R1C)	70-75	200	2	600	0.335
[55] Yu (1R1C)	25-80	92	2.8	1055	0.1055
[55] Yu (2R2C)	25-80	92	2.8	929, 39.73**	0.1055, 0.003**
[55] Yu (2R2C)	25-80	92	2.8	0.4041, 1017*	0.1055, 0.074*
[55] Yu (3R3C)	25-80	92	2.8	855.2, 1004*, 66.72**	0.1055, 0.001*, 0.0017**
[56] DTU	50-95	788	3 x 3	120.627	1.0781

Table 22: $R \left(\frac{^{\circ}C}{kWkg} \right)$ and $C \left(\frac{kWh}{^{\circ}Ckg} \right)$ compared with other papers.

Reference	V (L)	$R \left(\frac{^{\circ}C}{kWkg} \right)$	R combined	$C \left(\frac{kWh}{^{\circ}Ckg} \right)$	C combined
Case 1.2 (1R1C) Middle	281	1.2739	1.2739	0.00131	0.00131
Case 1.2 (2R2C) Middle	281	1.253, 0.00618*	1.25918	0.00134, 0.00006*	0.00140
Case 1.2 (3R3C) Middle	281	0.00615, 1.2657*, 0.403**	1.67485	0.000847, 0.00035*, 0.000004**	0.00123
Case 2 (3R3C) Middle	281	0.0062, 0.516*, 0.021**	0.5432	0.00067, 0.00098*, 0.00004**	0.00119
Case 3 (3R3C) Middle	281	0.0121, 0.655*, 0.01504**	0.68214	0.00011, 0.00066*, 0.00020**	0.00159
Case 3 (3R3C) Upper	281	0.2849, 0.00749*, 0.00550**	0.29789	0.00076, 0.00017*, 0.00061**	0.00154
[2] Løvstakken (1R1C)	281	1.0185	1.0185	0.00066	0.00066
[2] Løvstakken (1R1C)	281	1.0533	1.0533	0.00056	0.00056
[2] Løvstakken (1R1C)	281	1.0505	1.0505	0.00056	0.00056
[2] Løvstakken (1R1C)	281	0.87039	0.87039	0.00066	0.00066
[51] Svendsen (1R1C)	281	1.018	1.018	0.0006	0.0006
[51] Svendsen (2R2C)	281	1.008	1.008	0.0006	0.0006
[6] Lakshmanan (1R1C)	200	3	3	0.0016	0.0016
[55] Yu (1R1C)	92	11.467	11.467	0.0011	0.0011
[55] Yu (2R2C)	92	10.097, 0.431**	10.528	0.0011, 0.00003**	0.00113
[55] Yu (2R2C)	92	0.0043, 11.054*	11.0583	0.0011, 0.0008*	0.0019
[55] Yu (3R3C)	92	9.29, 10.91*, 0.725**	20.925	0.0011, 0.00001*, 0.00001**	0.00112
[56] DTU	788	0.153	0.153	0.0013	0.0013

R = Resistance between water and wall/(water and ambient if it is 1R1C). R* = Resistance between wall and ambient. R** = Resistance between heating element and water.

C = Heat capacity of water. C* = Heat capacity of wall. C** = Heat capacity of heating element.

Table 23 and Table 24 shows the specific heat capacity of water. Comparing capacitance values

with these tables is interesting because the parameter fitted capacitance should be at least equal to the values in these tables. Table 2 shows the heat capacity of isolation. This is interesting when considering the 2R2C and 3R3C-models, as these split the capacitance and resistance into several capacitances and resistances, including looking at the heat capacity of the wall.

Table 23: Specific heat capacity of water.

Temperature ($^{\circ}C$)	Specific Heat Capacity of Water	
20	$4184 \frac{J}{kg^{\circ}C}$	$0.001162 \frac{kWh}{kg^{\circ}C}$
80	$4198 \frac{J}{kg^{\circ}C}$	$0.0011661 \frac{kWh}{kg^{\circ}C}$

Table 24: Specific heat capacity of water at different volumes (L).

Volume (L)	$C(\frac{kWh}{^{\circ}C})$ at $20^{\circ}C$	$C(\frac{kWh}{^{\circ}C})$ at $80^{\circ}C$
200	0.232	0.233
281	0.327	0.328
788	0.916	0.920

9.1 Case 1

Experiments in Case 1.1 are the same as those performed in the project thesis, Løvstakken [2]. However, the experiments span a more extensive period, and the set-point temperature is adjusted during the experiments. This was to obtain a richer dataset at a steady state. More temperature sensors and improved insulation of the lower temperature sensor improved the results. The parameter fitting is equal to the parameters obtained in other research papers. The temperature measurements depend on the temperature sensor location. The lower temperature sensor measures a lower temperature than the temperature sensor located in the middle and the upper parts of the tank. The difference between the temperatures is around $5^{\circ}C$. The parameter fittings are lower for the measurements using the lower temperature sensor. The lower temperature sensor is also more sensitive to disturbances, such as temperature change and water draining. There occurred some water draining during both simulations. This is because the lab is a functional bathroom, and people may use hot water. There occurred noticeable water draining during Experiment 1.1, which can be seen in the parameter fitting using the lower temperature sensor values.

9.1.1 Case 1.1

Lower Temperature Sensor: The initial parameters are given an extensive range between upper and lower boundaries. The temperatures ranged from $0-100^{\circ}C$, capacitances from $0.0001-1 \frac{kWh}{^{\circ}C}$, and resistances from 0.1 to $500 \frac{^{\circ}C}{kW}$. The 1R1C-model and the 2R2C-model obtained equal thermal resistance and thermal capacitance values. The summation of resistances and capacitances in the 2R2C-model equals the parameter values obtained for the 1R1C model. This makes sense, as the resistance in the 1R1C-model spans the area of the two resistances in the 2R2C-model combined. When performing parameter fitting of the 3R3C model, initial values had to be specified more thoroughly. The boundaries of the initial parameters had to be narrowed down. There are a lot of possible parameter fittings, and the best solution considering model validation, as stated in 6.4, may not be the best solution to the parameter fitting.

If forcing R_{ww} (resistance between water and wall) to a higher minimum value, in the 3R3C-model, the other parameters automatically adjust accordingly. The combined resistance becomes around $270 \frac{^{\circ}C}{kW}$. Combined value of capacitance equals $0.336 \frac{kWh}{^{\circ}C}$. This parameter fitting gives

a good model validation, but there are other parameter fittings with better model validation. These other parameter fittings are not chosen because the fitted parameters did not make sense compared to other parameters obtained in other scientific papers.

The R-values obtained using the lower-temperature sensor are some lower for Case 1.1 than for Case 1.2. There is some use of hot water by visitors during both experiments. This is very clear when looking at Case 1.1, Figure 31. There is a clear drop in the blue line at around 45 hours. This use of hot water disturbs the results, especially considering the lower temperature sensor.

Upper Temperature sensor: Both 1R1C and 2R2C-models give the same results for parameter fitting of resistance and capacitance. There are some differences in the 3R3C-model, as the resistance value is much lower than calculated in the 1R1C and 2R2C-models. Combined capacitance is at the same level for the 3R3C model as the 1R1C- and 2R2C-models. It was much easier to fit the 3R3C model using the upper-temperature sensor compared with the 3R3C model with the lower temperature sensor. This is because the sensor is not as sensitive to water drained from the tank.

9.1.2 Case 1.2

There was not as much disturbance in the measurements in case 1.2 as in Case 1.1, but some water draining occurred at around hour 70. This can be seen in Figure 34.

Lower Temperature Sensor: It was difficult to fit the parameters of the lower sensor. This is probably because of some water being drained from the tank at hour 70. The resistance obtained is of a higher value than what was obtained in Case 1.1. The resistance obtained lies between 290 and 330 $\frac{^{\circ}\text{C}}{\text{kW}}$. The capacitance is between 0.3 and 0.38716 $\frac{\text{kWh}}{^{\circ}\text{C}}$.

Middle Temperature Sensor: It was easier to fit the parameters for the middle sensor. The resistances obtained using the middle sensor lie between the parameter fitting for the upper sensor (Case 1.1) and the lower sensor. The resistance had a value of 350 - 370 $\frac{^{\circ}\text{C}}{\text{kW}}$. The capacitance is more or less the same for all parameter fittings and is similar to values obtained in Case 1.1. Combined capacitance lies between 0.3 and 0.39 $\frac{\text{kWh}}{^{\circ}\text{C}}$.

9.1.3 Take home from experiments without draining water

The resistances obtained using the middle sensor lie between the values obtained by the high and the low-temperature sensor. This is a good observation and makes sense because of the lag in temperature change when cold water flows into the bottom of the tank. The upper and the middle-temperature sensor is located inside the thermowell located inside the tank. The lower temperature sensor is located on the outside of the water heater. The middle and the upper-temperature sensor is favorable considering water draining and location. Given that the water is drained from the top of the water heater, one can argue for the upper-temperature sensor as the best base when deciding on the model. The middle, however, is more centered on the water heater and may give a more general overview of the water's behavior. The resistances are measured to be between 270 and 410 $\frac{^{\circ}\text{C}}{\text{kW}}$ and the capacitance is between 0.3 and 0.5 $\frac{\text{kWh}}{^{\circ}\text{C}}$. During the project thesis, Løvstakken [2] the resistance was decided to be 295.47 $\frac{^{\circ}\text{C}}{\text{kW}}$ and the capacitance was decided to be 0.157 $\frac{\text{kWh}}{^{\circ}\text{C}}$, which is similar to what was established in Svendsen [51]. The new measurements and models are improving the results. By looking at the parameter fittings of Case 1, it is possible to establish new values for the resistance and capacitance. Considering

the case using the middle-temperature sensor, an average value of resistances and capacitance are chosen as a possible parameter fitting. This gives a resistance of $357.408 \frac{\text{°C}}{\text{kW}}$ for the whole system and capacitance of $0.366 \frac{\text{kWh}}{\text{°C}}$ for the whole system. When considering the case with the upper-temperature sensor, the capacitance can be chosen as $0.453 \frac{\text{kWh}}{\text{°C}}$ for the whole system. The resistance is more difficult to decide, but an estimate is that it holds a value of around $400 \frac{\text{°C}}{\text{kW}}$. The parameters obtained using the middle sensor are used in the predicted-value plots. These experiments are considered the best, and the parameters are great compared to other research papers.

9.2 Case 2

Case 2 considers the middle-temperature sensor. This sensor was chosen because it gave the best measurements and parameter fitting in Case 1. It was also chosen because it represents the average of the system. It is challenging to fit the parameters in Case 2. Adjustments were made to the initial parameters and their boundaries to be able to fit the model. The most challenging fit was the 2R2C-model.

The lower temperature sensor gives poor results when water is drained from the tank. The inlet water enters the bottom of the tank, where the lower temperature sensor is located. This means that the temperature measured by this sensor quickly drops to a temperature of around 20 °C . The outgoing water leaves the tank from the top. The middle and upper-temperature sensor is not as influenced by the inlet water. It takes time for the cold water to mix with the hot water in the middle and upper parts.

The obtained heat capacity for the different RC models varies a lot. The thermal capacitance of the 1R1C model is fitted to be $0.507 \frac{\text{kWh}}{\text{°C}}$, which is very high, but can make sense considering that the 1R1C-model looks at the complete system from water to ambient described by only 1 R and 1 C. The 2R2C-model estimated a thermal capacity of $0.3845 \frac{\text{kWh}}{\text{°C}}$ for water and $0.42463 \frac{\text{kWh}}{\text{°C}}$ combined value. The 3R3C-model estimated a heat capacity of 0.14499 and a combined heat capacity of $0.336 \frac{\text{kWh}}{\text{°C}}$. The thermal resistance of the 1R1C-model is estimated to a value of $167.69 \frac{\text{°C}}{\text{kW}}$. The 2R2C model estimates a combined value of $128.3671 \frac{\text{°C}}{\text{kW}}$. The 3R3C model estimates a value of $125.4674 \frac{\text{°C}}{\text{kW}}$.

The reason for the low resistance in Case 2 compared with Case 1 is the draining of water. The water heater loses much thermal energy when hot water leaves and cold water enters the water heater. When several long showers are taken in a short period, the heating element struggles to maintain a desirable temperature in the tank. This leads to a quick drop in temperature for the middle sensor as well as the lower sensor. It is also observable that the water heater is good at keeping a high temperature as long as no cold water enters the system. This may be the reason for the low thermal resistance in Case 2. The 3R3C model had a combined heat capacity similar to the one of the middle-temperature sensor in Case 1. It is optimistic that the heat capacity fittings equal those obtained in Case 1.

9.3 Case 3

Case 3 was tested for both upper and middle temperature sensors. This was to see if there were significant differences in parameter fitting of the two different temperature sensors. The results of Case 2 were surprising regarding the thermal resistance. Two different experiments in Case 3 would form a solid basis for comparison. It was challenging to fit the parameters in Case 3 but more manageable than the parameter fittings of Case 2. Many adjustments had to be made to the initial parameters and their boundaries. The most challenging fit was the 2R2C-model.

9.3.1 Case 3.1

Case 3.1 investigates the middle temperature sensor. The results are similar to the ones obtained in Case 2. The thermal resistances are low, and the heat capacity is more or less the same as in Case 1. It is interesting to see that higher combined thermal resistance gives lower combined heat capacitance. This is the opposite of both Case 1 and Case 2, where the capacitance and resistance followed each other. The reason for this is because the EWH is off for more extended periods. The heat capacity of just water is reduced as the model adds more resistances and capacitances. This also happens in Case 1 and Case 2. The combined resistance is estimated to be 170 - 195 $\frac{\circ C}{kW}$ and the combined capacitance has a value of 0.316 - 0.446 $\frac{kWh}{\circ C}$.

9.3.2 Case 3.2

The heat capacity fitted after experiments using the upper temperature sensor is of higher value than for the experiment using the middle temperature sensor. The heat capacity equals the heat capacity obtained in Case 1 for the upper temperature sensor. The thermal resistance is at its lowest during Case 3.2. Combined thermal resistance has a value of 103 to 138 $\frac{\circ C}{kW}$. Higher heat capacity gives lower thermal resistance, just as in Case 3.1 The combined heat capacity has a value of 0.48 and 0.557 $\frac{kWh}{\circ C}$.

9.4 Take home from experiments where water is drained from the EWH

The measurements of the lower temperature sensor are poor and hence not further used when draining water. When looking at Figure 37 and Figure 40 from Case 2 and case 3.1, it is clear that the blue line, which describes the lower temperature sensor, quickly drops to a temperature of around 20 $\circ C$. The green line shows the middle-temperature sensor and a more appropriate temperature behavior. The fitted thermal capacitance values are very similar to the values obtained in Case 1. The thermal resistance deviates a lot from case 1. The value of the resistance is more than half from Case 1 to Case 2 and 3. This is a lot but can be because of the draining of water. When looking at the Residual plots, ACF, and cumulated periodograms, it shows that the 3R3C-model is the best. The RMSE and LogLikelihood verify this. The simulated-value plots show that the best parameters to use are the ones obtained in Case 3. The parameters used in Case 1 lead to poorer simulated-value plots. A combined resistance for Case 3 using the middle-temperature sensor is 170.545 $\frac{\circ C}{kW}$ and combined capacitance is 0.446 $\frac{kWh}{\circ C}$. The combined resistance for Case 3 using the upper-temperature sensor is 104.286 $\frac{\circ C}{kW}$ and combined capacitance is 0.557 $\frac{kWh}{\circ C}$. The reason for using the combined heating capacity is that the 3R3C model splits the capacity into three more or less equal capacities. This is something the model does to easier obtain a good model validated fit. It is possible to fit the model with the heat capacity of water or water-ambient being 0.327 $\frac{kWh}{\circ C}$. The middle-temperature sensor is chosen as a good temperature sensor because of its location in the tank. The

9.5 Parameter fitting computed with CTSM-R

The first obtained parameter fitting is not necessarily the best one, and it is important to not just look at the model validation when choosing parameter fittings. The 1R1C-model can often be used as an indication of how the fittings of the 2R2C and 3R3C-models are going to be. The 1R1C-model does not need initial parameters with strict upper/lower boundaries to find a good parameter fitting. The obtained parameter fittings of the 1R1C-model are therefore used when fitting parameters for the 2R2C and 3R3C-models. What characterizes the 2R2C and 3R3C-models is that it is necessary to actively change the initial parameters and their upper/lower

boundaries to fit the model in the best possible way. There are several possible parameter fittings of each case with good model validation. Some of these validated parameter fittings are not chosen because they could contain very high/low resistance and capacitance values. Some parameters are forced to specific values by adjusting the upper and lower boundaries for which the parameters can operate. This means that the parameter fittings chosen for the 2R2C and 3R3C-models are evaluated regarding other scientific papers, the 1R1C-models, and the model validation. An example of this is the 3R3C-model of Case 1.1. By looking at the correlation matrix of this case, 30, the dPen/dPar value of the parameter The0 (temperature of heating element) is at 10.4694. This should be close to 0 if the only desire is to obtain the best possible model validation. The reason for this parameter fitting to be chosen is that all obtained parameters are good compared to other scientific papers and 1R1C-models.

It is possible to decide how good the model is by comparing the specific heat capacity of water with the fitted value of C_{water} . Table 24 and Table 23 shows the specific heat capacity of water. Last year's project thesis obtained a heat capacity of $0.185 \frac{kWh}{\text{kg}^\circ C}$, $0.000658 \frac{kWh}{\text{kg}^\circ C}$. This is a lot lower than the specific heat capacity of water. The experiments performed during Case 1 - Case 3 gave the lowest combined estimate of $0.303 \frac{kWh}{\text{kg}^\circ C}$ ($0.001078 \frac{kWh}{\text{kg}^\circ C}$). Some estimates of C_{water} in the 3R3C models gave smaller values than this, but combined values for water to ambient all gave results above $0.3 \frac{kWh}{\text{kg}^\circ C}$, $0.001 \frac{kWh}{\text{kg}^\circ C}$. This is very similar to the specific heat capacity of water. Table 2 in Section 2.4 shows the heat capacity of isolation materials. This is significantly lower than the heat capacity of water. This is considered when choosing proper parameter fittings for the heat capacity of the wall. Most of the estimated heat capacities for the wall are of lower value than the heat capacity of water. Glass wool has a specific heat capacity of $0.000286 \frac{kWh}{\text{kg}^\circ C}$. In contrast, water has a heat capacity of $0.001162 \frac{kWh}{\text{kg}^\circ C}$. The heat capacity of the heating element is considered the lowest heat capacity. It does not store any heat, but it adds heat to the system.

By comparing the fitted heat capacity with earlier research, it is noticeable that both the project thesis, Løvstakken [2] and Svendsen [51] had approximately half the predicted value for their parameters compared to the other references. These references do not have good experiments because of weaknesses in the lab setup. The other scientific papers all have a specific heat capacity around the specific heat capacity of water. The new estimations in this thesis do also estimate a specific heat capacity to be around the heat capacity of water.

The RMSE and LogLikelihood of all the cases favor the 3R3C-model in all the cases. The Log-Likelihood of Case 2 and Case 3 is negative, but the 3R3C-model has the most negligible negative value and is, therefore, a better fit. The residual plots show that the peaks are lower for the 3R3C model compared to the 1R1C and 2R2C models. The 1R1C and 2R2C-models are very similar in residual plots. The cumulated periodogram shows that the 1R1C model is very off the designated boundary area. The 2R2C and 3R3C-models are equal to each other with small variations. The ACF plot also indicates that the 2R2C and 3R3C-models are the better options. The 3R3C-model has minor peaks. One-step-ahead plots show that each case model is a good fit for the measured values. The Simulated-value-plots show that the 3R3C is the better fit, as it is almost equal to the measured values. The 1R1C and 2R2C-models are more alike but do not fit the measured temperature. The 1R1C and 2R2C models miss the significant drop in temperature.

10 Further Work

There are still possible to improve the NTNU Smart House Lab. Installing an OSO Charge R to the OSO Saga S 300 enables better control of the water heater. It enables the opportunity to control hot water heating at times of the day with the lowest electricity price. It also gives insight into how much hot water is available and other functions such as "sleep mode." With this installation, further insights and control are added to the system.

The next step will be to make an optimization model that minimizes the cost of operation and shows the flexibility potential of water heaters. Using the one-day-ahead power price and simulating a case with a given number of water heaters, it is possible to estimate the water heater's cost savings and flexibility potential. The 3R3C-model is the better model to use and should be investigated more thoroughly if one is to simulate the water heaters.

It would be great to fit more temperature sensors inside the tank. The lower temperature sensor can be ignored as it does not give good enough measurements.

11 Conclusion

By insulating the existing temperature sensor, the results improve significantly. This is possible by comparing the measurements and the predicted parameters of this thesis and the project thesis [2]. The new sensor installations do also improve the results. The new parameters fittings are similar to other scientific papers. An expanded thermoelectric equivalent also improves the model. By calculating the root-mean-square-error and LogLikelihood it is possible to see that the 3R3C model is favorable in all cases. By looking at the simulated-value plots, it is easy to see that the plotted 3R3C-model fits the measured plots better than the 1R1C and 2R2C-models.

By draining water, the thermal resistance changed a lot. The thermal resistance more than halves its value in Case 2 and Case 3 compared to Case 1. This is because of the water draining. The temperature quickly drops when the shower is in use. The tank used 30 to 40 liters of hot water per 5 minutes, which means much cold water enters the tank. The thermal capacitance did not change significantly when water was drained from the EWH. There were more minor changes in the capacitance, but this is normal when simulating different experiments and models.

It was interesting to perform experiments by looking at different temperature sensors, as the results differed. The low-temperature sensor gave poor measurements as it was too dependent on the air surrounding the sensor and the cold inlet water. The middle and upper-temperature sensors gave better results as they had a delay in temperature change. This makes sense as the out-water leaves the tank from the top of the tank. Testing for different set-point temperatures was also interesting. this gave a rich dataset.

The parameter fittings vary for the different scientific papers mentioned in Section 3. The heat capacitance obtained in this thesis is equal to the heat capacitance obtained in Reference [6] Lakshmanan, [55] Yu, and [56] DTU. Reference [51] and [2] have approximately half the thermal capacitance-value. This is because these two references used the old lab setup at NTNU without insulation on the lower temperature sensor and new temperature sensors and flow meter.

The preferred model is the 3R3C-model, and the preferred thermal capacitance of water to ambient for this model is a minimum of $0.3 \frac{kWh}{^\circ C}$, and $0.446 \frac{kWh}{^\circ C}$ for the combined thermal capacitance. The preferred thermal resistance of this model is $170 \frac{kWh}{^\circ C}$ for water to ambient. This parameter values are obtained using the middle temperature sensor. The heating element's heat capacity and thermal resistance are regarded as low.

The lab setup can be further improved by adding the OSO Charge R or buying a new smart water heater. This would make it easier to monitor the EWH and obtain its flexibility potential. It would also be exciting to optimize the operation of the EWH regarding electricity price. This is possible by making use of the model established in this thesis.

References

1. Viseth E. Høye strømpriser: Dette trekker mest strøm hjemme hos deg. 2021. Available from: <https://www.tu.no/artikler/hoye-strompriser-i-sor-norge-dette-trekker-mest-strom-hjemme-hos-deg/513128>. accessed 30.05.2022
2. Løvstakken EM. Predicting flexibility potential of domestic hot water. PhD thesis. 2021
3. Nations U. Science, Solutions, Solidarity. 2021. Available from: https://www.un.org/climatechange?gclid=CjwKCAiA7dKMBhBCEiwAO_crFHjnk4aGOaVqSzqqw9y6DbRUVWZ_n5sZRj9VWUvI4blwdes1wTD1RoCJNYQAvD_BwE
4. Medepalli N, Joy M, Gorre R, and Rabbani M. MITIGATION OF POWER QUALITY ISSUES IN GRID INTEGRATED RENEWABLE ENERGY RESOURCES. 2020. DOI: 10.13140/RG.2.2.35224.21764. Available from: <https://www.researchgate.net/publication/345959213>
5. Rajasekharan J. ELK-15: Hydro Power Scheduling and Miscellaneous Topics on Electricity Markets. University Lecture. 2021. accessed: 18.10.2021
6. Lakshmanan V, Sæle H, and Degefa MZ. Electric water heater flexibility potential and activation impact in system operator perspective – Norwegian scenario case study. *Energy*. Vol. 236. Elsevier Ltd, 2021 Dec. DOI: 10.1016/j.energy.2021.121490
7. Wikipedia. Specific heat capacity. Available from: https://en.wikipedia.org/wiki/Specific_heat_capacity. (accessed: 07.10.2021)
8. NordPool. Market Data. 2022. Available from: <https://www.nordpoolgroup.com/en/Market-data1/Power-system-data/Consumption1/Consumption/ALL/Hourly1/?view=table>. accessed 01.06.2022
9. Elvia. Hva er nettleie? 2021. Available from: <https://www.elvia.no/nettleie/alt-om-nettleie/hva-er-nettleie>. accessed: 14.12.2021
10. Skatteetaten. 2021. Available from: <https://www.skatteetaten.no/bedrift-og-organisasjon/avgifter/saravgifter/om/elektrisk-kraft/>. accessed: 14.12.2021
11. Elvia. De nye nettleieprisene fra 1. januar 2022 er nå klare. 2021. Available from: <https://www.elvia.no/nettleie/alt-du-ma-vite-om-ny-nettleie-for-2022/>. accessed: 14.12.2021
12. Nve. Value of flexibility from electrical storage water heaters. 2021. Available from: www.nve.no
13. Statnett. Balance Agreement. Tech. rep. 2018 :1–4. Available from: <https://www.statnett.no/contentassets/6d34576d29d042859511eda73bbacd45/balanseavtale-gjeldende-fra-01.05.18.pdf>
14. Demand Flexibility. 2021. Available from: <https://buildings.lbl.gov/demand-flexibility>. accessed: 10.11.2021
15. Pudjianto D, Djapic P, Aunedi M, Gan CK, Strbac G, Huang S, and Infield D. Smart control for minimizing distribution network reinforcement cost due to electrification. *Energy Policy* 2013 Jan; 52:76–84. DOI: 10.1016/j.enpol.2012.05.021. Available from: <https://www.sciencedirect.com/science/article/pii/S0301421512004338>
16. Institute of Electrical and Electronics Engineers, IEEE Signal Processing Society, and Hydro-Québec. Symposium 3i. 2017 IEEE Global Conference on Signal and Information Processing. 2017. Available from: <https://ieeexplore.ieee.org/abstract/document/8309115>
17. Ryssdal MB, Fiksen K, Ådnanes OK, and Christiansen CH. Value of flexibility from electrical storage water heaters. 2020 :1–40. Available from: www.thema.no
18. Elvia. AMS-måler: dette må du vite. Available from: <https://www.elvia.no/smart-forbruk/alt-om-din-strommaler/ams-maler-dette-ma-du-vite/>. (accessed: 07.10.2021)

-
19. Walnum HT, Justo Alonso M, Clauß J, and Lindberg K. Characterization of heat load profiles in buildings and their impact on demand side flexibility. *IOP Conference Series: Materials Science and Engineering*. Vol. 609. 5. Institute of Physics Publishing, 2019 Oct. DOI: 10.1088/1757-899X/609/5/052035. Available from: <https://iopscience.iop.org/article/10.1088/1757-899X/609/5/052035/pdf>
 20. Hashemi MH, Hashemi MH, Moradlou M, and Bigdeli M. Energy Management of Industrial Loads In a Smart Micro grid Using Particle Swarm Optimization Algorithm Reserve Management in Restructured Power System Considering Loads Reliability View project Energy Management of Industrial Loads In a Smart Microgrid Using PSO Algorithm. Tech. rep. 2015. Available from: <https://www.researchgate.net/publication/286556977>
 21. Malone K. Electrical Load Management. 2010. Available from: <http://large.stanford.edu/courses/2010/ph240/malone1/>. accessed 18.12.2021
 22. Tumino P. Frequency Control in a Power System. 2020. Available from: <https://eepower.com/technical-articles/frequency-control-in-a-power-system/#>. accessed: 12.11.2021
 23. Engineering. PRIMARY SECONDARY AND TERTIARY FREQUENCY CONTROL. 2015. Available from: <https://top10electrical.blogspot.com/2015/10/primary-secondary-and-tertiary.html>. accessed: 12.11.2021
 24. Bompard E, Mazza A, and Toma L. Classical grid control: Frequency and voltage stability. *Converter-Based Dynamics and Control of Modern Power Systems* 2021 Jan :31–65. DOI: 10.1016/B978-0-12-818491-2.00003-1
 25. Wei C, Wu Q, Xu J, Sun Y, Jin X, Liao S, Yuan Z, and Yu L. Distributed scheduling of smart buildings to smooth power fluctuations considering load rebound. *Applied Energy* 2020 Oct; 276. DOI: 10.1016/j.apenergy.2020.115396. Available from: <https://www.sciencedirect.com/science/article/abs/pii/S0306261920309089>
 26. Csoknyai T, Legardeur J, Akle AA, and Horváth M. Analysis of energy consumption profiles in residential buildings and impact assessment of a serious game on occupants' behavior. *Energy and Buildings* 2019 Aug; 196:1–20. DOI: 10.1016/j.enbuild.2019.05.009. Available from: <https://www.sciencedirect.com/science/article/pii/S0378778818334790>
 27. Elvia. Smarte varmtvannsberedere vil redusere ressursbruken. 2021. Available from: <https://www.elvia.no/drift-og-vedlikehold/utbygginger-og-prosjekter/smar-te-varmtvannsberedere-vil-redu-sere-ressursbruken/>
 28. Høiax. Høiax CONNECTED - smart varmtvannsbereder med skyløsning. 2021. Available from: <https://www.hoiax.no/om-hoiax/articles/hoiax-connected-smart-varmtvannsbereder-med-skylosning>. accessed: 03.12.2021
 29. Høiax. Høiax CONNECTED - smart varmtvannsbereder med skyløsning. 2022. Available from: <https://www.hoiax.no/om-hoiax/articles/hoiax-connected-smart-varmtvannsbereder-med-skylosning>. accessed 14.03.2021
 30. Energy O. Vi frigjør kraften i varmtvannsberedere. 2022. Available from: <https://osoenergy.no/>. accessed 25.05.2022
 31. Enova. varmekapasitetSmart Varmtvannsbereder. 2022. Available from: <https://www.enova.no/privat/alle-energitiltak/smart-varmtvannsbereder/>. accessed 14.03.2021
 32. Tibber. Aeotec - Heavy Duty Switch. 2022. Available from: <https://tibber.com/no/store/produkt/aeotec-heavy-duty-switch>. accessed 14.03.2021
 33. Power TE. Smart Water Heater Pilot Program. 2021. Available from: <https://www.tep.com/water-heater-pilot/>. accessed: 03.12.2021
 34. BPA. Smart Water Heater Pilot. 2021. Available from: <https://www.bpa.gov/EE/Technology/EE-emerging-technologies/Projects-Reports-Archives/Field-Tests/Pages/Smart-Water-Heater-Pilot.aspx>. accessed: 03.12.2021
-

-
35. Rheem. SMART WATER HEATER, SMART CHOICE. 2022. Available from: <https://www.rheem.com/smarthelectric/>. accessed 14.03.2021
 36. aquanta. Make Your Water Heater Smart. Save Money. Stay Comfy. 2022. Available from: <https://aquanta.io/>. accessed 14.03.2021
 37. OSO hotwater AS. Saga - S datablad. 2021. Available from: https://www.bademiljo.no/globalassets/bluestone-assets/document/146061-12_20bw_20mont_20anv_20saga_20s_20_20no.pdf
 38. hotwater O. SAGA Standard - S. Available from: <https://osohotwater-no.kmc.fless.co.uk/produkt/saga-standard-s/>. (accessed: 06.10.2021)
 39. Norge C. BETYDNINGEN AV VARMEKAPASITETEN I ISOLASJONSMATERIALET. 2022. Available from: <https://www.cbinorge.no/celluloseisolasjon/hva-er-celluloseisolasjon/betydningen-av-varmekapasiteten-i-isolasjonsmateriale>. accessed 16.05.2022
 40. FHI. Fordelingsnett til dusjer og andre aerosoldannede tappepunkter. Available from: <https://www.fhi.no/nettpub/legionellaveilederen/temakapitler/interne-vannfordelingsnett-som-forsyner-dusjer-og-andre-aerosoldannende-tappepunkter/>. (accessed: 23.09.2021)
 41. Embedded. LogicMachine4. 2021. Available from: <https://openrb.com/logicmachine4/>. accessed: 17.12.2021
 42. Wikipedia. KNX (standard). 2021. Available from: [https://en.wikipedia.org/wiki/KNX_\(standard\)](https://en.wikipedia.org/wiki/KNX_(standard)). accessed: 19.10.2021
 43. KNX. A brief introduction. 2021. Available from: <https://www.knx.org/knx-en/for-professionals/What-is-KNX/A-brief-introduction/>. accessed: 19.10.2021
 44. Wikipedia. White box (software engineering). Available from: [https://en.wikipedia.org/wiki/White_box_\(software_engineering\)](https://en.wikipedia.org/wiki/White_box_(software_engineering)). (accessed: 20.09.2021)
 45. Walnum HT, Lindberg KB, and Sartori I. Evaluating Input Influence in Grey-box models for Demand Response in Buildings. *Proceedings of Building Simulation 2019: 16th Conference of IBPSA*. Vol. 16. IBPSA, 2020 Mar :4729–36. DOI: 10.26868/25222708.2019.211410. Available from: http://www.ibpsa.org/proceedings/BS2019/BS2019_211410.pdf
 46. Amara F, Agbossou K, Cardenas A, Dubé Y, and Kelouwani S. Comparison and Simulation of Building Thermal Models for Effective Energy Management. *Smart Grid and Renewable Energy* 2015; 06:95–112. DOI: 10.4236/sgre.2015.64009. Available from: https://www.researchgate.net/publication/236138545_Model_Identification_Using_Stochastic_Differential_Equation_Grey-Box_Models_in_Diabetes
 47. Wikipedia. Black Box. Available from: https://en.wikipedia.org/wiki/Black_box. (accessed: 20.09.2021)
 48. Zong Y, Böning GM, Santos RM, You S, Hu J, and Han X. Challenges of implementing economic model predictive control strategy for buildings interacting with smart energy systems. *Applied Thermal Engineering*. Vol. 114. Elsevier Ltd, 2017 Mar :1476–86. DOI: 10.1016/j.applthermaleng.2016.11.141. Available from: <https://www.sciencedirect.com/science/article/pii/S1359431116334871>
 49. Wikipedia. Grey box model. Available from: https://en.wikipedia.org/wiki/Grey_box_model. (accessed: 20.09.2021)
 50. Duun-Henriksen AK, Schmidt S, Røge RM, Møller JB, Nørgaard K, Jørgensen JB, and Madsen H. Model identification using stochastic differential equation grey-box models in diabetes. *Journal of Diabetes Science and Technology* 2013; 7:431–40. DOI: 10.1177/193229681300700220. Available from: https://www.researchgate.net/publication/236138545_Model_Identification_Using_Stochastic_Differential_Equation_Grey-Box_Models_in_Diabetes
 51. Svendsen I. Modelling Electrical Flexibility from Domestic Water Heaters. PhD thesis. 2021
-

-
52. Parnis G. Building Thermal Modelling Using Electric Circuit Simulation. Tech. rep. 2012
 53. Roma SU di. Thermal-electrical analogy: thermal network. 2021. Available from: http://www.ingaero.uniroma1.it/attachments/2176_Cap_320Thermal-electrical20analogy.pdf
 54. CTSM-R Development Team. Continuous Time Stochastic Modeling in R User's Guide and Reference Manual CTSM-R Development Team CTSM-R Version 1.0.0. Tech. rep. 2021. Available from: www.r-project.org
 55. Yu X, You S, Cai H, Georges L, and Bacher P. Data-Driven Modelling and Optimal Control of Domestic Electric Water Heaters for Demand Response. *Environmental Science and Engineering*. Springer, 2020 :77–86. DOI: 10.1007/978-981-13-9528-4{_}9
 56. Halvgaard R, Bacher P, Perers B, Andersen E, Furbo S, Jørgensen JB, Poulsen NK, and Madsen H. Model predictive control for a smart solar tank based on weather and consumption forecasts. *Energy Procedia*. Vol. 30. Elsevier Ltd, 2012 :270–8. DOI: 10.1016/j.egypro.2012.11.032
 57. Hu M, Xiao LF, and Xiao F. Model Predictive Control Of Inverter Air Conditioners Responding to Real-Time Electricity Prices In Smart Grids. Tech. rep. 2018. Available from: <https://www.researchgate.net/publication/333825450>
 58. Fjordkraft. Strømforbruket til varmtvannsberederen. Available from: <https://www.fjordkraft.no/strom/stromforbruk/varmtvannsbereder/>. (accessed: 07.10.2021)
 59. Bjelland Eriksen A, Hansen H, Hole J, Jonassen T, Mook V, Steinnes S, and Varden Lars. Reguleringsmyndigheten for energi-RME. Vol. 1. 2020 :1–84. Available from: www.reguleringsmyndigheten.no
 60. Saele H and Grande OS. Demand response from household customers: Experiences from a pilot study in Norway. *IEEE Transactions on Smart Grid* 2011; 2:102–9. DOI: 10.1109/TSG.2010.2104165. Available from: <https://ieeexplore.ieee.org/document/5710614>
 61. Haider A, Stark W, and Brekken TKA. Electric Hot water Heater Primary Frequency Control. 2018 :2670–5. Available from: <https://ieeexplore.ieee.org/stamp/stamp.jsp?arnumber=8557350&tag=1.&tag=1>
 62. Haugan I. Åpnet nytt smarthus-laboratorium. 2019. Available from: <https://gemini.no/2019/09/apner-nytt-smarthus-laboratorium/>. accessed: 19.10.2021
 63. Compute D. ctsmr - Continuous Time Stochastic Modelling for R. 2021. Available from: <http://www.ctsm.info/documentation.html>. accessed 21.12.2021
 64. Hyndman Robert J & Athanasopoulos G. Residual diagnostics. 2021. Available from: <https://otexts.com/fpp2/residuals.html>. accessed 18.12.2021

12 Appendix

12.1 Case 1.1

12.1.1 2R2C

Table 25: Coefficient Matrix of the 2R2C-model in Case 1.1, using the upper temperature sensor.

	Estimate	Std.Error	t value	Pr(> t)	dF/dPar	dPen/dPar
Twater0	7.732e+01	8.6653e-02	8.923e+02	0.000e+00	6.1929e-05	0.0018
Twall0	9.9302e+01	1.5247e+01	6.4474e+01	1.5613e-10	2.297e-07	0.3409
Cwall	1.2308e-02	8.206e-02	1.4999e-01	8.8079e-01	-4.7484e-08	0.0000
Cwater	4.2516e-01	9.6554e-03	4.4034e+01	0.0000e+00	-8.7699e-07	0.0001
e11	-2.6010e+01	1.3828e+02	-1.8809e-01	8.5083e-01	-1.9623e-07	0.0000
p11	-1.1263e+00	2.0619e-02	-5.4624e+01	0.0000e+00	3.7367e-06	0.0000
p22	-6.2691e+00	1.9165e+01	-3.271e-01	7.4364e-01	1.6107e-07	0.0000
Rwa	9.6805e+00	6.0233e+01	1.6072e-01	8.7234e-01	-3.0721e-08	0.0000
Rww	3.9287e+02	5.0927e+01	7.7143e+00	2.2871e-14	-1.9202e-06	0.3093

Table 26: Correlation Matrix for the 2R2C model in Case 1.1 using the upper temperature sensor.

	Twater0	Twall0	Cwall	Cwater	e11	p11	p22	Rwa
Twall0	0.02							
Cwall	-0.03	-0.03						
Cwater	-0.07	0.02	0.00					
e11	-0.02	-0.02	-0.16	0.00				
p11	0.06	0.00	0.03	0.14	0.02			
p22	0.00	-0.01	0.62	-0.05	-0.86	-0.02		
Rwa	0.05	0.03	-0.95	-0.01	0.15	-0.04	-0.62	
Rww	-0.06	-0.03	0.66	0.03	-0.11	0.04	0.43	-0.72

Table 27: Coefficient Matrix of the 2R2C-model in Case 1.1, using the lower temperature sensor.

	Estimate	Std.Error	t value	Pr(> t)	dF/dPar	dPen/dPar
Twater0	8.2800e+01	5.6222e-02	1.4727e+03	0.000e+00	1.7993e-02	0.0049
Twall0	2.8797e+01	1.3750e+01	2.0942e+00	3.6385e-02	-3.9631e-05	-0.007
Cwall	1.8206e-02	1.2479e-03	1.4589e+01	0.0000e+00	2.0393e-04	0.0000
Cwater	3.2110e-01	6.1827e-03	5.1936e+01	0.0000e+00	-1.18856e-03	0.0005
e11	-2.4639e+01	5.3256e+00	-4.6265e+00	4.0021e-06	-1.6230e-05	0.0000
p11	5.6947e-07	4.0027e-02	1.4227e-02	9.9999e-01	1.9134e-10	0.0000
p22	6.7807e+00	7.5915e-02	8.9320e+01	0.0000e+00	5.4212e-03	0.0000
Rwa	1.7295e+00	1.2047e-01	1.4357e+01	0.0000e+00	9.2444e-04	0.0000
Rww	2.8846e+02	1.4023e+01	2.0571e+00	0.0000e+00	-8.9207e-04	-0.0002

Table 28: Correlation Matrix for the 2R2C model in Case 1.1 using the lower temperature sensor.

	Twater0	Twall0	Cwall	Cwater	e11	p11	p22	Rwa
Twall0	0.00							
Cwall	0.00	-0.70						
Cwater	0.01	0.03	0.22					
e11	0.01	0.27	-0.33	-0.47				
p11	0.00	0.06	0.02	0.03	-0.02			
p22	0.01	0.54	-0.77	-0.14	0.41	0.02		
Rwa	0.01	0.66	-0.31	0.25	0.09	-0.02	-0.06	
Rww	0.01	0.8	-0.6	-0.14	0.58	0.03	0.67	0.5

12.1.2 3R3C

Table 29: Coefficient Matrix for the 3R3C-model in Case 1.1 using the upper temperature sensor.

	Estimate	Std. Error	t value	Pr(> t)	dF/dPar	dPen/dPar
The0	7.8409e+01	3.6278e-01	2.1614e+02	0.0000e+00	-1.2965e-04	0.0001
Twater0	7.7332e+01	5.2899e-02	1.4619e+03	0.0000e+00	1.0544e-04	0.0021
Twall0	4.6231e-29	1.8046e-27	2.5619e-02	9.7956e-01	-2.1631e-06	0.0000
Che	9.5786e-02	2.1518e-03	4.4514e+01	0.0000e+00	-1.4964e-03	0.0539
Cwall	2.0408e-01	1.2624e-01	1.6166e+00	1.0619e-01	1.1330e-04	0.0000
Cwater	2.3947e-01	5.3025e-03	4.5161e+01	0.0000e+00	-1.0152e-03	-0.0001
e11	-6.8882e+00	1.4990e-01	-4.5953e+01	0.0000e+00	-4.8095e-05	0.0000
p11	4.5481e-08	4.2350e-01	1.0739e-07	1.0000e+00	1.0752e-14	0.0000
p22	-1.6237e-01	1.3964e-02	-1.1628e+01	0.0000e+00	-7.9994e-06	0.0000
p33	-4.7349e+01	1.1236e+1	-4.2141e+00	2.6668e-05	1.8057e-04	0.0000
Rhew	2.4732e+00	1.0578e-01	2.3381e+01	0.0000e+00	-7.9994e-04	0.0000
Rwa	2.5422e+00	1.7499e+00	1.4528e+00	1.4650e-01	1.8849e-04	0.0000
Rww	3.3412e+02	9.7013e+00	3.4441e+01	0.0000e+00	-2.4211e-04	-0.0006

Table 30: Correlation Matrix for the 3R3C-model in Case 1.1 using the upper temperature sensor.

	The0	Twater0	Twall0	Che	Cwall	Cwater	e11	p11	p22	p33	Rhew	Rwa
Twater0	-0.17											
Twall0	-0.02	0.00										
Che	-0.03	0.01	0.19									
Cwall	0.03	0.00	-0.98	-0.17								
Cwater	-0.03	0.01	0.08	-0.28	0.00							
e11	0.00	0.03	-0.10	0.00	0.02	-0.18						
p11	0.01	0.01	-0.02	-0.01	0.02	-0.01	0.01					
p22	-0.01	0.05	-0.11	0.01	-0.01	-0.25	0.85	0.00				
p33	0.02	-0.04	0.21	0.08	-0.02	0.33	-0.54	-0.01	-0.68			
Rhew	0.09	0.00	-0.14	-0.48	0.15	-0.14	0.05	0.00	0.08	-0.18		
Rwa	-0.02	-0.01	0.96	0.20	-0.88	0.22	-0.21	-0.02	-0.26	0.45	-0.15	
Rww	-0.05	0.00	0.01	-0.60	0.01	0.64	-0.10	0.01	-0.16	0.05	-0.27	0.06

Table 31: Coefficient Matrix for the 3R3C-model in Case 1.1 using the lower temperature sensor.

	Estimate	Std. Error	t value	Pr(> t)	dF/dPar	dPen/dPar
The0	8.9722e+01	1.0836e+00	8.2798e+01	0.0000e+00	-2.6755e-04	10.4694
Twater0	7.3300e+01	4.5020e-02	1.6282e+03	0.0000e+00	-8.7234e-04	0.0008
Twall0	7.2425e+01	3.8918e-01	1.8610e+02	0.0000e+00	2.9028e-04	0.0013
Che	3.1260e-03	2.3549e-03	1.3275e+00	1.8457e-01	6.4033e-05	-0.0001
Cwall	2.1301e-01	9.0528e-03	2.3530e+01	0.0000e+00	-4.8777e-05	0.0000
Cwater	1.2239e-01	8.0710e-03	1.5164e+01	0.0000e+00	9.7048e-06	0.0000
e11	-1.2766e+02	1.4456e+01	-8.8306e+00	0.0000e+00	4.6406e-04	0.0005
p11	2.9695e-05	3.1880e+00	9.3145e-06	9.9999e-01	8.8250e-11	0.0000
p22	-1.7389e-01	4.9278e-03	-3.5288e+01	0.0000e+00	-1.0051e-05	0.0000
p33	2.7549e-01	1.9369e-02	1.4223e+01	0.0000e+00	6.7141e-06	0.0000
Rhew	4.4071e+01	3.3038e+01	1.3340e+00	1.8243e-01	-6.4147e-06	0.0000
Rwa	3.0155e+02	1.2584e+01	2.3963e+01	0.0000e+00	6.6350e-05	0.0004
Rww	1.8313e+00	9.0577e-02	2.0218e+01	0.0000e+00	-9.8286e-05	0.0000

Table 32: Correlation Matrix for the 3R3C-model in Case 1.1 using the lower temperature sensor.

	The0	Twater0	Twall0	Che	Cwall	Cwater	e11	p11	p22	p33	Rhew	Rwa
Twater0	0.02											
Twall0	-0.88	0.06										
Che	-0.27	-0.04	0.06									
Cwall	0.14	0.03	0.04	-0.08								
Cwater	-0.20	-0.03	-0.01	0.15	-0.83							
e11	-0.17	-0.03	0.04	0.45	-0.13	0.20						
p11	0.00	0.01	0.02	-0.07	0.00	-0.01	-0.05					
p22	0.00	0.00	0.01	-0.04	0.05	-0.07	-0.02	0.01				
p33	-0.04	-0.01	-0.07	0.04	-0.27	0.28	0.06	-0.01	0.26			
Rhew	0.32	0.05	-0.05	-0.83	0.50	-0.62	-0.47	0.07	0.05	-0.18		
Rwa	-0.04	-0.02	-0.01	0.10	0.00	0.07	0.23	-0.03	-0.01	0.01	-0.13	
Rww	-0.23	-0.02	0.04	0.09	-0.55	0.65	0.11	-0.02	0.04	0.49	-0.37	0.06

12.2 Case 1.2

12.2.1 1R1C

Table 33: Coefficient Matrix for the 1R1C-model in Case 1.2.

	Estimate	Std. Error	t value	Pr(> t)	dF/dPar	dPen/dPar
Tewh0	8.9200e+01	4.0515e-02	2.2016e+03	0.0000e+00	5.4235e-03	0.0252
C	3.6721e-01	3.6721e-01	9.9680e+01	0.0000e+00	-2.0304e-04	0.0000
e11	-1.8972e+01	5.2572e+00	-3.6087e+00	3.1658e-04	2.2276e-05	0.0359
p11	-1.8935e+00	2.0831e-02	-9.0895e+01	0.0000e+00	4.2487e-04	0.0000
R	3.5798e+02	1.0673e+01	3.3541e+01	0.0000e+00	-8.5413e-06	0.0000

Table 34: Correlation Matrix for the 1R1C-model in Case 1.2.

	Tewh0	C	e11	p11
C	0.06			
e11	0.23	-0.41		
p11	0.11	0.15	-0.088	
R	-0.07	-0.17	0.19	-0.13

12.2.2 2R2C

Table 35: Coefficient Matrix of the 2R2C-model of Case 1.2 with middle temperature sensor.

	Estimate	Std. Error	t value	Pr(> t)	dF/dPar	dPen/dPar
Twater0	8.9194e+01	3.9466e-02	2.2600e+03	0.0000e+00	1.1881e-03	0.0248
Twall0	9.3266e+01	1.4841e+01	6.2845e+00	4.1798e-10	5.3357e-03	0.2947
Cwall	1.5927e-02	1.5884e-03	1.0027e+01	0.0000e+00	-6.7542e-04	0.0000
Cwater	3.7598e-01	5.2299e-03	7.1890e+01	0.0000e+00	4.1120e-04	0.0000
e11	-1.8142e+01	8.9702e+01	-2.0225e-01	8.3975e-01	-1.5465e-03	0.0000
p11	-6.3790e+00	1.8028e+01	-3.5384e-01	7.2350e-01	-2.6914e-03	0.0000
p22	6.7858e+00	6.8865e-02	9.8537e+01	0.0000e+00	3.5496e-05	0.0000
Rwa	1.7388e+00	1.7467e-01	9.9550e+00	0.0000e+00	-3.0537e-04	0.0000
Rww	3.5210e+02	1.2856e+01	2.7388e+01	0.0000e+00	3.7293e-04	0.0008

Table 36: Correlation Matrix of the 2R2C-model for case 1.2 using the middle temperature sensor.

	Tewh0	Twall0	Cwall	Cwater	e11	p11	p22	Rwa
Twall0	0.05							
Cwall	0.00	0.33						
Cwater	0.02	0.01	0.12					
e11	0.01	-0.12	-0.86	-0.1				
p11	-0.01	0.01	0.83	0.01	-0.99			
p22	-0.01	-0.05	-0.35	-0.07	0.00	0.00		
Rwa	0.00	-0.32	-0.70	0.08	0.86	-0.83	-0.27	
Rww	-0.04	-0.07	-0.08	-0.22	-0.02	0.02	0.52	0.03

12.2.3 3R3C

Table 37: Coefficient Matrix for the 3R3C-model in Case 1.2 using the middle temperature sensor.

	Estimate	Std. Error	t value	Pr(>(abs(t)))	dF/dPar	dPen/dPar
The0	9.1944e+01	1.2075e+00	7.6147e+01	0.0000e+00	-8.3765e-04	0.0002
Twater0	8.9200e+01	2.4559e-02	3.6321e+03	0.0000e+00	1.9872e-03	0.0250
Twall0	7.2112e-19	1.6017e-17	4.5021e-02	9.6410e-01	0.0000e+00	0.0000
Che	1.1636e-02	1.7000e-03	6.8447e+00	1.0707e-11	-2.5353e-03	0.0000
Cwall	1.0655e-02	1.3217e-03	8.0617e+00	1.3323e-15	6.3950e-03	-0.0248
Cwater	3.1734e-01	3.3207e-03	9.5566e+01	0.0000e+00	3.1612e-03	0.0000
e11	-9.3295e+01	3.5298e+01	-2.6431e+00	8.2907e-03	7.5185e-05	0.0001
p11	2.3390e+00	4.0575e-01	5.7646e+00	9.7189e-09	-2.7997e-05	0.0000
p22	-9.3453e-02	3.0556e-01	-3.0584e+01	0.0000e+00	3.8998e-05	0.0000
p33	-1.0412e-04	1.4441e+01	-7.2101e-06	9.9999e-01	5.4329e-11	0.0000
Rhew	7.2524e+00	8.9805e+01	8.0757e+00	1.3323e-15	4.5175e-03	0.0010
Rwa	2.6142e+01	2.5027e+01	1.0446e+00	2.9637e-01	-2.5766e-04	0.0000
Rww	3.3329e+02	2.2795e+01	1.4621e+01	0.0000e+00	-9.9088e-04	-0.0006

Table 38: Correlation Matrix for the 3R3C-model in Case 1.2 using the middle temperature sensor.

	The0	Twater0	Twall0	Che	Cwall	Cwater	e11	p11	p22	p33	Rhew	Rwa
Twater0	0.03											
Twall0	-0.52	0.00										
Che	-0.53	0.00	0.99									
Cwall	-0.50	0.00	0.99	0.99								
Cwater	0.31	0.01	-0.57	-0.59	-0.60							
e11	-0.52	0.00	1.00	0.99	0.99	-0.57						
p11	0.49	0.00	-0.85	-0.88	-0.84	0.45	-0.85					
p22	0.04	-0.05	-0.05	-0.07	-0.03	-0.07	-0.05	0.36				
p33	0.01	-0.04	-0.01	-0.02	-0.02	0.03	-0.01	-0.01	-0.03			
Rhew	0.53	0.00	-0.99	-0.98	-0.98	0.52	-0.99	0.89	0.08	0.02		
Rwa	0.52	0.01	-0.90	-0.87	-0.82	0.43	-0.90	0.78	0.09	0.00	0.88	
Rww	-0.53	0.00	0.99	0.97	-0.53	0.99	-0.85	-0.07	0.00	0.97	-0.96	0.01

12.3 Case 2

12.3.1 1R1C

Table 39: Coefficient Matrix for the 1R1C-model in Case 2.

	Estimate	Std. Error	t value	Pr(> t)	dF/dPar	dPen/dPar
Tewh0	5.9008e+01	3.4713e-01	1.6999e+02	0.0000e+00	9.3661e-05	4e-04
C	5.0712e-01	2.4470e-02	2.0724e+01	0.0000e+00	1.9742e-05	0e+00
e11	-2.2969e-01	6.3934e+1	-3.5925e-01	7.1947e-01	-1.3706e-06	0e+00
p11	1.9057e-01	2.4138e-02	7.8951e+00	6.4393e-15	1.1399e-05	0e+00
R	1.6769e+02	3.2970e+01	5.0863e+00	4.2293e-07	1.0991e-05	0e+000

Table 40: Correlation Matrix for the 1R1C-model in Case 2.

	Tewh0	C	e11	p11
C	-0.07			
e11	0.00	-0.00		
p11	0.05	-0.01	0.00	
R	-0.03	0.20	-0.04	-0.08

12.3.2 2R2C

Table 41: Coefficient Matrix of the 2R2C-model in Case 2, using the middle temperature sensor.

	Estimate	Std.Error	t value	Pr(> t)	dF/dPar	dPen/dPar
Twater0	5.8994e+01	1.3439e-01	4.3899e+02	0.000e+00	-9.2049e-03	-0.0032
Twall0	9.6296e+01	4.4318e+01	2.1728e+00	2.9983e-02	5.9726e-03	0.0702
Cwall	4.0130e-02	2.8057e-02	1.4303e+00	1.5288e-01	1.8207e-03	0.0000
Cwater	3.8450e-01	2.1690e-02	1.7728e+01	0.0000e+00	-6.6839e-04	0.0001
e11	-2.2163e+01	6.1321e+00	-3.6143e+00	3.1346e+00	-1.8053e-04	0.0000
p11	1.0884e-08	4.7086e-02	2.3116e-07	1.0000e+00	5.2616e-14	0.0000
p22	6.5242e+00	2.6685e-01	2.4449e+01	0.0000e+00	5.7031e-04	0.0000
Rwa	4.5472e+00	3.2899e+00	1.3822e+00	1.6717e-01	-1.5766e-03	0.0000
Rww	1.2382e+02	3.09397e+01	4.0023e+00	6.6535e-05	-2.2175e-05	0.0000

Table 42: Correlation Matrix for the 2R2C model in Case 2 using the middle temperature sensor.

	Twater0	Twall0	Cwall	Cwater	e11	p11	p22	Rwa
Twall0	0.33							
Cwall	-0.33	-1.00						
Cwater	0.06	-0.07	0.05					
e11	-0.21	-0.47	0.45	0.15				
p11	0.00	-0.01	0.01	0.00	0.00			
p22	-0.09	-0.16	0.13	0.35	0.92	-0.01		
Rwa	0.33	1.00	-0.99	-0.08	-0.47	0.00	-0.17	
Rww	-0.11	-0.16	0.14	0.13	0.95	0.00	0.97	-0.16

12.3.3 3R3C

Table 43: Coefficient Matrix of the 3R3C-model of Case 2 with middle temperature sensor.

	Estimate	Std. Error	t value	Pr(> t)	dF/dPar	dPen/dPar
The0	5.9276e+01	1.2298e+00	4.8361e+01	0.0000e+00	3.0267e-03	0.0004
Twater0	5.9008e+01	1.5323e-01	3.8508e+02	0.0000e+00	7.1823e-03	-0.0002
Twall0	5.1429e+01	2.2800e+00	2.2557e+01	0.0000e+00	-8.0904e-03	0.0003
Che	2.8879e-01	6.9906e-02	4.1311e+00	3.8599e-05	-7.5477e-04	0.0001
Cwall	1.6214e-01	1.0457e-02	1.5506e+01	0.0000e+00	6.5839e-04	-0.0004
Cwater	1.4499e-01	8.1630e-03	1.7762e+01	0.0000e+00	-2.6914e-03	-0.0007
e11	-2.0165e+01	1.5116e+00	-1.3341e+01	0.0000e+00	-6.7890e-04	0.0000
p11	-9.1383e-04	1.0937e+01	-8.3551e-05	9.9993e-01	-1.6634e-08	0.0000
p22	-3.2263e-07	5.4511e-02	-5.9186e-06	1.0000e+00	5.3382e-01	0.0000
p33	-2.3817e+02	1.4168e+01	-1.6811e+01	0.0000e+00	-9.6701e-04	0.0425
Rhew	1.9024e+00	3.6085e-01	5.2721e+00	1.5986e-07	-7.2748e-04	0.0000
Rwa	3.9850e+00	7.7696e-01	5.1290e+00	3.3938e-07	3.8182e-04	0.0000
Rww	1.1958e+02	1.2538e+01	9.5373e+00	0.0000e+00	2.8549e-03	0.0000

Table 44: Correlation Matrix of the 3R3C-model for Case 2 using the middle temperature sensor.

	The0	Twater0	Twall0	Che	Cwall	Cwater	e11	p11	p22	p33	Rhew	Rwa
Twater0	0.74											
Twall0	0.07	-0.09										
Che	0.08	0.13	-0.72									
Cwall	-0.04	-0.17	0.92	-0.63								
Cwater	-0.03	-0.05	0.38	-0.45	0.24							
e11	-0.12	-0.22	0.88	-0.75	0.92	0.18						
p11	0.04	0.17	-0.97	0.77	-0.96	-0.35	-0.93					
p22	-0.02	-0.02	0.05	-0.03	0.05	0.04	0.12	-0.05				
p33	-0.14	-0.22	0.92	-0.86	0.88	0.4	0.94	-0.96	0.04			
Rhew	0.14	0.12	-0.38	0.48	-0.2	-0.50	-0.17	0.36	-0.05	-0.45		
Rwa	0.05	0.11	-0.68	0.88	-0.5	-0.59	-0.59	0.70	-0.04	-0.78	0.62	
Rww	0.11	0.15	-0.68	0.78	-0.54	-0.80	-0.55	0.69	-0.05	-0.77	0.73	0.85

12.4 Case 3.1

12.4.1 1R1C

Table 45: Coefficient Matrix for the 1R1C-model in Case 3.1.

	Estimate	Std. Error	t value	Pr(> t)	dF/dPar	dPen/dPar
Tewh0	8.8224e+01	3.5607e-01	2.4777e+02	0.0000e+00	3.2613e-04	0.0182
C	3.1663e-01	9.4934e-03	3.3353e+01	0.0000e+00	-1.4953e-04	0.0000
e11	-2.2747e+01	1.1633e+02	-1.9554e-01	8.4500e-01	-1.5582e-07	0.0000
p11	2.3705e-01	2.2676e-02	1.0453e+01	0.0000e+00	2.2198e-06	0.0000
R	1.9594e+02	2.9350e+01	6.6760e+00	3.9015e-11	1.4359e-06	0.0000

Table 46: Correlation Matrix for the 1R1C-model in Case 3.1.

	Tewh0	C	e11	p11
C	0.10			
e11	-0.01	0.04		
p11	0.03	0.01	0.00	
R	0.02	0.10	0.02	-0.03

12.4.2 2R2C

Table 47: Coefficient Matrix of the 2R2C-model in Case 3.1 using the middle temperature sensor.

	Estimate	Std.Error	t value	Pr(> t)	dF/dPar	dPen/dPar
Twater0	8.8223e+01	1.8923e-01	4.6622e+02	0.000e+00	2.4692	0.0179
Twall0	7.4891e+01	1.3184e+01	5.6804e+00	1.7229e-08	-1.0780e-04	0.0018
Cwall	4.5212e-02	2.9192e-03	1.5488e+01	0.0000e+00	6.8519e-05	0.0001
Cwater	3.1164e-01	1.4340e-02	2.1731e+01	0.0000e+00	1.3447e-03	0.0001
e11	-1.5503e+02	1.2864e+01	-1.2051e+01	0.0000e+00	1.9885e-04	0.0002
p11	1.0760e-06	1.5386e-01	6.9935e-06	9.9999e-01	4.2927e-11	0.0000
p22	7.2317e+00	1.5222e-01	4.7509e+01	0.0000e+00	-6.8476e-03	0.0000
Rwa	2.1938e+00	3.86883e-01	5.6711e+00	1.8168e-08	-5.2650e-04	0.0000
Rww	1.8016e+02	2.0560e+01	8.7628e+00	0.0000e+00	2.4502e-05	0.0001

Table 48: Correlation Matrix for the 2R2C model in Case 3.1 using the middle temperature sensor.

	Twater0	Twall0	Cwall	Cwater	e11	p11	p22	Rwa
Twall0	0.06							
Cwall	0.03	-0.25						
Cwater	0.00	0.13	0.14					
e11	-0.07	-0.78	-0.31	-0.23				
p11	0.06	0.03	0.05	0.02	-0.07			
p22	0.06	0.3	0.61	0.50	-0.79	0.08		
Rwa	-0.03	0.03	-0.66	-0.13	0.55	-0.05	-0.78	
Rww	0.08	0.3	0.74	0.27	-0.79	0.09	0.91	-0.67

12.4.3 3R3C

Table 49: The coefficient Matrix of the 3R3C-model for Case 3.1 using the middle temperature sensor.

	Estimate	Std. Error	t value	Pr(> t)	dF/dPar	dPen/dPar
The0	8.8177e+01	7.5310e-01	1.1709e+02	0.0000e+00	-2.7783e-03	0.0180
Twater0	8.8219e+01	2.0210e-01	4.3652e+02	0.0000e+00	5.1375e-03	0.0181
Twall0	8.7626e+01	4.8467e+00	1.8080e+01	0.0000e+00	6.0126e-04	0.0153
Che	1.5520e-01	1.6319e-02	9.5108e+00	0.0000e+00	1.0736e-04	0.0000
Cwall	1.6464e-01	3.6680e-03	4.4886e+01	0.0000e+00	-6.2218e-04	-0.0004
Cwater	1.2567e-01	7.1632e-03	1.7544e+01	0.0000e+00	4.0965e-04	-0.0019
e11	-2.3556e+01	1.9797e+00	-1.1898e+01	0.0000e+00	2.4032e-04	0.0000
p11	1.5693e-04	1.1585e+00	1.3779e-04	9.9989e-01	7.3794e-10	0.0000
p22	7.1438e-07	9.1108e-02	7.8410e-06	9.9999e-01	6.1379e-11	0.0000
p33	5.3016e+02	3.4509e+01	1.5363e+01	0.0000e+00	-1.4208e-03	0.0065
Rhew	8.6995e-01	8.0608e-02	1.0792e+01	0.0000e+00	-3.7817e-07	0.0000
Rwa	1.5448e+00	1.4411e-01	1.0719e+01	0.0000e+00	-2.7115e-04	0.0000
Rww	1.6813e+02	1.3683e+01	1.2287e+01	0.0000e+00	6.8522e-04	0.0001

Table 50: Correlation Matrix of the 3R3C-model for Case 3.1 using the middle temperature sensor.

	The0	Twater0	Twall0	Che	Cwall	Cwater	e11	p11	p22	p33	Rhew	Rwa
Twater0	0.63											
Twall0	0.04	0.05										
Che	-0.04	-0.03	-0.03									
Cwall	-0.04	-0.01	0.66	0.01								
Cwater	-0.04	-0.05	0.03	-0.40	-0.02							
e11	-0.03	-0.04	-0.99	0.03	-0.66	-0.04						
p11	0.07	0.06	0.24	-0.16	0.18	-0.15	-0.23					
p22	0.00	-0.03	-0.04	0.01	-0.04	-0.04	0.17	0.04				
p33	0.05	0.01	-0.85	-0.11	-0.59	0.18	0.84	-0.11	0.01			
Rhew	-0.01	-0.02	0.00	-0.34	0.27	-0.13	0.00	0.19	0.01	-0.08		
Rwa	-0.04	-0.03	-0.09	0.05	0.40	-0.12	0.10	0.06	0.01	0.02	0.52	
Rww	0.04	0.02	-0.72	-0.06	-0.31	-0.39	0.72	0.12	0.06	0.66	0.39	0.39

12.5 Case 3.2

12.5.1 1R1C

Table 51: Coefficient Matrix for the 1R1C-model in Case 3.2.

	Estimate	Std. Error	t value	Pr(> t)	dF/dPar	dPen/dPar
Tewh0	7.6256e+01	4.2200e-01	1.8070e+02	0.0000e+00	-4.3801e-07	0.002
C	4.7953e-01	2.8420e-02	1.6873e+01	0.0000e+00	-8.2417e-07	0.000
e11	-2.2055e+01	6.5886e+02	-3.3474e-02	9.7330e-01	1.3121e-06	0.000
p11	3.9613e-01	3.0391e-02	1.3034e+01	0.0000e+00	-6.4529e-07	0.000
R	1.3789e+02	3.5107e+01	3.9277e+00	9.2917e-05	9.8318e-07	0.000

Table 52: Correlation Matrix for the 1R1C-model in Case 3.2.

	Tewh0	C	e11	p11
C	-0.01			
e11	0.00	0.00		
p11	-0.05	0.04	0.00	
R	0.01	0.14	0.00	-0.04

12.5.2 2R2C

Table 53: Coefficient Matrix of the 2R2C-model in Case 3.2 using the middle temperature sensor.

	Estimate	Std.Error	t value	Pr(> t)	dF/dPar	dPen/dPar
Twater0	7.6288e+01	1.8880e-01	4.0407e+02	0.000e+00	-4.8746e-04	0.0015
Twall0	2.1191e+01	5.5656e+00	3.8075e+00	1.5077e-04	-5.3744e-04	-0.0299
Cwall	1.8046e-01	2.6837e-02	6.7243e+00	3.3123e-11	-6.1924e-04	0.0000
Cwater	3.6097e-01	2.5563e-02	1.4121e+01	0.0000e+00	7.0129e-05	0.0001
e11	-1.9257e+01	1.3225e+00	-1.4562e+01	0.0000e+00	-6.1937e-04	0.0000
p11	4.2471e-01	2.2532e-02	1.8849e+01	0.0000e+00	5.1255e-07	0.0000
p22	6.3991e+00	1.5642e-01	4.0911e+01	0.0000e+00	-6.1937e-04	0.0000
Rwa	1.3731e+00	2.0209e-01	6.7944e+00	2.0943e-11	4-1093e-04	0.0000
Rww	1.0208e+02	1.3129e+01	7.7749e+00	2.2871e-14	-1.8162e-03	-0.2363

Table 54: Correlation Matrix for the 2R2C model in Case 3.2 using the middle temperature sensor.

	Twater0	Twall0	Cwall	Cwater	e11	p11	p22	Rwa
Twall0	0.03							
Cwall	0.05	0.76						
Cwater	0.03	0.12	-0.25					
e11	0.02	0.97	0.68	0.19				
p11	-0.02	0.00	-0.02	-0.04	0.01			
p22	0.00	-0.66	-0.87	0.57	-0.57	0.00		
Rwa	-0.05	-0.77	-0.68	0.01	-0.71	-0.04	0.62	
Rww	-0.04	-0.95	-0.89	0.04	-0.89	0.00	0.79	0.87

12.5.3 3R3C

Table 55: Coefficient Matrix of the 3R3C-model for Case 3.2 using the middle temperature sensor.

	Estimate	Std. Error	t value	Pr(> t)	dF/dPar	dPen/dPar
The0	7.6898e+01	1.9805e+00	3.8828e+01	0.0000e+00	-2.6908e-03	0.0022
Twater0	7.6256e+01	1.9125e-01	3.9873e+02	0.0000e+00	1.4694e-02	0.0018
Twall0	4.8561e+01	8.7191e-01	5.5695e+01	0.0000e+00	-5.4196e-03	0.0001
Che	1.7316e-01	4.2636e-02	4.0613e+00	5.3479e-05	-2.0223e-04	0.0000
Cwall	1.7010e-01	7.1467e-03	2.3801e+01	0.0000e+00	-3.4846e-03	-0.0003
Cwater	2.1461e-01	1.4698e-02	1.4601e+01	0.0000e+00	2.7557e-04	-0.0001
e11	-1.5751e+01	2.2276e-01	-7.0706e+01	0.0000e+00	1.1592e-03	0.0000
p11	5.3901e+00	7.3066e-01	7.3770e+00	4.0035e-13	-2.6629e-04	0.0000
p22	4.1010e-01	2.7015e02	1.5180e+01	0.0000e+00	8.1052e-05	0.0000
p33	1.7950e+02	1.3295e+01	1.3501e+01	0.0000e+00	9.9716e-04	0.0000
Rhew	1.5251e+00	2.4129e-01	6.3206e+00	4.2883e-10	-4.5321e-05	0.0000
Rwa	4.8837e+00	1.3614e+00	3.5873+00	3.5383e-04	6.5383e-04	0.0000
Rww	9.7877e+01	2.7614e+01	3.544e+00	4.1564e-04	-2.8338e-04	0.0000

Table 56: Correlation Matrix of the 3R3C-model for Case 3.2 using the middle temperature sensor.

	The0	Twater0	Twall0	Che	Cwall	Cwater	e11	p11	p22	p33	Rhew	Rwa
Twater0	0.57											
Twall0	0.36	0.15										
Che	0.01	-0.08	0.53									
Cwall	-0.07	-0.14	0.24	0.37								
Cwater	0.32	0.15	0.36	0.04	-0.04							
e11	0.05	0.05	0.05	0.06	0.01	0.12						
p11	0.20	0.15	-0.08	-0.34	0.26	0.26	0.13					
p22	0.05	0.08	0.06	0.21	0.02	0.03	0.38	0.16				
p33	-0.05	-0.05	0.21	0.44	0.29	-0.13	0.06	0.08	0.15			
Rhew	0.10	0.12	-0.25	-0.29	0.06	-0.33	0.09	0.68	0.22	0.12		
Rwa	-0.05	-0.12	0.28	0.45	0.92	-0.04	0.02	0.28	0.05	0.39	0.07	
Rww	-0.09	-0.10	0.23	0.40	0.72	-0.12	0.05	0.34	0.13	0.59	0.14	0.82

12.6 Tables

Table 57: Flexibility service for TSO.

Flexibility service for TSO	Pros
Primary control	Maintain system stability and reliability (fast reaction)
Secondary control	Maintain system stability and reliability
Tertiary control	Maintain system stability and reliability
National Capacity Market	Reduce requirement for peak generation capacity
Congestion Management	Delay grid reinforcements Avoid grid reinforcements
Grid Capacity Management	Optimize Asset Use Reduce grid losses
Controlled islanding	Reduce frequency and duration of outage
Redundancy (n-1) support	Reduce frequency and duration of outage

Table 58: Flexibility services for DSO.

Flexibility service of DSO	Pros
Congestion Management	Delay grid reinforcement Avoid grid reinforcement
Voltage control	Avoid grid reinforcement
Grid Capacity Management	Optimize asset use reduce grid losses
Controlled islanding	Reduce frequency and duration of outage
Redundancy (n-1) support	Reduce frequency and duration of outage
Power quality support	Avoid grid investments

Table 59: Flexibility services for BRP.

Flexibility services for BRP	Pros
Day-ahead Optimisation	Reduce sourcing costs
Intraday Optimization	Reduce sourcing costs
Self-/Passive Balancing	Reduce balancing costs
Generation Optimization	Reduce sourcing costs

Table 60: Flexibility services for Prosumers.

Flexibility services for Prosumers	Pros
ToU Optimization	Reduce energy costs
KWmax Control	Reduce grid connection costs
Self Balancing	Reduce energy costs
Controlled islanding	Increase availability

12.7 Code

```

1- ## ----setup, include=FALSE-----
2- ## Set options and default
3- library(knitr)
4- opts_chunk$set(fig.path='genfig/', fig.align='center', fig.show='hold', size='footnotesize',cache=TRUE)
5- options(replace.assign=TRUE, width=76)
6-
7- ## ----init-----
8- ## Init by deleting all variables and functions
9- rm(list=ls())
10- ## Set the working directory
11- setwd(".")
12- ## Use the ctsmr package
13- library(ctsmr)
14-
15- ## List with global parameters
16- prm <- list()
17- ## Number of threads used by CTSM-R for the estimation computations
18- prm$threads <- 1
19-
20- ## ----sourcefunctions, results="hide"-----
21- ## Source the scripts with functions in the "functions" folder. Just a neat way of arranging helping functions in R
22- sapply(dir("functions", full.names=TRUE), source)
23-
24- ## ----definemodel-----
25- ## initialize the model
26- model <- ctsm$new()
27- ## Specify the system equations
28- model$addSystem(dThe ~ ((Twater-The)/(Rhew*Che) + Q/Che) * dt + p11 * dw1)
29- model$addSystem(dTwater ~ (M*0.001666667*(Tin-Twater)/Cwater + (Twall-Twater)/(Rww*Cwater)+(The-Twater)/(Rhew*Cwater)) * dt + p22 * dw2)
30- model$addSystem(dTwall ~ ((Twater-Twall)/(Rww*Cwall)+(Ta-Twall)/(Rwa*Cwall)) * dt + p33 * dw3)
31-
32- ## The inputs
33- model$addInput("Ta", "Q", "Tin", "M")
34-
35- ## The observation equation
36- model$addObs(yTwater ~ Twater )
37- ## Set the variance of the measurement error
38- model$setVariance(yTwater ~ exp(e11))

```

Figure 55: Code for initializing and system equations.

```

40- ## ----initvalues, tidy=FALSE-----
41- model$setParameter( Twater = c(init=75 ,lb=40 ,ub=95) )
42- model$setParameter( Twall = c(init = 40, lb = 0, ub = 95))
43- model$setParameter( The = c(init = 40, lb = 0, ub = 100))
44- ## Set intial values
45- model$setParameter( Cwater = c(init=0.15 ,lb=0.1 ,ub=0.5) )
46- model$setParameter( Cwall = c(init=0.15 ,lb=0.1 ,ub=0.5) )
47- model$setParameter( Che = c(init=0.01 ,lb=0.0001 ,ub=0.5) )
48- model$setParameter( Rww = c(init=450 ,lb=390 ,ub=600 ) )
49- model$setParameter( Rwa = c(init=10 ,lb=0.001 ,ub=300 ) )
50- model$setParameter( Rhew = c(init=1 ,lb=0.001 ,ub=10 ) )
51- model$setParameter( p11 = c(init=1 ,lb=-350 ,ub=350) )
52- model$setParameter( p22 = c(init=1 ,lb=-350 ,ub=350) )
53- model$setParameter( p33 = c(init=1 ,lb=-350 ,ub=650) )
54- model$setParameter( e11 = c(init=-1 ,lb=-350 ,ub=350) )
55- |
56- ## Read the data csv
57- X <- read.csv("experiment11.csv",sep=";",header=FALSE)
58-
59- X <- read.csv("Experiment2.csv",sep=";",header=FALSE)
60-
61- X <- read.csv("Experiment3.csv",sep=";",header=FALSE)
62-
63- X <- read.csv("Experiment 4.csv",sep=";",header=FALSE)
64-
65- X <- read.csv("Experiment 5.csv",sep=";",header=FALSE)
66- ## show file
67- X
68- ## set the names of the columns in X
69- names(X) <- c("Moling", "Tsetpoint", "t","q","yTwater2","yTwater", "Ta", "Tin", "Tut", "M")

```

Figure 56: Code for reading files and setting initial values.

```

70 ▾ ## ----plotdata-----
71 ## Plot the data
72 ## add extra space to right margin of plot within frame
73 par(mfrow=c(1,1),mar=c(5, 4, 4, 6)+0.1)
74
75 ## Plot first set of data and draw its axis
76 plot(X$t,X$ytwater, pch=16, axes=FALSE, xlab="", ylab="", type="l",col="blue", lwd = 2)
77 axis(2, ylim=c(0,1),col="blue",col.axis="blue",las=1) ## las=1 makes horizontal labels
78 mtext("Temperature (°C)",side=2,line=3, cex = 1.5)
79 box()
80
81 ## Allow a second plot on the same graph
82 par(new=TRUE)
83
84 ## Plot the second plot and put axis scale on right
85 plot(X$t,X$Q, pch=15, axes=FALSE, xlab="", ylab="", type="l", col="red", lwd = 2)
86 ## a little farther out (line=4) to make room for labels
87 mtext("Power (kw)",side=4,line=4, cex = 1.5)
88 axis(4, ylim=c(0,7000), col="red",col.axis="red",las=1)
89
90 ## Draw the time axis
91 axis(1,pretty(range(X$t),10))
92 mtext("Time of day(h)",side=1,col="black",line=2.5, cex=1.5)
93
94 ## Add Legend
95 legend("topleft",legend=c("Temperature","Power"),
96       text.col=c("blue","red"),pch=c(16,15),col=c("blue","red"))
97

```

Figure 57: Code for plotting temperature and power graphs.

```

100 fit <- model$estimate(data=X, threads=prm$threads)
101
102 ▾ ## ----summary-----
103 ## Print the parameters estimates and the Correlation Matrix of the estimates
104 print(summary(fit,extended=TRUE))
105 ▾ ## ----comparePrmEstimates,cache=FALSE-----
106 ## The parameter estimates in a data.frame
107 Prm <- data.frame(xm=fit$xm)
108 row.names(Prm) <- names(fit$xm)
109 ## The true parameter values
110 Prm$xmtrue <- c(63,0.18,-8,0.5,297, 0, 0, 0, 0, 0, 0, 0, 0)
111 ## Approximately lower 95% confidence bound
112 Prm$lower <- (fit$xm - 2*fit$sd)
113 ## Approximately upper 95% confidence bound
114 Prm$upper <- (fit$xm + 2*fit$sd)
115 ## Print it all
116 #round(Prm,digits=2)
117 format(Prm,digits=4)
118
119 ▾ ## ----acfAndCP,fig.height=4-----
120 ## Calculate the one-step ahead predictions
121 tmp <- predict(fit, newdata=x)
122 ## calculate the residuals and put them with the data in a data.frame x
123 X$ytwaterHAT <- tmp$output$pred$ytwater
124 X$ytwaterHAT
125 X$residuals <- X$ytwater - X$ytwaterHAT
126 ## Auto-correlation function and cumulated periodogram
127 par(mfrow=c(1,2)) # Setup plot
128 acf(X$residuals, main="Residuals ACF")
129 cprgram(X$residuals, main="Cumulated periodogram")
130
131 ## Calculate the loglikelihood value
132 print(paste("Loglikelihood", fit$loglik))
133
134 ## calculate RMSE|
135 sqrt(mean((X$ytwater - X$ytwaterHAT)^2))
136
137 ▾ ## ----timeseriesresiduals-----
138 ## Plot of inputs, output, one-step ahead predicted output, and residuals
139 par(mfrow=c(3,1),mar=c(3,3.5,1,1),mgp=c(2,0.7,0)) # Setup plot
140 plot(X$t,X$Q,type="l", xlab = "time (h)", ylab = "Power (kw)")
141 plot(X$t,X$residuals,type="l", xlab = "time (h)", ylab = "residuals")
142 plot(X$t, X$ytwater, ylim=range(X[,c("ytwater","ytwaterHAT")]), type="n", xlab="time (h)", ylab="Temperature EWH")
143 lines(X$t, X$ytwater, lwd = 2, col = "blue")
144 lines(X$t, X$ytwaterHAT, col=2, lwd = 2)
145 legend("topleft",legend=c("Measured","Simulated"),
146       text.col=c("blue","red"),pch=c(16,15),col=c("blue","red"))

```

Figure 58: Code for parameter fitting, RMSE and LogLikelihood value and Residual plots.

